

AN INTEGRATIVE APPROACH TO MANAGING A SPECIES
OF CONSERVATION CONCERN:
RESOURCE SELECTION, SPATIAL ECOLOGY, AND POPULATION GENETICS
OF THE GREEN SALAMANDER
(ANEIDES AENEUS)

A Ph.D. Dissertation
Presented to
the Graduate School of
Clemson University

In Partial Fulfillment
of the Requirements for the Degree
Doctor of Philosophy
Biological Sciences

by
Megan Veronica Novak
December 2023

Accepted by:
Dr. Kyle Barrett, Committee Chair
Dr. Saara DeWalt, Co-chair
Dr. Robert Baldwin
Dr. James Nichols

ABSTRACT

The relationship between wildlife and the environment they inhabit is dependent on both spatial and temporal scales. It is therefore crucial that biological investigations account for ecological scale when analyzing patterns and processes established, particularly when such investigations inform conservation management plans. This dissertation provides extensive insight into the conservation biology of the green salamander (*Aneides aeneus*), a critically imperiled species in South Carolina. The green salamander is a species that exists in a patchy network of rock outcrops within mountainous forest landscapes, and most studies on habitat suitability for green salamanders have been conducted on the macrohabitat, neglecting the interaction between individuals and their immediate microhabitat. Assessments of within-habitat features can help determine habitat suitability for sites with unknown occupancy status. I evaluated within-site resource selection using logistic regression to inform the interaction between individuals and their immediate microhabitat and identified features that contribute to microclimate stability and within-habitat connectivity as significant predictors of green salamander presence. Spatial and temporal variability in population demographics were addressed by implementing a three-year population survey across upstate South Carolina. In this study, I concurrently implemented two methods of estimating abundances, a capture-mark-recapture (CMR) approach and an unmarked repeated count approach (N-mixture modeling). I surveyed twenty-one green salamanders across upstate South Carolina and implemented a two-tiered survey design to analyze the data in a robust framework that accounted for open and closed population assumptions. Survey results provided the first

evidence of a green salamander migrating between two discrete rock outcrops (50 m). Our top CMR model estimated average seasonal abundances to range from 3–32 individuals across twelve sites. The top N-mixture model estimated abundances to vary from 10–51 individuals across nineteen sites throughout the three-year study period. Further, I analyzed the genetic structure within and between discrete green salamander locales across South Carolina. I used RADSeq sequencing to identify SNPS, estimate population genetic statistics including F_{ST} , F_{IS} , H_O , H_S , and N_e , and used fastSTRUCTURE to detect fine-scale population patterns. Results identified no evidence of inbreeding and little genetic differentiation among sites but showed evidence of isolation by distance (IBD). To investigate the influence of landscape heterogeneity on gene flow, I evaluated the genetic structure among green salamander sites against IBD and isolation by resistance (IBR) models. We used pairwise F_{ST} values as the genetic response to evaluate resistance landscape surfaces that included water bodies and land cover features. Genetic structure was best described by the IBD model. Forested land provided little resistance to gene flow, suggesting arboreal behaviors may provide a mechanism for animal dispersal among rock outcrops. Cumulatively, this body of work provides an extensive analysis on the conservation biology within, between, and among populations of a species of conservation concern. My evaluation of the selection of microhabitat helps in identifying the threshold of features required for an overall site to be suitable. The demographic results provided the first reports of site-specific abundances. Continued monitoring practices and can help conservationists track past demographic patterns and predict future trajectories. The report of an individual

migrating between sites and empirical results from our larger-scale landscape genetic analysis offer evidence of a stepping-stone dispersal network between neighboring site locales, and ultimately identified forested land cover to be a mechanism for gene flow. Results have been reported to the South Carolina Department of Natural Resources and US Forest Service to inform future species management plans.

ACKNOWLEDGMENTS

I would like to extend my deepest gratitude to my advisor, Dr. Kyle Barrett. Dr. Barrett's support and mentorship was unwavering and invaluable throughout this tremendous task. I would not be the scientist, teacher, and leader that I am today without him. I would also like to express my sincere thanks to my co-advisor, Dr. Saara DeWalt, and my committee, Dr. Rob Baldwin and Dr. James Nichols. Their willingness, support, and belief in me was consistently expressed throughout the entirety of this dissertation, and it was all incredibly and genuinely appreciated.

I acknowledge and thank the South Carolina Department of Natural Resources, the United States Forest Service, and the Clemson Creative Inquiry Program, all of which supported this work financially. I also thank Tangled Bank Conservation for their invaluable collaboration in our genetic work.

I extend my gratitude and sincere love to my dear friends for their encouragement throughout this journey, especially Kara Titus, Amanda Palecek, David Munteanu, Emma Rogers, Anwar Hanano, and Andie Eaton, all of whom played a tremendous role in my success. I could not have undertaken this degree without the limitless support and love from my family, who have been my cheerleaders since day one. My sister, Jessie Novak, was the cornerstone of my confidence and inspiration. And lastly, words cannot express my gratitude and love to my wife, Caitlin Novak, who was my sounding board and voice of reason for the past six years. Her encouragement, love, and unconditional support carried me through the finish line.

TABLE OF CONTENTS

	Page
TITLE PAGE	i
ABSTRACT.....	ii
ACKNOWLEDGMENTS	v
LIST OF TABLES	ix
LIST OF FIGURES	xii
CHAPTER	
I. INTRODUCTION	1
II. WITHIN-SITE MICROCLIMATE AND CONNECTIVITY CAN HELP PREDICT THE PRESENCE OF DISCRETE PATCH INHABITANTS, <i>ANEIDES AENEUS</i>	7
Abstract.....	7
Introduction.....	8
Methods.....	10
<i>Study Site</i>	10
<i>Field Methods</i>	11
<i>Statistics</i>	11
Results.....	12
Discussion.....	13
III. EVALUATING MARK-RECAPTURE AND REPEATED COUNT APPROACHES WHEN SETTING A RELIABLE BENCHMARK FOR A NEAR-THREATENED SPECIES.....	16
Abstract.....	16
Introduction.....	17
Methods.....	20
<i>Survey Methods and Data Collection</i>	20
Study Area	21
A robust survey design.....	21
Capture-mark-recapture data collection.....	22

	N-mixture model data collection	23
	Habitat and landscape data collection.....	23
	<i>Data analysis</i>	24
	Capture-mark-recapture data analysis.....	24
	N-mixture model data analysis	27
	Results	30
	<i>CMR analysis</i>	30
	<i>N-mixture models</i>	32
	Discussion	33
	<i>Survival probability, S</i>	33
	<i>Detection probability, p</i>	34
	<i>Temporary emigration, γ and availability probability, ϕ</i>	35
	<i>Abundance covariates</i>	35
	<i>Comparison of CMR and N-mixture model abundance estimates</i> ...	37
IV.	UNEXPECTED HIGH GENETIC RELATEDNESS ACROSS DISCRETE PATCHES OF A TERRESTRIAL SALAMANDER	39
	Abstract	39
	Introduction.....	40
	Methods.....	42
	<i>Field Methods</i>	42
	<i>Lab Methods</i>	43
	3RAD Library Preparation and Sequencing.....	43
	Data Processing and SNP calling	44
	Quantifying Population Structure.....	44
	Genetic diversity and Effective Population Size within Sampling Units	46
	Results	47
	<i>Sequencing</i>	47
	<i>Population Structure</i>	47
	<i>Genetic Diversity and Effective Population Size within Sampling Units</i>	48
	Discussion	48
V.	ISOLATION BY DISTANCE BEST EXPLAINS SPATIAL GENETIC STRUCTURE IN GREEN SALAMANDERS IN SOUTH CAORLINA.....	53
	Abstract	53
	Introduction.....	53
	Methods.....	56
	<i>Study site and sample collection</i>	56

<i>DNA extraction and population genetic analyses</i>	57
<i>Resistance models</i>	58
<i>Resistance surface optimization and evaluation</i>	59
Results.....	60
Discussion.....	60
VI. CONCLUSION.....	65
APPENDIX	106
Supplemental 1	107
Supplemental 2	108
Supplemental 3	109
Supplemental 4.....	110
REFERENCES	111

LIST OF TABLES

Table	Page
2.1. Predicted and modeled relationships between crevice use and features of the crevice for populations of Green Salamanders (<i>Aneides aeneus</i>) across five sites in Greenville, Oconee, and Pickens counties, South Carolina, USA. Predictions are listed as being either positively (+) or negatively (-) correlated with salamander presence	71
2.2. Mean \pm standard deviation of crevice features that were both occupied and unoccupied by Green Salamanders (<i>Aneides aeneus</i>) across five sites (rock outcrops) in Greenville, Oconee, and Pickens counties, South Carolina, USA	72
2.3. MANOVA (Multivariate Analysis of Variance) results indicating how crevice features differ across the five sites we visited of Green Salamanders (<i>Aneides aeneus</i>) in Greenville, Oconee, and Pickens counties, South Carolina, USA. We expected the features crevice density, nearest crevice, and nearest tree to be the best predictive rock characteristics for salamander presence. Canopy cover, crevice density, distance to nearest crevice, and distance to nearest tree differed significantly between sites	73
3.1. Descriptions of the capture probability (p), recapture probability (c), and survival (S) parameter covariates incorporated into the robust design framework for our CMR analysis	74
3.2. Descriptions of the detection probability (p), availability probability (Φ), and abundance (λ) parameter models incorporated into the N-mixture models for the unmarked analysis	75
3.3. AIC _C results for candidate CMR models describing the 214 capture histories of green salamanders (<i>Aneides aeneus</i>) across 12 sites by various survival (S), capture probability (p), and recapture probability (c) covariates. ~1 indicates a null model; blank cells indicate the covariate was not incorporated into the model	76

List of Tables (Continued)

Table	Page
3.4. Green salamander (<i>Aneides aeneus</i>) survival and capture probability estimates across the surveyed South Carolina populations as described by the top ranked CMR model. Survival (S) was site-specific and capture probability (p) was constant across sites and sampling periods. NA's indicate estimates were removed because the standard errors were larger than the estimates.....	78
3.5. Green salamander (<i>Aneides aeneus</i>) availability probability estimates across the five primary periods. These availability estimates indicate the probability that green salamanders were available for capture within the super-population (i.e., site)	79
3.6. Results of the AIC analysis for candidate N-mixture models describing the unmarked counts of green salamanders (<i>Aneides aeneus</i>) across 19 sites by various detection (p), availability (Φ), and abundance (λ) models. All models are fit to a Poisson distribution. All availability models include the best-fit detection probability covariate (temperature). All abundance models include the top ranked detection covariate and availability covariate (primary period)	80
4.1. Pairwise F_{ST} values for green salamander (<i>Aneides aeneus</i>) populations across sampling sites in South Carolina, USA. We have results on thirteen of the seventeen total sites used in this study because four sites were not included in the analysis as they contained only one tissue sample each. Mean $F_{ST}=0.06\pm 0.008$	81
4.2. Pairwise F_{ST} values for populations of green salamanders (<i>Aneides aeneus</i>) separated into three groups separated by Lake Jocassee/Eastatoee Creek (between Groups 1 and 2) and the South Saluda River/Table Rock Reservoir (between Groups 2 and 3). Mean $F_{ST}=0.080\pm 0.003$	82

List of Tables (Continued)

Table	Page
4.3. All genetic population statistics estimated for individual green salamander populations in upstate South Carolina, USA. Populations are individual rock outcrops separated by at least 50 m, and n dictates the number of tissue samples removed from the respective site. Sites with only one tissue sample were not included in the population statistic analysis. H_O is a measure of observed heterozygosity, H_S is a measure of expected heterozygosity under Hardy-Weinberg Equilibrium, F_{IS} is the inbreeding coefficient, and N_e represents the estimated effective population size (95% CI). N_e estimates denoted as “NA” indicate the estimate could not be distinguished from the sampling error; it does not indicate an infinitely large population	83
4.4. Genetic population statistics estimated for green salamander populations culminated into three groups in upstate South Carolina, USA. Groups are separated by notable water bodies, and n dictates the number of tissue samples removed from the respective site. H_O is a measure of observed heterozygosity H_S is a measure of expected heterozygosity under Hardy-Weinberg Equilibrium, F_{IS} is the inbreeding coefficient, and N_e represents the estimated effective population size (CI). N_e estimates denoted as “NA” indicate the estimate could not be distinguished from the sampling error; it does not indicate an infinitely large population.....	84
5.1. A comparison of the resistance surfaces optimized and evaluated using ResistanceGA (v. 4.1-16) to evaluate isolation by distance versus isolation by resistance models in response to green salamander (<i>Aneides aeneus</i>) genetic connectivity. Models include distance-only (Distance), a water resistance layer (Water), a land cover resistance layer (NLCD), an intercept only model (Null), and two resistance layers run simultaneously (nlcd.water). Models were evaluated using Akaike information criterion (AIC_C). Results show the distance-only model (IBD) outperformed the other surfaces.	85
5.2. Resistance values associated with the two resistance models analyzed as single, independent layers within ResistanceGA. Response values for the resistance surface optimization and evaluation were pairwise F_{ST} estimates across green salamander (<i>Aneides aeneus</i>) sites across upstate South Carolina. Resistance values were set to a maximum of 500; higher values indicate higher resistance	86

LIST OF FIGURES

Figure	Page
<p>2.1. Each survey of Green Salamanders (<i>Aneides aeneus</i>) of rock outcrops in Greenville, Oconee, and Pickens counties, South Carolina, USA, began by first laying a field tape across the length of the outcrop (solid yellow line). This long axis was divided every 5 m (dashed yellow lines), and a random number generator was used to determine where a perpendicular transect (white lines) was laid within these 5 m segments. Every crevice crossed by these perpendicular transects was surveyed for salamander presence and assessed for crevice depth, width, length, humidity, distance from the nearest tree, distance from the nearest crevice, and crevice density.....</p>	87
<p>2.2. Crevice density surrounding the crevice of interest (ten-point center star) of Green Salamanders (<i>Aneides aeneus</i>) was calculated by identifying the point within the crevice of interest that is surrounded by the most crevices. A 1-m² area was measured around this point and every crevice that fell within this designated space was counted (shown as individual stars), including the crevice of interest.....</p>	88
<p>2.3. Violin plots for the significant ($\alpha=0.05$) site features in crevices unoccupied (grey) and occupied (green) by Green Salamanders (<i>Aneides aeneus</i>) in Greenville, Oconee, and Pickens counties, South Carolina, USA. (A) Crevice width; (B) canopy cover; (C) crevice density.....</p>	89
<p>2.4. Odds ratio curves for probability of presence of Green Salamanders (<i>Aneides aeneus</i>) in relationship to (A) crevice width, (B) canopy cover, and (C) crevice density with the respective confidence intervals.....</p>	90
<p>3.1. County-level distribution of the green salamander (<i>Aneides aeneus</i>). The Blue Ridge Escarpment (BRE) populations exists in Georgia, North Carolina, and South Carolina, disjunct from the main Appalachian population. Map downloaded from the Amphibian and Reptile Monitoring Initiative's National Amphibian Atlas website</p>	91

List of Figures (Continued)

Figure	Page
3.2. The robust design used for the marked population analysis of green salamander (<i>Aneides aeneus</i>) populations in the Blue Ridge Escarpment. This design includes primary sampling periods, K , with secondary periods nested within each primary, k . Primary periods were pooled into cool and warm seasons in the year, determined post hoc as sampling days that achieved temperatures higher (warm period) or lower (cool period) than the annual average. Primary periods assume an open population where births, deaths, immigration, and emigration can occur between them. Secondary periods assume a closed population.....	92
3.3. Photo-identification process with the Interactive Individual Identification System (I ³ S) software. Uploaded photographs of individual animals are assessed for reference points (e.g., patterns), and the I ³ S software compares those reference points to others previously made for individuals already uploaded into the system.....	93
3.4. An illustration of the relationships between γ' and γ'' at time $i-1$ and i . The super-population is represented by the entire rock outcrop. Crevices on the outer portions of the rock outcrop are easily surveyed, and animals present in these areas are available for capture. Crevices deep within the rock outcrop are unable to be surveyed. Animals present in the inner circle are unable to be encountered by the surveyors, but still members of the super-population. Adapted from Powell and Gale 2015.....	94
3.5. Kendall Tau's correlation scatterplots illustrating the relationship between the average abundance as estimated by the CMR analysis and [A] site elevation (m); [B] aspect (degrees); [C] site size (m ²); [D] the average number of crevices totaled across each site	95
3.6. Abundance estimates for 19 green salamander (<i>Aneides aeneus</i>) populations across upstate South Carolina. Black bars represent site-specific abundances estimated through count data in an N-mixture model framework with count data fit to a Poisson distribution. N-mixture model estimates are informed by $p \sim$ temperature, $\Phi \sim$ primary period, and $\lambda \sim$ site size + total number of crevices. Gray bars represent the site-specific abundances estimated using a CMR approach and averaged across the five primary periods that assumed an open population. Within the CMR model, $\gamma \sim 1$, $p \sim 1$, and $S \sim$ site	96

List of Figures (Continued)

Figure	Page
3.7. Correlative scatterplot illustrating the relationship between our CMR averaged green salamander (<i>Aneides aeneus</i>) population abundance estimates and the N-mixture model population abundance estimates. Results indicate a weak relationship ($R^2 = 0.0072$) with no notable association.....	97
4.1. Some analyses incorporated population units as numerous sampling locations combined into three groups. This map shows the grouped population units, each separated by a water body that we hypothesized would be large enough to hinder gene flow and create three potential population groupings of green salamanders in upstate South Carolina, USA. Red pin represents Group 1 (n=15 tissue samples); blue pins represent Group 2 (n=53 tissue samples); yellow pins represent Group 3 (n=45 tissue samples)	98
4.2. Principal component analyses identifying population differentiation among green salamander (<i>Aneides aeneus</i>) sites in upstate South Carolina. Each color represents a unique population, and each dot represents an individual green salamander. (A) The analysis conducted with one single nucleotide polymorphism per RAD locus (851 unlinked SNPs). (B) Results of the analysis that included a more stringent filtering scheme that included only SNPs present in more than 50% of individuals, and SNPs present in more than 50% of individuals and SNPs present in at least one individual per sampling location (247 unlinked SNPs). (C) and (D) illustrate the same filtering schemes as (A) and (B), respectively; however, the population units are now separated by geographic grouping rather than individual sites sampled. Neither (A) nor (B) show strong population separation among sampling sites, but (C) and (D) begin to show more population structure among the three groups	99
4.3. Population genetic differentiation showed evidence of isolation by distance ($R^2=0.24$) across pairwise combinations of 17 green salamander (<i>Aneides aeneus</i>) populations in upstate South Carolina.....	101
4.4. Taken from Gordon (1952). A description of population locales and habitat type used by green salamanders (<i>Aneides aeneus</i>) along the species range. Population locations were taken from various sources from 1924 to 1950 (see Figure 1 in Gordon 1952). Note no record of green salamander populations within the Appalachian Valley, and apparent disjunct populations within the Blue Ridge Escarpment in North Carolina and South Carolina	102

List of Figures (Continued)

Figure	Page
5.1. Topographic map showing the sampling locations for green salamanders (<i>Aneides aeneus</i>) across upstate South Carolina, USA.....	103
5.2. Resistance maps made in ArcGIS Pro (v. 3.0.1). Locations of green salamander (<i>Aneides aeneus</i>) sampling sites are represented by yellow dots. Panel A shows the original National Land Cover Database (NLCD, Esri 2019) and National Hydrography Dataset (NHD, USGS 2021). Panels B and C represent two resistance surfaces with features aggregated from the original NLCD and NHD layers. Panel B illustrates the water resistance surface with three class features: large water bodies (blue), which combines streams classified as third order and higher as well as lakes; streams (green), which combines first and second order streams; and land (gray). Panel C illustrates the land cover resistance surface with five class features: water (blue), a combination of open water, woody wetlands, and emergent herbaceous wetlands; developed space (white), which aggregated developed open space, and developed land from low, medium, and high intensities; early successional (black), a category that joined barren land, shrub land, scrub land, grassland, and herbaceous cover; forest cover (green) which combined deciduous, evergreen, an mixed forests; and agriculture (yellow), which incorporated pasture, hay, and cultivated crop land.....	104

CHAPTER ONE

DISSERTATION INTRODUCTION

George Hutchinson (1965) described our world as an ecological theater that plays on various levels of time and space, a metaphor highlighting how different biological patterns emerge depending upon the scales at which they are viewed. Mating behaviors, population structure, migration, individual home ranges, and foraging efforts are all examples of biological processes that can be studied independently of one another, but they do not truly exist as independent concepts. Rather, these dynamics are nested in a hierarchical structure, and they are each spatially and temporally governed (Wiens 1989). With this shared governance, different patterns of each process can be found based on the scale in which it was studied. For example, Semlitsch (1998) proposed a buffer of protected land around salamander breeding ponds to extend approximately 164 m from the pond, based on within-population movement studies. Charney (2012) revisited the estimated buffer zone width in the same population system, but in the context of salamander migration movements between populations instead of within-population movement. When viewed from this larger scale, Charney found the species' migrational movement capabilities to range from 1000 - 3000 m and suggested the buffer zone be increased to accommodate migratory behaviors. These paired studies offer insight into the concept of determining the scale of an investigation: the appropriate scale of a study depends on the questions asked, the organisms investigated, and the time periods of interest.

Animal movement is a characteristic of life that can drive ecological dynamics across scales and influence biological organization from subpopulation dynamics to population distribution. An individual organism's movement and habitat selection within its immediate environment helps to explain habitat requirements needed to meet behavioral (e.g., hunting,

mating, predator avoidance; see Isley 1938, Sandoval 1994, Sperry and Weatherhead 2009) and physiological (e.g., thermoregulation and cutaneous respiration; see Spotila 1972, Kingsolver and Watt 1983, Huey 1991) demands. Resources that meet these immediate biological requirements exist on a localized scale, relative to the larger landscape, as suitable patches of habitat. The distribution and abundance of species across the landscape is defined by resource availability, the movement of individuals among those resources, and the limits of animal dispersal capabilities. Research examining these many moving parts is becoming increasingly important with human urbanization and expansion into previously undeveloped lands, influencing animal behaviors within the subpopulation, and potentially reshaping the total population structure.

Wildlife populations are often defined as occupying contiguous habitat where the quality of resources can vary, and animals distribute themselves amongst those resources (McCullough 1996). A contrasting concept is that of a patchy population structure distributed among a network of homogeneous habitat interspersed throughout a heterogeneous landscape (Levins 1970). Both population structures describe how animals are distributed throughout an environment, with the key distinction lying in the spatial arrangement of subpopulations and the level of connectivity between them (Moilanen and Hanski 1998, Briers 2002). Connectivity across populations provides a means for interaction between individuals and gene flow, thereby maintaining genetic diversity throughout the species range. A review by Kindlmann and Burel (2008) distinguished two subsets of connectivity: structural and functional. Structural connectivity is defined as the physical pathways available within a landscape that organisms can use to disperse or interact within. These features include corridors for movement that facilitate animal dispersal and gene flow. Functional connectivity refers to the degree to which components within the landscape

permit animal movement. Within this, functional connectivity defines the effectiveness of corridors provided by the structural components within the habitat. Functional connectivity ensures features within the landscape are not only physically (structurally) connected, but also ecologically meaningful.

Improving our understanding of the structural and ecological components inhibiting and strengthening connectivity among a patchy population may provide insight for applied species management programs. Such an understanding could inform conservation efforts aimed at species that naturally exist in continuous populations but are forced into a patchy distribution throughout an anthropogenically fragmented landscape. Conservation biology rests on the concept that the ability to restore or preserve natural ecosystems is firmly intertwined with a scientific understanding of how that ecosystem functions. Therefore, it is crucial that a conservation-based investigation consider the scales of the biological processes of interest and the different patterns that can emerge across those scales. **The goal of this dissertation is to advance the scientific understanding of patchy population structures and interpopulation dispersal mechanisms used to maintain population persistence** by investigating a species of conservation concern across a range of spatial and temporal scales. Specifically, I examined the population demographics and the physical and genetic structures within an amphibian species, the green salamander (*Aneides aeneus*).

Many amphibians exist in patchy and discretely bound habitats and are thus reliant on the functional connectivity between those patches for dispersal opportunities. Two traits that contribute to a disjunct subpopulation structure among amphibian populations include poor dispersal ability and site fidelity (Duellman and Trueb 1986, Sinsch 1990, Blaustein et al. 1994). Amphibians are often limited in their dispersal ability because of their physiological makeup,

and concurrently have strict habitat requirements. The amphibian integumentary system is remarkable for its permeability, which is a critical feature for gas exchange and osmoregulation (Hopkins 2007) but limiting in regards to habitats that are suitable for such a sensitive anatomy. Many amphibians are thus restricted to wet or moist habitats interspersed throughout a terrestrial landscape to reduce the likelihood of desiccation. Further, some amphibians exhibit a biphasic life history with an aquatic larval stage and a terrestrial adulthood. This life history trait often requires mating, oviposition, and larval development to occur at discrete aquatic breeding sites (i.e., permanent ponds, ephemeral ponds, streams, etc.). Adult amphibians can exhibit high fidelity to their natal ponds (Pechmann et al. 1991), thereby perpetuating the paradigm of patchy subpopulations expressed in amphibian species. The degree of dispersal capabilities and levels of habitat fidelity determine the bounds within which amphibian populations operate.

The green salamander is a fully terrestrial salamander that inhabits vertical rock outcrops along the Appalachian Mountains. There has been evidence of arboreal behaviors of green salamanders witnessed in trees adjacent to rock outcrops (Wilson 2003, Waldron and Humphries 2005), though the full extent of this is unknown. Generally, the species is considered “weakly” arboreal and predominantly rock-dwelling (Bishop 1928, Snyder 1991). The patchy distribution of rock outcrops inhabited by the terrestrial green salamander mirrors the distribution of ponds inhabited by biphasic amphibians. Rocks are physically discrete habitat structures in an otherwise heterogeneous landscape, and green salamander populations thereby exhibit a patchy distribution throughout the species range.

Green salamander populations range from Alabama to Pennsylvania, with a notable disjunct outlier population in the Blue Ridge Escarpment (BRE) that falls within North Carolina, South Carolina, and Georgia, USA (Figure 2.1). The species is listed as “Near threatened with

decreasing populations” by the IUCN Red List (IUCN 2022), and as “Critically imperiled” in South Carolina (in the BRE). Information on salamander dispersal capabilities indicate the species exhibits limited mobility (generally ≤ 50 m; Gordon 1952, Williams and Gordon 1961, Waldron and Humphries 2005, John 2017). Shorter dispersal distances exhibited by individuals may be a consequence of the species’ lungless anatomy. The metabolic capacity and oxygen consumption of lungless salamander species is limited to 20-40% of what a lunged salamander can sustain (Full 1986; Full et al. 1988), and this limitation on energy expenditure directly affects lungless salamander dispersal capabilities.

Population estimation efforts have been conducted within the BRE in the past few decades, but most of these studies only include raw count data of either individuals, brooding mothers, or green salamander nest counts. These count surveys have results ranging from as few as one salamander per site to as many as 141 individuals across an unlisted number of sites (Gordon 1952, Snyder 1971, Snyder 1991, Corser 2001). In 2016 an N-mixture model was developed to estimate population sizes that incorporated surveyor detection probabilities (Newman et al. 2016, unpublished data). Much of the information on green salamander population demographics is poorly understood, not well documented, or unpublished.

Within this dissertation I investigated green salamanders within the BRE to answer questions related to within-habitat patch suitability, subpopulation demographics, and within- and between-subpopulation genetic structure. To address the larger goal of expanding our understanding of patchy population structures and interpopulation dispersal mechanisms, the individual aims of this work sought to answer the following questions:

1. What features within a discrete habitat patch (i.e., rock outcrop) are related to microhabitat suitability?
2. Do abundance and survival rates vary between discrete habitat patches based on habitat and environmental covariates?
3. How do inbreeding and effective population sizes differ across disjunct, patchy, subpopulations with varying sizes and distances from each other?
4. Which intervening landscape features are associated with the genetic connectivity of subpopulations of a species restricted to discrete habitat patches?

The answers to these questions provided an analysis on the conservation biology within, between, and among green salamander populations in South Carolina to ensure results found are relevant to the scale in which they were observed. Question 1 was scaled to a microhabitat use (rock crevices) within the macrohabitat patch (rock outcrops). Question 2 investigated population demographics within habitat patches (i.e., rock outcrops) and defines the perimeter of the patch as the boundaries for subpopulations. Questions 3 and 4 exhibited the largest spatial and temporal scale of the dissertation. In these chapters, we analyzed demographic and genetic connectivity across subpopulations in upstate South Carolina. By specifying spatial and temporal extent of each of our four questions and designing the scale of our approaches accordingly, we can be confident that the pattern-process relationships we infer from our results are relevant to the ecological questions we sought to investigate.

CHAPTER TWO

WITHIN-SITE MICROCLIMATE AND CONNECTIVITY CAN HELP PREDICT THE PRESENCE OF DISCRETE PATCH INHABITANTS, *ANEIDES AENEUS*

Abstract.—Many animal species inhabit environments where resources are patchily distributed. In circumstances where species' populations are restricted to exist in a patchy network within an otherwise inhospitable environment, assessments of within-habitat features can help determine habitat suitability for sites with unknown occupancy status. The Green Salamander (*Aneides aeneus*) is an example of a species with a patchy distribution that inhabits rock outcrops embedded within mountainous forest landscapes. Most studies on habitat suitability for Green Salamanders have been conducted on the macrohabitat (rock outcrops), neglecting the interaction between individuals and their immediate microhabitat (rock crevices). The small size and lungless nature of Green Salamanders limit movements, affecting behaviors such as foraging, predation evasion, and searching for mates. As a result of these constraints, we predicted crevices with features related to within-habitat connectivity (i.e., structural connectivity between microhabitats) are likely to be associated with Green Salamander presence. We evaluated features that contribute to microclimate and within-habitat connectivity, including crevice width (cm), length (cm), depth (cm), temperature (°C), crevice density ($1/m^2$), nearest crevice (cm), and nearest tree (m). We surveyed 424 crevices across five sites; we found salamanders occupying 116 of the crevices, but we did not find salamanders in 310 crevices, which we classified as available but unused microhabitats. A Global Logistic Regression Model identified crevice width, canopy cover, and crevice density as significant predictors of salamander presence. Understanding critical within-site features is as equally important for conservation

management as the larger site-level criteria, especially for small animals with a patchy distribution.

1. Introduction

For species that inhabit discrete patches of habitat on the landscape (e.g., wetlands, reefs, rock outcrops), the suitability of the habitat is typically assessed across the entire patch to provide conservation managers with spatially explicit suitability maps to guide protection or prioritization of habitats. For example, landscape-level indices for modeling habitat selection of organisms with patchy distributions have included minimum/maximum patch area (Chapin et al. 1998; Garabedian et al. 2017), patch connectivity (Nikolakaki 2004; Kindlmann and Burel 2008), landscape topography and vegetation coverage (Goldberg et al. 2004; Dustan et al. 2013; Newman et al. 2018), and prey availability (Lewis and Garrison 1984; Benoit-Bird et al. 2013). It is equally important, however, to assess the selection of microhabitats within discrete patches (i.e., third-order habitat *sensu* Johnson, 1980) because some threshold of suitable microhabitats must exist for the overall patch to be suitable. An understanding of the third-order selection of microhabitats provides insight into how ectothermic individuals address ecological needs, such as those related to temperature (Blouin-Demers and Weatherhead 2001; Hofmann and Fischer 2002) and humidity (Reagan 1974; Lunghi et al. 2015).

Species management decisions backed by an understanding of second-order (macrohabitat) selection and third-order (microhabitat) selection are likely the most effective. A habitat conservation approach across these spatial scales would not only account for population structure (e.g., locales of presence/absence) but also within-site patterns and dynamics (e.g., distribution and movement). Some terrestrial salamanders, for example, exhibit different ecological patterns across macro- and microhabitats because they exist in homogeneous, discrete

patches throughout an otherwise heterogeneous landscape. The differences between these two scales of habitat are essential in allowing regional population persistence (i.e., by maintaining heterogeneity in the macrohabitat), and individual fitness (i.e., fitness met by acquiring resources in the microhabitat).

Compared to other species of salamanders in the Southeastern U.S., Green Salamanders (*Aneides aeneus*) inhabit a highly specialized niche of moist crevices in rocky outcrops found within mixed oak forests (Wake 1963; Corser 2001) and are one of the few arboreal salamanders in the region (Gordon 1952; Waldron and Humphries 2005). Unsurprisingly for a species with a distinctly narrow habitat niche, Green Salamanders have a decreasing population trend and are globally ranked as Near Threatened (Hammerson 2004). To ensure clarity of our definitions of scale for this paper, we will hereby refer to second-order habitat as discrete rock outcrops and third-order habitat as the crevices within the rock. Previous habitat suitability studies for Green Salamanders have focused on identifying landscape features of rock outcrop locations that are presumed to influence the physiology of a species (Bruce 1968; Hafer and Sweeny 1993; Newman et al. 2018). Past studies have identified landscape characteristics associated with maintaining stable temperature and moisture as important for the species. For example, south-facing aspect and low elevation were found to be influential factors in both presence and abundance of Green Salamanders (Bruce 1968; Newman 2018). On a third-order microhabitat scale (i.e., rock crevices), resource preferences for Green Salamanders are thought to include features maintaining stable climates; thus, deep and narrow crevices with high humidity are commonly reported predictors of abundance for Green Salamanders (Gordon and Smith 1949; Rosell et al. 2009; Smith et al. 2017).

The current literature on habitat preferences of Green Salamanders has neglected the importance of connectivity within a habitat (specifically, within a rock outcrop). As a lungless salamander relying on cutaneous respiration, the metabolic capacity and oxygen consumption of Green Salamanders are limited to 20–40% of what a lunged salamander can sustain (Full 1986; Full et al. 1988). Additionally, the surface activity of plethodontid salamanders, including Green Salamanders, is largely limited to nights with either high humidity or rainy conditions (Feder 1983; Keen 1984). These limitations on movement directly affect salamander behaviors, including hunting capabilities, evading predators, and searching for mates. Because of this, we predict within-habitat connectivity for lungless salamanders to be central for survival. We hypothesized increased within-habitat connectivity would increase the probability of Green Salamander presence, and features related to connectivity would rank among the most influential for Green Salamander occupancy. Specifically, we predicted the likelihood of finding a Green Salamander would increase with crevice density and decrease as the distance to the nearest crevice and nearest tree increased. We also predicted Green Salamander presence would decrease as crevice width and depth increases, and increase with higher canopy cover because these features may contribute to stabilizing the microclimate of the rock crevices (Table 2.1, Column 1).

2. Methods

2.1 Study site

We surveyed microhabitat (rock crevice) feature composition across five sites from July 2018 through July 2019. We completed a minimum of six surveys for each site throughout the year, with no surveys conducted in the winter season. Each site was known to be occupied by Green Salamanders in the past, as they were identified from historical records. Surveys occurred

across Oconee, Pickens, and Greenville counties, South Carolina, USA, between 0900–2000. Sites varied in size from 136–1,792 m² (mean = 828 ± 759 m²) and were in state parks, protected land owned by the South Carolina Department of Natural Resources, and private land. One site was directly parallel to a major roadway, and one site was adjacent to powerlines. All sites were within hardwood and pine forests, with species of Great Laurel (*Rhododendron maximum*) and Mountain Laurel (*Kalmia latifolia*) common in the understory.

2.2 Field Methods

At every site, we laid a field tape across the long axis of the outcrop. Along every 5 m of this axis, we generated a random number to determine where a perpendicular transect would be placed (Figure 2.1). We assessed every crevice that the perpendicular transect crossed for crevice depth (cm), width (cm), length (cm), canopy cover (%), distance from the nearest tree (m), distance from the nearest crevice (cm), and crevice density within a 1 m² area (Figure 2.2). We measured percentage canopy cover using a spherical crown densiometer (Forestry Suppliers Inc., Jackson, Mississippi, USA). We defined crevice length as the distance from one end of the crevice opening to the other and we measured the width at the widest part of the crevice. We were unable to measure depth past 40 cm because most crevices are angled sharply beyond this distance. While assessing the microhabitat features, we actively searched for Green Salamanders in each crevice along each transect. When we found a salamander, we recorded the microhabitat feature data where we located the individual. We categorized crevices as used if a salamander was present or unused if no salamander was present. Instances of false unused categorizations may have occurred in deep (> 40 cm, n = 12 crevices) or jagged crevices where the entirety of the crevice was unable to be observed.

2.3 Statistics

We fit a binomial Generalized Linear Mixed Model using the `glmer` function in the `lme4` package in R (R Core Team 2018) to conduct an exploratory analysis. This analysis allowed us to identify the significant microhabitat features associated with salamander presence. We tested crevice depth, width, length, canopy cover, distance from the nearest tree, distance from the nearest crevice, and crevice density for multicollinearity (correlation assigned at $|r| > 0.70$) before being added into the global model. We also performed a Multivariate Analysis of Variance (MANOVA) to determine if any of the crevice features varied by site. We centered all predictor variables to a mean of 0 and scaled them to 1 standard deviation prior to analysis. We used coefficient estimates to calculate odds ratios (95% Confidence Intervals) for the significant variables included in the global model.

3. Results

We surveyed 426 crevices across five sites. We found salamanders occupying 116 of these crevices, and the remaining 310 were classified as available but unoccupied habitat (Table 2.2). A collinearity test showed no combination of any two variables was strongly correlated (all r among all pairwise tests < 0.60), and a MANOVA showed crevice morphologies varied by site ($F = 11.646$, $df = 5$, $P < 0.001$; Table 2.3), so we included site as a random effect in the Generalized Linear Mixed Model to account for the shared variance between crevice features within the same rock outcrop.

Crevice width, canopy cover, and crevice density were significant features in predicting salamander presence (Table 2.1; Figures 2.3 and 2.4). Crevice width was negatively associated with the probability of salamander presence. The average crevice width of the occupied crevices was 1.4 cm (± 1.6 SE). The probability of presence increased with canopy cover and crevice density. The average canopy coverage for occupied crevices was 99% (± 4.4 SE). The average

crevice density surrounding occupied crevices was 8.0 crevices per m² (\pm 4.9 SE). Our data show an overall increase in the predicted probability of salamander presence as crevice density increases, and at a density of more than seven crevices per m², the rate of change in the probability of a Green Salamander being present increases by approximately 7% with every additional 2.56 crevices.

4. Discussion

As we predicted, the probability of finding a Green Salamander in a crevice decreased with an increase in crevice width, and the probability increased in crevices with increasing canopy cover, and with an increase in crevice density. Narrow-width crevices and a high canopy cover are often considered necessary components of habitat for Green Salamanders (Bruce 1968; Smith et al. 2017), presumably because these features minimize water loss. Canopy cover shades crevices and thereby prevents large temperature fluctuations from change in sunlight intensity. Furthermore, narrow crevices likely maintain a moist environment that aids in cutaneous respiration. Although high canopy cover promotes site-level occupancy (Smith et al. 2017), our results show the importance of canopy cover at individual crevices. The average percentage of canopy cover above unoccupied crevices was 95%, and the average coverage over occupied crevices was 99%. This distinction illustrates that near-complete shade is an important microhabitat feature for crevice use by Green Salamanders.

Crevice depth as a predictor for the presence of Green Salamanders has had mixed results in the past, being highly ranked as a predictor of salamander occupancy by Smith et al. (2017), but not significant by Rossell et al. (2009). Our results complement the latter, but the possibility of false absences of salamanders in deep crevices increases because of the difficulty of seeing past 40 cm and around angles within a crevice. Crevice density has a positive correlation with

the probability of presence of Green Salamanders and is one of the three features (crevice density, distance to nearest crevice, and distance to nearest tree) we tested related to within-site connectivity. Of these connectivity-related features, high crevice density indicates multidirectional connectivity and a potential increase in nearby suitable microhabitats. In contrast, distance to nearest crevice and distance to nearest tree measures a linear connection between only two potential microhabitats. A high density of crevices within a square meter provides a network of potentially suitable microhabitats and reduces the cost of movement between crevices. Our data show a positive relationship between use and crevice density, and there is an increase in slope beyond approximately seven crevices per m². This threshold could offer a tool for managers evaluating site-level suitability. Having high crevice density within a habitat is important because Green Salamanders are lungless and are, therefore, unable to sustain long continuous movements (Full et al. 1988). Higher densities of suitable habitat also allow for more efficient foraging, predation evasion, and mate searching (Abrahams and Dill 1989; Pitt 1999; Stephens 2008).

Our results also indicate that aspects of within-site features are essential in determining site-level suitability for Green Salamanders. Canopy cover and all within-site connectivity features (crevice density, distance to nearest crevice, and distance to nearest tree) vary significantly between sites. Understanding within-site features that are important for habitat selection is equally pragmatic for conservation management as identifying site-level features. Habitat suitability has often been described as a function of aggregate features (i.e., temperature, humidity, nutrient levels, hydroperiod, etc.; e.g., Newman et al. 2018); however, for smaller organisms, considering small-scale, patchy resources may be equally helpful when determining the suitability of potential habitat (Gade and Peterman 2019). For example, Bog Turtles

Glyptemys muhlenbergii) require not only a hydrologically suitable wetland, but hummocks for nesting within the site (Zappalorti et al. 2015), and Hairy Woodpeckers (*Picoides villosus*) are cavity-nesters that select habitat based on snag density (Zarnowitz and Manuwal 1985). For Green Salamanders, conservation management practices should not only focus on macrohabitat features (e.g., rock outcrop size, aspect, and elevation), but also the microhabitat features associated with refugia, nesting, and foraging. Based on our results, we propose management priorities should be given to Green Salamander habitats with thinner crevice widths (< 3 cm), very high canopy cover at sites (> 95%), and sites with high crevice density (at least seven crevices per m²). If rock outcrops that meet the landscape level features preferred by Green Salamanders do not also contain these within-site features, it is possible the outcrop as a whole may not be suitable for the species.

We encourage future research on species inhabiting discrete patches to evaluate microhabitat features that could shed light on species behavior and site-level selection. Variations in microhabitat composition between sites could indicate discrepancies in site-level habitat suitability and the resulting population abundances across sites. Explicitly evaluating how the selection of microhabitat components (third-order habitat selection) influences population persistence and population growth within selected sites (second-order habitat selection) will likely benefit the conservation of patchily distributed species and identifying the threshold of microhabitat features required for an overall site to be suitable could guide how sites are prioritized within broader wildlife management efforts.

CHAPTER THREE

EVALUATING MARK-RECAPTURE AND REPEATED COUNT APPROACHES WHEN SETTING A RELIABLE BENCHMARK FOR A NEAR-THREATENED SPECIES

Abstract.—Estimating population abundances is a cornerstone to population monitoring practices. Obtaining accurate population size estimates can help conservationists track past demographic patterns and predict future trajectories. In this study, we sought to provide the first site-specific population estimates for green salamanders (*Aneides aeneus*), a species experiencing population declines across its range. We concurrently implemented two methods of estimating abundances, a capture-mark-recapture (CMR) approach and an unmarked repeated count approach (N-mixture modeling). We surveyed twenty-one green salamander populations across upstate South Carolina. We implemented a two-tiered survey design to analyze the data in a robust framework that accounted for open and closed population assumptions. We had 219 green salamander captures and 584 observations from 2019–2021. Our top CMR model included a null capture probability ($p=0.105$) and site-specific survival probabilities. Survival estimates ranged from 0.83–1.00 (average= 0.93 ± 0.04 SE). CMR seasonal average abundance estimates ranged from 3–32 individuals across sites. Site size had a weak but positive relationship with the CMR abundance estimates ($R=0.31$, $p=0.22$). The top N-mixture model defined detection probability as a function of temperature (0.14–0.30), availability probability as a function of the primary survey period, and abundance as a function site size and the total number of crevices at a site. Site-specific abundance estimates from the top N-mixture model ranged from 10–51 green salamanders (average= 20.66 ± 2.72 SE) across the entire three-year period. Results illustrate two temporally different abundance estimates from our CMR and N-mixture model approaches. We encourage future studies to continue population monitoring efforts for this species to better

inform conservation management plans for this species, and we advise the survey design implemented be based on the temporal scale of interest. Further, we suggest if a CMR approach is being implemented, researchers should consider simultaneously collecting repeat count data as well, as it is logistically cheap to implement concurrently.

1. Introduction

Accurately estimating population sizes is a crucial when evaluating the conservation status of a species and monitoring demographic trajectories. Anthropogenic changes to environments have caused many species to suffer population declines, with some already driven to extinction and many facing it (Hughes et al. 1997, Ehrlich and Pringle 2008). With the increasing severity of threats to species persistence coupled with the growing list of species declining in population, the need to monitor population statuses is evident. Some species are not monitored unless declines are already reported, therefore, population trend data are scarce, and knowing the population status with certainty is difficult from the start (Bonebrake et al. 2010).

Population research tends to be examined in the short-term and lack continuous monitoring programs (Bonebrake et al. 2010). Often, assessments of species persistence probability are based on temporally fragmented population estimates and subsequent conservation practices can be subject to a shifting baseline syndrome (Pauly 1995, Soga and Gaston 2018). A concatenation of long-term and reliable population status data will help aid and promote conservation efforts by identifying population fluctuations that are distinct from human-caused declines. Amphibian species are of particular concern for population monitoring practices. There is a notable dearth of demographic and life history information available across all amphibian species, where we have published information on only 0.2% of the 1,714 threatened amphibian species, and a striking 88% of all amphibian species have no information

(Conde et al. 2019). Many amphibians are limited to strict abiotic requirements because of their physiological makeup, making them susceptible to environmental disturbances, and global amphibian populations are declining at an accelerated and unprecedented rate due to anthropogenic influences (Hopkins 2007).

The green salamander (*Aneides aeneus*) is listed as “Near-threatened with decreasing populations” by the IUCN Red List, “Vulnerable” by NatureServe, and ranked as “Critically imperiled” by the South Carolina Department of Natural Resources. Green salamanders are a fully terrestrial species that inhabit rock outcrops embedded in mountainous forested landscapes. Existing in discrete rock outcrops ensures reliable population boundaries that are useful for population parameter analyses and conservation management approaches. In the mid-1970’s there was evidence of a green salamander population collapse within the Blue Ridge Escarpment (BRE; Figure 3.1). This collapse was noted from accumulating historic records, not active surveys (Snyder 1991). After this finding, researchers began count surveys for populations within the BRE. These surveys consisted of unpublished raw count data (see Corser, 2001) or examined the environmental variables that affect spatial variation in green salamander abundances (Newman et al. 2018). To date, there have been no site-specific abundance estimates published for this species of conservation concern.

Unfortunately, in many cases, detecting the individuals of the species of interest is a challenging task, and imperfect detection probabilities can lead to biased abundance estimations (Royle and Nichols 2003, Royle et al. 2005). Many field and statistical approaches have surfaced to expand our understanding of populations from raw count data to estimated abundances while accounting for the probability that the surveyors detect individuals that are present. Advancements in population abundance estimation methods include double observer, removal,

unmarked N-mixture, and modifications to capture-mark-recapture methods (Powell and Gale 2015).

A capture-mark-recapture (CMR) design incorporates the *in-situ* capture and marking of animals for the purpose of individually identifying them (via visual implant elastomers, collars, ear tags, photographs, etc.), and immediate release back into the habitat. The subsequent surveys can then identify individuals that are recaptured or newly captured. These capture histories help to inform the probability of detecting individuals during a survey period, and this detection probability along with the frequency of marked, or previously identified, individuals in future surveys is used to estimate abundance (Jolly 1965, Pollock 1982). These methods have been used to produce reliable abundance estimates of long-term surveys but are labor and time intensive and are only suitable when species can be reliably captured and marked. When individual identification or marking is unreliable, unmarked studies utilizing N-mixture models offer an alternative via count data. With an unmarked approach, the number of individuals detected in a sampling unit (e.g., a discrete site, small plots, along transects) is counted, and each sampling unit has repeated visits. Counts from repeated visits are used to estimate detection probability of individuals, which is in turn used to estimate population abundance (Royle 2004, Dail and Madsen 2011). N-mixture models have been growing in popularity in recent years because they do not require animal manipulation, are less costly in survey time and effort, and can be used for species difficult to mark or individually identify. N-mixture models, however, have been criticized for potential information loss from not incorporating information from individual animals encountered more than once during subsequent surveys, the models require the inclusion of multiple sites whereas CMR studies can be performed on one site, and N-mixture models are

more sensitive to violating model assumptions than CMR models (Barker et al. 2018, Duarte et al. 2018, Link et al. 2018).

Choosing a marked or unmarked approach for estimating population parameters is dependent on the biologist' time, funding, and the nature of the species being studied. While Barker et al. (2018) expressed hesitation for using N-mixture models because of the loss of information caused by uncontrolled variation in detection probabilities, many others have reported strong parallels between N-mixture and CMR abundance estimates (Courtois et al. 2016, Ficetola et al. 2018, Costa et al. 2020). For this study, we implemented both a marked and unmarked study design to estimate abundances across 21 discrete green salamander populations because the unique fingerprint-like dorsal patterning allowed for a reliable and non-invasive means of “marking” individuals for the CMR approach. By applying two common methods of estimating population abundances to multiple green salamander populations, we aimed to (1) identify which method is logistically feasible for the species; (2) provide the first published estimates of abundances across several green salamander populations within the BRE that can be used for repeatable benchmarks in future population monitoring efforts. We define a benchmark as an estimate corresponding to a given site at a given time, and within this context, subsequent benchmarks will illuminate population size trends over time. Within this second objective, we predicted abundance estimates would increase with landscape features known to be related to green salamander presence: larger rock outcrop sizes, low elevations, south-facing sites, and high crevice densities (Bruce 1968, Smith et al. 2008, 2017, Newman et al. 2018, Novak and Barrett 2023).

2. Methods

2.1 Survey methods and data collection

2.1.1 Study area

We surveyed 21 discrete green salamander populations (i.e., rock outcrops) in South Carolina within the Blue Ridge Escarpment (BRE) of the larger species range. Sites were chosen based on verified occupancy of green salamanders in the past (Newman et al. 2018). Exact locations of these sites will not be specified but have been submitted to the South Carolina Department of Natural Resources. Endemic flora include oak and mixed oak-pine forests with great laurel (*Rhododendron maximum*) and mountain laurel (*Kalmia latifolia*) common in the understory. Outcrops were comprised of granitic or sandstone rocks ranging from 12–1,252 m². Adjacent outcrops were considered separate sites if they were separated by at least 50 m, which is half the longest distance recorded for a green salamander (106 m; Gordon, 1961; Smith and Green, 2005), and more than twice as long than the average dispersal distance of green salamanders across studies (average distance dispersed = 18.14 m; Gordon, 1961, 1952; Williams and Gordon, 1961). Elevations of the sites extended from 361–865 m and aspects ranged from 100–306°.

2.1.2 A robust survey design

We surveyed 21 sites from 2019 through 2021 using both a marked (CMR) and unmarked (N-mixture model) design. For both data collection approaches, our sampling schematic followed a robust design that uses two levels of sampling, primary (K) and secondary (k) periods (Figure 3.2). Primary sampling periods are assumed to function in an open population where births, deaths, immigration, and emigration can occur between primary periods. Our survey efforts were designed with short intervals between primary periods (e.g., days rather than weeks or months) because we surveyed populations year-round, so the assumption of open populations is interpreted as intervals between the midpoints of the primary periods. Secondary

sampling periods are nested within K and are sampled closer together in time so that a closed population can be reasonably assumed (i.e., births, deaths, immigration, and emigration area assumed to not occur between secondary sampling periods). We established primary sampling periods based on warm and cool months of the year. We determined delineations between warm and cool post hoc as sampling days that achieved temperatures higher (warm period) or lower (cool period) than the annual average. Occupancy patterns of green salamanders in rock outcrops have been shown to oscillate along this pattern, being less abundant within rock outcrops in the warmer seasons and present within outcrops in the cooler seasons (Gordon 1952, Waldron and Humphries 2005).

2.1.3 Capture-mark-recapture data collection

A minimum of two surveyors actively and independently searched for green salamanders in rock outcrop crevices during each secondary population survey (k). We attempted to remove all green salamanders we detected in crevices and, if successful, we placed the individual into a Ziplock bag. We assigned each salamander an identification number and photographed the individuals that were successfully removed from the crevices. We took photographs of the unique green patterns from the dorsal view of the salamander to “mark” individuals for the CMR analysis. We returned salamanders to the location of extraction once the photographs were collected.

We used the free software Interactive Individual Identification System (I³S Pattern ver. 4.02) for photo-identification of every salamander that was successfully removed from a rock crevice and photographed (i.e., captured; download at <http://www.reijns.com/i3s/index.html>; Sannolo et al., 2016; Van Tienhoven et al., 2007). We identified reference points in the dorsal pattern once the photographs were uploaded into the application (Figure 3.3), and the output

results included a ranked list of every photo uploaded that the program identified as a potential match (i.e., recaptured individual). The software produced all potential matches, regardless of the site of origin. This allowed us to identify any individuals migrating from one study site to another. We manually compared the photograph of interest to all photos in the ranked list output by I³S to make our final determination of whether an individual salamander was a new capture or recaptured animal.

2.1.4 N-mixture model data collection

We collected unmarked count data simultaneously with the marked data. A single survey occasion consisted of a minimum of two surveyors actively and independently searching for green salamanders. After the survey, we identified the number and locations of each salamander found to provide the total number of salamanders found at each site per visit. After this total count was recorded, we removed, photographed, and returned all salamanders found in compliance with our CMR method.

2.1.5 Habitat and landscape data collection

We collected habitat data for each green salamander population that included rock outcrop size (m²), elevation (m), aspect (degrees), and the average total number of crevices per site. We used a tally counter to count every crevice inspected each survey day across the entirety of the three-year study. We averaged those counts to obtain the average total number of crevices available at each of our 21 sites. We also collected temperature (°C) and relative humidity (%) data at each visit. All surveys took place between 08:00–20:00 hrs. Time of day was not included as a detection covariate in the study, since most of the surveys took place during the day, and surveys after sunset were rare and typically only occurred when we were processing a large number of individuals for CMR analysis.

There was not enough variation in the time of our surveys to include a diurnal (e.g., day/night) covariate. All surveys took place between 0800–2000 hrs.

2.2 *Data analysis*

2.2.1 Capture-mark-recapture data analysis

We used the results of the photo-identification across all sampling occasions (five primary periods with two to six secondary samples each) to construct capture histories for each individual salamander at 18 of the 21 populations, because three of the 21 populations did not elicit any salamander captures. Secondary sampling events ranged from two to six survey days per primary period based on logistic restraints and site access limitation as a result of the COVID-19 pandemic quarantine. We did not include individuals that were unable to be removed from the crevices because they were not photographed (i.e., marked).

We implemented the capture history data into a robust design framework using package ‘MARK’ in R (Laake 2013, R Core Team 2021). The robust design allows for the estimation of key parameters in population dynamics including population abundance, survival rate, and temporary emigration by analyzing the capture histories of all animals across the study period. Within a robust design, individual salamanders within sampling units (rock outcrops) are assumed to exist as “super-populations.” Super-populations are larger than the subset of the population that is available for encounter (Bailey et al. 2004). For example, green salamanders are available for encounter if they are visible in rock crevices or on the rock face, but are unavailable for encounter if they are deep in the rock crevices or in adjacent arboreal habitats that are not surveyed or detected (Figure 3.4). All salamanders present within a rock outcrop, available for encounter or not, are a part of the super-population. Movement within the super-population and between areas where animals are available or unavailable for capture are

described by γ . Specifically, γ' represents the probability that animals that are a part of the super-population but unavailable for capture at primary period K remain unavailable for capture in the next primary sampling period, $K+1$. In contrast, γ'' represents the probability that animals available for capture in primary period K move into an area where they are unavailable for capture in the next primary sampling period, $K+1$.

We fit our capture history data to a stepwise series of models. We first tested movement models. We then implemented the best fit movement parameter to a series of detection probability models. The top ranked detection covariate was then incorporated into numerous abundance models. We used Akaike's Information Criterion (AIC_C) to identify model rankings at each step. We outline the parameter models in more detail below.

We fit the green salamander CMR data to a series of three temporary movement (i.e., temporary emigration) models to determine whether no movement, random movement, or Markovian movement was best represented (Kendall et al. 1997, Powell and Gale 2015). The no movement (null) model describes a population where all individuals are available for capture at each primary period, and no individuals are outside the bounds of being encountered ($\gamma' = \gamma'' = 0$). Random movement describes the probability of an individual animal being in the sampled area within a primary period as equal for animals that were and were not in the sampled area in the previous sampling period, $K-1$ ($\gamma' = \gamma''$). Markovian movement defines the probability that an animal is available or unavailable during primary period K as dependent on whether the animal was available or unavailable at time $K-1$. Within these three movement models, apparent capture probability, p , recapture probability, c , and survival, S , were assumed to remain constant (null). After identifying the top-ranked movement model, we implemented that movement parameter

into all subsequent models that included variations of capture probability, recapture probability, and survival covariates (Table 3.1).

In this CMR design, capture probability is the likelihood of detecting, successfully removing, and marking (photographing) individual salamanders. We included models with various capture probability covariates, p , to determine which best fit the data. Each model tested only included one capture probability covariate for simplicity and to reduce the number of parameters in each model. The capture probability covariates tested included “site,” “removal difficulty,” “layout,” “primary period,” and “secondary period.” Logically, “site” as a covariate tested if capture probability was site-specific. “Removal difficulty” was a covariate that defined the probability of capture as a function of a categorical capture difficulty of three levels: easy, medium, and hard. These difficulty rankings were assigned prior to the analysis based on how many salamanders were successfully removed from the rock crevices relative to the total number of salamanders observed at that site. “Layout” was a binomial covariate incorporating individual sites that were classified as being either comprised of a single rock outcrop (0), or numerous rocks adjacent to each other (1). “Primary period” and “secondary period” were two covariates that defined capture probability as being a function of the primary and secondary period the sampling effort took place in, respectively. In other words, within the “primary period” and “secondary period” covariates, capture probability was allowed to differ across those sampling periods, but not within them.

We also tested various covariates for survival, again with each model incorporating only one survival covariate for simplicity and to reduce the number of parameters involved. Covariates included for survival included: “site,” “cover,” and “layout.” Logically, “site” defined survival as site-dependent. “Cover” was a binomial covariate that categorized sites as either open

(0) or wooded (1) based on the presence of tree canopy cover. Sites that were adjacent to roadways or had substantial tree falls were categorized as ‘open’ coverage. “Layout” as a survival covariate had the same definition as the capture probability covariate.

The package ‘MARK’ outputs estimated abundances for each of the primary sampling periods K at each site j as the quotient between the number of individuals caught at least once in primary period, n_{Kj} , and the probability of being caught at least once in the primary period, \hat{p}^* (Equation 1, Equation 2).

$$\hat{N}_{Kj} = \frac{n_{Kj}}{\hat{p}_{Kj}^*} \quad (1)$$

$$\hat{p}_{Kj}^* = 1 - (1 - p_j)^k \quad (2)$$

Where p represents the probability of being detected during a secondary period. We removed primary periods with an abundance estimate of zero because these resulted from no salamander captures during those primary periods and they are unlikely to be representative of stochastic population crashes. We also removed primary periods that provided abundance estimate standard errors that were larger than the estimate itself. We averaged the remaining primary period estimates to estimate the site-specific abundances.

We performed post-hoc Kendall’s Tau correlation analyses to identify the relationships between site features (elevation, aspect, size, and the total number of crevices) and the estimated population abundances. Weather conditions (temperature and relative humidity) were not included in the marked analysis because they varied at each secondary survey, and we did not expect abundance to change day-to-day because of extreme weather.

2.2.2 N-mixture model data analysis

N-mixture models leverage a “mixture” or combination of a binomial distribution and a Poisson distribution to estimate abundance. The binomially distributed portion of the likelihood statement defines the probability of detecting an observed count of animals (y_{jk}) at site j during

visit k , given a population size of N_j animals and a detection rate of p . The Poisson portion describes the probability that there are N_j number of animals at site j , given that the mean abundance across all sites being studied is λ (Equation 3; Powell and Gale, 2015; Royle, 2004).

$$p(y_{jk}|\lambda, p_{jk}, N_j) = \prod_{j=1}^R (\prod_{i=1}^S \text{Bin}(y_{jk}|N_i, p_{jk}) \text{Pois}(N_j|\lambda)) \quad (3)$$

The N-mixture model assumes (1) the binomial and Poisson distributions are good approximations of reality; (2) observers do not double-count any individuals within a survey; (3) the number of animals at one site is independent of the number of animals at another; (4) detection is constant across sites and secondary periods, unless modeled by covariates; (5) all N_j individuals at visit k have the same detection probability, p_{jk} .

We used package ‘unmarked’ in R (Fiske and Chandler 2011) to fit the model of Chandler et al. (2011) to our repeated count. The model used was a generalization of the N-mixture models provided by Royle (2004) but expanded to accommodate temporary emigration ($1 - \phi$) across primary sampling periods. The likelihood of the population abundance λ , probability of availability for capture ϕ , and the probability of being detected p , given the count data y_{jk} provided from site j at time k is expressed in Equation 4 for three site visits:

$$L(\lambda, \phi, p|y_{jk}) = \prod_{j=1}^R \left\{ \sum_{j=\max(y_{jk})}^{\infty} \left(\frac{M_j!}{y_{j1}! y_{j2}! y_{j3}! y_{jk0}!} \right) \times (\phi\pi_1)^{y_{j1}} (\phi\pi_2)^{y_{j2}} (\phi\pi_3)^{y_{j3}} (\phi\pi_0)^{M_j - y_{j\cdot}} \right\} f(M_j|\lambda) \quad (4)$$

where R is the total number of sampling units (i.e., rock outcrops), M_j is the superpopulation size (i.e., latent number of salamanders present at a rock outcrop j), and π is the vector of multinomial cell probabilities estimated from a function of the detection probability, p . This model has since been extended for binomial mixture models for repeated counts with function “gpcount” in R.

Within this extension, at any time t , only a fraction of the super-population (M_j) is available (Φ_{jk}), leading to estimated population sizes of N_{jk} .

We used the “unmarkedFrameGPC” function in R to construct the data frame for data collected in the two-tiered primary and secondary sampling design. This function distinguished abundance covariates (λ ; elevation, site size, slope, aspect, total number of crevices per site), availability covariates (ϕ ; primary period, thermal season), and detection covariates (p ; temperature, relative humidity, and the number of surveyors) across primary periods. Availability covariates describe what may influence whether green salamanders are available for capture, or within the super-population but unavailable for capture. We used “gpcount” function to fit the repeated count data to the model of Chandler et al. (2011). We employed a stepwise modeling approach similar to that of our CMR methods (Table 3.2). We tested data fit to a negative binomial and a Poisson distribution, but implemented all subsequent models independently to both distribution types regardless of which had the lowest AIC value as a precaution to the negative binomial mixture fitting the count data but providing unrealistic abundance estimates (Kéry et al. 2005, Joseph et al. 2009, Kéry 2018). We first built and compared detection models to identify which covariate(s) best fit the data. We then implemented that top-ranked detection covariate into each of three availability models. We incorporated primary period (a covariate with five levels, one corresponding with each primary sampling period), thermal season (a binomial covariate that categorized each primary period into either a warm or cool season), and a null availability model. We chose these temporal availability covariates because green salamander presence probabilities have been reported to oscillate temporally (Waldron and Humphries 2005). Lastly, we used the top ranked distribution and availability covariates in a series of abundance models to identify which site-level spatial

features influence population abundances. We included site size (m^2), aspect, elevation (m), slope ($^\circ$), the total number of crevices at a site, and site layout as abundance covariates in separate models. We converted each covariate to z-scores and used the “gpcount” function to fit the N-mixture models to the repeated count data. We used AIC to identify model rankings. After identifying the best fit abundance model, we used the “predict” function to calculate site-specific population sizes based on the top-ranked site covariates that best predicted the count data. This provided a single estimate of the total number of green salamanders within the super-population at each site across the entire three-year study period.

3. Results

We had 584 green salamander observations during $k_{total}=279$ secondary visits across 21 sites from 2019–2021 (range=0–17 individuals observed per site in each survey). We successfully removed and photographed 219 salamanders from rock crevices (i.e., capture). Fifty-eight salamanders of the 219 captured individuals were identified as recaptures (26%). Two of the 21 sites did not yield any salamander observations throughout the study period. One site generated one salamander capture with no subsequent recaptures or observations. Only one salamander was identified as immigrating between two sites (50 m).

3.1 CMR analysis

Any sites with too few recaptures that caused capture probability $\hat{p} < 0.001$ were removed post-hoc and all marked analysis models were run again without them, providing results on 12 of the 21 sites. The null movement model (i.e., no temporary emigration outside the study system) was ranked as the best fit ($AIC_C=1084.01$, $w=0.626$) among the three movements tested. Random movement (i.e., the probability of an animal being in the sampled area within a primary period is equal for animals that were and were not in the area in the previous sampling period, K -

I) was a competitive second model ($\Delta\text{AIC}=1.39$, $w=0.293$). Both movement parameterizations (null and random) were individually incorporated in all subsequent models, but not simultaneously.

Of all tested, the model incorporating null movement, a null capture probability, and site-specific survival probabilities was ranked highest ($\text{AIC}_C=1065.67$, $w=0.23$, Table 3.3). The second-ranked model included null movement, capture probability as a function of site, and survival as a function of the rock layout ($\Delta\text{AIC}=1.21$, $w=0.13$). The third-ranked model was defined by random movement, capture probability as a function of site, and survival as a function of rock layout ($\Delta\text{AIC}=1.85$, $w=0.09$).

Within the top model, the estimated likelihood of detecting and capturing salamanders (p) was 10.5% across all sampling periods and all sites. Site-specific survival probabilities across primary periods ranged from 0.83 – 1.00 with an average of 0.93 (± 0.04 SE; Table 3.4). These survival estimates pertained to the time between the mid-points of each primary period (approximately 6 weeks). Population abundance estimates ranged from 3 – 32 salamanders across the analyzed sites with an average of 15.86 (± 6.11 SE; Figure 3.6). More detailed results on the covariate estimates of the second- and third-ranked models can be found in the supplemental material (Appendix S1, S2, S3).

No correlation coefficients between site covariates exceeded $r=|0.70|$. The highest correlation between site covariates was between site size and the total number of crevices ($r=0.51$). Kendall's Tau correlations indicate the average estimated abundance of the twelve green salamander populations had a weakly positive trend with site size ($R=0.31$, $p=0.22$). There was no evidence of correlations between estimated population abundance and the total number of crevices ($R=0.09$, $p=0.76$), aspect ($R=-0.07$, $p=0.75$), or elevation ($R=0.02$, $p=1.00$; Figure 3.5).

3.2 *N*-mixture models

No correlation coefficients between detection covariates exceeded $r=|0.70|$. The highest correlations between detection covariates were between day of year and humidity ($r=0.31$), and day of year and temperature ($r=0.27$). While these correlations are low, we removed day of year from the *N*-mixture models because we felt humidity and temperature were more explanatory variables than day of year.

During initial model fitting, the single-parameter negative binomial distribution fit the count data better than the Poisson; however, we continued to fit all models separately to both distributions. After all models were built and compared, the top negative binomially distributed model produced a few unreasonably high population abundances (range 7–95 salamanders; see Appendix S4). Previous studies found negative binomial mixtures provide unidentifiable models and produce inflated abundance estimates (Dennis et al. 2015, Kéry 2018). Therefore, we subsequently fit all detection models using a Poisson distribution. Among these models, two had the most support with a cumulative weight of 0.98. These two models defined detection probability, p , as a function of temperature ($\Delta\text{AIC}=0$), and an additive function between temperature and humidity ($\Delta\text{AIC}=1.97$). The number of surveyors present was not shown to be a useful predictor of green salamander detection ($\Delta\text{AIC}=6.75$). Detection probability coefficients of the top ranked model demonstrated a slightly negative relationship with temperature, with probabilities ranging from 0.14–0.30 with an average of 0.19 (± 0.0001 SE) across sites and all secondary periods. Availability models were fit using temperature as the covariate for our detection parameter, and the top model defined the probability of green salamander availability within the study area as a function of the primary period the surveys occurred in, with Period 1 having the highest probability (Table 3.5). Probability of availability was constant across sites

within a primary period. Abundance models were fit last and the top model incorporated detection probability as a function of temperature, availability probability as a function of primary period, and abundance as an additive function of site size and the total number of crevices present at a site (Table 3.6). Site-specific abundance estimates from this top N-mixture model ranged from 10–51 green salamanders with an average of 20.66 across sites (± 2.72 SE; Figure 3.6). These estimates represent the number of green salamanders in the super-population of each site across the three-year study period.

4. Discussion

Although green salamanders are a species of conservation concern, no published studies have performed population-level abundance analyses. Our results represent the first record of site-specific abundance estimates using both a marked (CMR) and unmarked (N-mixture modeling) approach from three-year survey efforts.

4.1 Survival probability, S

Survival estimates can distinguish spatial and temporal vulnerabilities for a species and provide insight for conservation management. We estimated the probability of survival between primary periods using only the capture-mark-recapture (CMR) method because confirmed recaptured individuals in subsequent sampling periods are helpful to inform a survival parameter. With two-tiered survey designs, gaps in time are allowed between primary periods during which an open population can be reasonably assumed; however, because we sampled year-round, we did not have long periods of time between our primary sampling periods. Therefore, our survival probability estimates should be interpreted as the likelihood of surviving between the mid-point of one primary period to the next. Interestingly, neither covariate describing specific patch characteristics (i.e., the spatial layout of the sites or the cover type) explained more of the

variation in the survival probabilities than the site-specific covariate. The 1.5 monthly survival estimates ranged from 83% to 100% across our sites. Spatial layout of the sites (i.e., the site was comprised of either a single rock or numerous rocks adjacent to one another) was the best descriptor for survival in the second and third top models (Appendix S1, S2). When considering all three top models, there is evidence that spatial variation within (layout) and across (site-specific) our populations influence the survival probabilities of green salamanders.

4.2 Detection probability, p

Detection probability is an integral aspect of the estimation of population abundances that refine the estimates by accounting for imperfect detection. It is seldom the case that animals are conspicuous enough to be detected at a near perfect rate during each population survey. Without accounting for imperfect detection, it is difficult to determine if variations in count data are representative of stochastic events or changes in detection probability throughout the study. The detection probability of our top CMR model was low (0.105). Our CMR detection probability was fit as a null parameter, defining detection as constant across all sites and survey periods. Models that included temporal variation in detection probability (among both primary and secondary survey periods) did not rank highly, indicating little evidence of temporal variation in the surveyors' ability to detect green salamanders throughout the study period.

The detection probabilities estimated using the unmarked N-mixture model ranged from ($p=0.14-0.30$) and were estimated as function of temperature, providing a different detection probability for each secondary survey period. Unsurprisingly, these were higher than our CMR estimate; CMR detection probabilities incorporate detecting and successfully capturing unique individuals (i.e., removing the salamander from the crevice and photographing the individual), whereas detection probabilities from count data only incorporate detecting a green salamander.

Our N-mixture model detection parameter had a negative relationship with temperature, indicating surveyors were more likely to detect a green salamander on secondary survey days that were cooler as opposed to the warmer.

4.3 Temporary emigration γ , and availability probability, ϕ

The null model movement model best explained temporary emigration in our CMR analyses. This indicated that our CMR data were best described when salamanders were always assumed to be available for capture within the super-population at each sampling period. Similarly, individuals that were unavailable for capture remained unavailable over all sampling periods.

Salamander availability was fit as a function of primary period (i.e., a covariate of five levels for each primary sampling period) within our unmarked N-mixture modeling results. This indicated that each primary period had a different estimate of probability of salamander availability held constant across all sites. Interestingly, while temperature showed a negative relationship with detection probability in our N-mixture model, thermal season (i.e., binomial variable of “cool” or “warm” that varied across primary periods) did not show evidence of influencing salamander availability for capture within the super-population. Salamander availability was highest in the first warm season of our five total seasons (Figure 3.2). We retained primary survey period as the availability coefficient in our N-mixture models because it had more support than the model where availability was equal across primary periods; however, there seems to be a source of variation explaining this heterogeneity in availability probability that we did not capture in the covariate data collected throughout the study.

4.4 Abundance covariates

In our CMR study, there was no evidence of correlations between the estimated population abundances and the site-level features measured, with the exception of a weakly positive trend with site size. The weak fit of the data to the regression models are perhaps unsurprising given our low number of sites in this analysis and the range of aspects, elevations, and sizes surveyed within those twelve sites. Recall we filtered out sites that had too few recaptures which biased our detection probabilities to be low enough to over-inflate abundance estimates. This limited the analysis to twelve sites. The sites that were applicable to the CMR analysis had an elevation range of 360–640 m, and an aspect range of 129–224 degrees (southeast–southwest). These ranges are more limited than those of all sites (n=19) we had surveyed (elevation: 360–865 m; aspect: 30–306 degrees). The range of site sizes and total crevices was not comparably different between the twelve sites in the CMR analysis and all sites surveyed. Our robust N-mixture models, which incorporated count data from all nineteen sites, indicated both size and the total number of crevices at a site were positively correlated and informative when predicting green salamander abundances.

An effect of outcrop size is consistent with Newman et al. (2018) and the general ecological assumption that habitat size correlates positively with local animal abundances (but see Holt et al., 1997 and Krebs et al., 1969 Holt et al., 1997 and Krebs et al., 1969 Holt et al., 1997 and Krebs et al., 1969 Holt et al., 1997 and Krebs et al., 1969 Holt et al., 1997 and Krebs et al., 1969 Holt et al., 1997 and Krebs et al., 1969 for mechanisms explaining deviations from that pattern). A second predictor in estimating green salamander abundance is the total number of crevices available at a given site. Rock crevices function as the immediate green salamander habitat, and >99% of our salamander observations came from instances of finding them in the crevice fissures as opposed to on the rock face. It is important to note that rock outcrop size was not correlated with the averaged total

number of crevices available ($r=0.51$). The observation that rock outcrop size is decoupled from the number of crevices may have important implications for management decisions that prioritize sites based on perceived habitat availability. Novak and Barrett (2023) showed green salamander presence had a strong relationship with crevice density (number of crevices per m^2), where the probability of a salamander being present increased with an increased number of crevices present, likely because higher crevice densities are associated with increased multidirectional microhabitat connectivity within the rock outcrop. More crevices provide a network of potentially suitable refugia for green salamanders to inhabit, which we believe explains total crevice count appearing in both the CMR and N-mixture models.

4.5 Comparison of CMR and N-mixture model abundance estimates

The CMR and N-mixture analyses produced estimates at two temporally different scales. The CMR model provided site-specific abundances averaged across primary survey periods, each representing warm and cool seasons from 2019 through 2021. The N-mixture model estimated site-specific abundances across the three-year study period. When estimates from both analyses were plotted against each other, there was a weak fit with no notable evidence of association across sites (Figure 3.7). Seasonally averaged abundance estimates from our robust CMR analysis ranged from 3–32 individuals across twelve sites, with site-specific estimates generally being smaller than those of the N-mixture model estimates that ranged from 10–51 across nineteen sites throughout the entire study period.

Provided we estimated two temporally different abundance estimates with our CMR and N-mixture model approaches, we cannot definitively suggest one design over the other in regard to future monitoring efforts for green salamanders. The analysis chosen must be based on the temporal scale of interest. That said, it is worth mentioning that the passive crevice-dwelling

behavior of green salamanders within discrete rock outcrops that provided reliable population boundaries, coupled with the ability to noninvasively use photography as a means of marking individuals led us to believe green salamanders were a logistically ideal system to use a CMR study. Surprisingly, our exhaustive survey efforts across three years showed limited capture and recapture rates compared to count data obtained. Often, conservation managers do not have the time or data budget to conduct CMR studies and instead resort to N-mixture models as a viable alternative. However, if a CMR approach is applicable, field efforts will inevitably have instances of detections but failed captures. This lends itself to simultaneously implementing an unmarked design (e.g., N-mixture modeling) and offering an opportunity to evaluate population demographics across seasonal and yearly temporal scales.

Rather than persuading future studies from one study or the other, we suggest researchers consider the temporal resolution of the abundance estimates of interest. If a CMR design is in consideration, we urge the concurrent implementation of repeated count surveys as well, because the latter are not logistically costly when already performing a CMR analysis. We also urge the continuation of green salamander population monitoring on a more regular basis to continue to provide concrete biological indicators on population health. Though our results represent the first site-specific abundance estimates for this species of conservation concern, we recognize this study is a single component of a larger monitoring program. Retesting predictions is an important doctrine of science, and single analyses rarely provide definitive results that can adequately contribute to a meticulous assessment of a body of knowledge (Nichols et al. 2019). This is of utmost importance when viewed through the lens of animal conservation. Repeated monitoring efforts will help provide valuable insight on this, and many other, species of conservation concern.

CHAPTER FOUR

UNEXPECTED HIGH GENETIC RELATEDNESS ACROSS DISCRETE PATCHES OF A TERRESTRIAL SALAMANDER

Abstract.— Understanding the genetic structure of populations is a cornerstone of conservation biology that can elucidate evolutionary processes and their consequences. It is of particular importance to investigate the genetic structure within and connectivity between demes of species that are experiencing population declines to identify which populations that may be vulnerable to inbreeding depression. In this study, we evaluated the genetic structure of green salamander (*Aneides aeneus*) populations in upstate South Carolina. The green salamander is experiencing population declines along the species range and particularly within the Blue Ridge Escarpment (BRE), a disjunct population subset in the Southern Appalachians. Additionally, the green salamander presents an interesting demographic population structure as individuals inhabit discrete rock outcrops interspersed along the landscape in a naturally patchy distribution. We sampled tissues across seventeen green salamander populations in upstate South Carolina. We used restriction-site-associated DNA sequencing (RADSeq) and identified SNPs across individuals to estimate population statistics including F_{ST} , F_{IS} , H_O , H_S , and N_e , and used fastSTRUCTURE to detect fine-scale population patterns. Results indicated little to no genetic differentiation among the sampling sites (mean $F_{ST} = 0.06 \pm 0.008$) and no evidence of inbreeding (mean $F_{IS} = -0.05 \pm 0.036$). fastSTRUCTURE results showed all samples analyzed across the seventeen sites were best described as one genetic population, from which we infer rock outcrops do not effectively serve as discrete population boundaries. From a conservation perspective, the genetic structure among green salamander sites suggest dispersal between rock

outcrops is occurring more frequently than expected, and the evidence of isolation by distance indicates structural connectivity between outcrops should be maintained.

1. Introduction

Genetic diversity among populations offers insight into population structure, past biogeographic changes, and demographic or life history characteristics that contribute to genomic patterns (Rosenbaum et al. 2007, Murphy et al. 2018). Populations undergoing habitat loss and fragmentation are typically of conservation interest because population isolation increases susceptibility to genetic drift and reduced genetic variation from stochastic processes, threatening the long-term persistence of the population (Nguyen et al. 2022). For example, habitat fragmentation within formerly contiguous populations may create subpopulations and hinder gene flow via increased geographic distance and/or impermeable barriers in the newly altered landscape. Consequently, the subpopulations may exhibit a loss of genetic diversity and the concomitant decrease in heterozygosity and increase in the frequency of deleterious alleles. Small, isolated populations are also more prone to inbreeding and genetic drift (Lynch et al. 1995, Frankham 2005, Kawamura 2005, Hoffmann et al. 2017, Kazitsa et al. 2018), which can contribute to lowered resistance to diseases (Spielman et al. 2004, Pearman and Garner 2005), and increased susceptibility to population declines following environmental fluctuations (Jump et al. 2009). Therefore, evaluating population genetics and identifying extrinsic (e.g., landscape matrix, biogeographical events) and intrinsic (e.g., life history, population demography) factors influencing the genetic structure is essential for the conservation management for species of concern.

Global amphibian populations are declining at an unprecedented rate (Stuart et al. 2004, Hopkins 2007). The deluge of causes for this modern-day extinction crisis includes habitat loss

and fragmentation (Cushman 2006, Gallant et al. 2007), climate change (Carey & Alexander, 2003), competition with invasive species (Kats and Ferrer 2003, Falaschi et al. 2020), environmental pollution (Carey and Bryant 1995, Fasola et al. 2015), disease (Lips et al. 2006, Kilpatrick et al. 2010), and overharvesting (Warkentin et al. 2009, Pan et al. 2016). Many amphibians are notably vulnerable to these threats because of their limited habitat tolerances, and environmental or anthropogenic changes to these habitats often result in poor health within individuals and instability within populations (Beebee 2005, Becker et al. 2007, Fusco et al. 2020).

Among the threatened amphibian herpetofauna is the green salamander (*Aneides aeneus*). The green salamander is a fully terrestrial species that inhabits discrete rock outcrops embedded within a matrix of hardwood forests. Accumulated historic records of green salamander populations have provided evidence of an apparent population collapse in the mid-1970's (Snyder 1971, 1991). The species ranges along the Appalachian Mountains, with an isolated range existing within the Blue Ridge Escarpment (BRE; Figure 3.1) in Georgia, North Carolina, and South Carolina. Green salamanders are now listed as “Near threatened with decreasing populations” by the IUCN Red List (IUCN 2022) and ranked as “Critically imperiled” in the state of South Carolina, where all populations exist within the disjunct BRE.

We were interested in the population genetics of green salamanders because (1) the species is experiencing a population decline and is of immediate conservation concern in South Carolina, and (2) the species exists in naturally discrete populations which may inform implications for species undergoing habitat fragmentation. Patchiness is a population distribution pattern that many naturally contiguous species are being forced into as anthropogenic habitat fragmentation intensifies. Understanding the genomic patterns of isolated populations may

become important as more species experience fragmentation. Our objectives were to examine the degree of genetic differentiation with and between discrete sites of known green salamander populations in South Carolina. Specifically, we used RADSeq to sequence green salamander DNA and estimate population genetic statistics including genetic diversity (F_{ST}), inbreeding (F_{IS}), and effective population size (N_e). We hypothesized that sites with higher green salamander abundances would have lower F_{IS} values, indicating a larger genetic distinction between individuals, because sites with higher abundances generally show a trend of greater allelic richness (Pflüger et al. 2019). We also hypothesized that sites geographically close to one another would have lower F_{ST} values, indicating genetic differentiation between populations, because green salamanders have limited movement capabilities, and short-distanced dispersal patterns are more likely to occur than long-distance movements (Full et al. 1988, Cupp Jr. 1991, Corser 2001).

2. Methods

2.1 Field Methods

We collected tissues samples from green salamanders at fifteen of twenty-one sites with known historical green salamander presence across Oconee, Pickens, and Greenville counties in South Carolina. We were unable to capture salamanders for tissue collection at the remaining sites. We manually identified green salamanders from photos to prevent removing tissue from an individual that was previously sampled. We collected tissue samples from salamanders by removing 2–5 mm of tissue from the tail tips. We immediately placed samples in a 2 mL vial of 95% ethyl alcohol and stored in a -80°C freezer within four hours of tissue removal. A total of 142 tissues were removed from seventeen sites. The number of tissue samples collected was not equal across sites. Five sites had 2 or fewer samples collected, and others ranged from 4–30

tissue samples removed (mean=6.65±1.61). Uneven tissue collection across sites was the result of the number of salamanders encountered at each site and the limited success in removing individuals from rock crevices.

2.2 Lab Methods

2.2.1 3RAD Library Preparation and Sequencing

We constructed 3RAD libraries for green salamander samples for sequencing. We followed a 3RAD protocol (Bayona-Vasquez et al. 2019) to produce dual-digest RADseq libraries. The protocol includes a double enzyme digest, adapter ligation, limited cycle PCR, and a 1.2X Sepure SpeedBead cleanup (Rohland and Reich 2012). We used ClaI, BamHI, and MspI enzymes (New England BioLabs) during the digestion step. To allow for sample pooling, we barcoded each sample with internal dual indices using i5 and i7 iTrue adapters (Glenn et al. 2019). We visualized the libraries on a gel, then quantified and pooled them to 100ng/μL in pools of 48 individuals. We removed small fragments using a 1.2X SpeedBead cleanup. We size-selected the pooled library to 400–600 base pairs (bp) using a Pippin Prep (Sage Science Inc., Beverly, MA, USA). The pooled library was sent to Azenta Life Sciences (South Plainfield, NJ, USA) for sequencing. 3RAD prepared library pools were quality checked using a D1000 ScreenTape on the Agilent TapeStation (Agilent Technologies, Palo Alto, CA, USA) and quantified using a Qubit 2.0 fluorometer at the Azenta facility. The DNA libraries were also quantified by real-time PCR. The libraries were each sequenced on one lane of an Illumina NovaSeq instrument using a 2x150 paired-end configuration.

This protocol provided us with consistent reads with reduced PCR duplicates. PCR duplicates can produce an incorrect representation of the organism's genome sequence and single

nucleotide polymorphisms (SNPs); therefore, reducing these duplicates provides greater confidence in the resulting library of DNA sequences.

2.2.2 Data Processing and SNP Calling

We first removed any individuals that did not have more than 5 million raw reads returned from the sequencer. We next removed adapter sequences and PCR clones, filtered and clustered reads into de novo RAD loci, aligned the reads to the RAD loci, called and filtered SNPs, and generated genotype files using ipyrad (v. 0.9.58; Eaton and Overcast 2020). We used the default settings for ipyrad, except for the minimum depth required to call a base (10X) and clustering threshold (0.88).

2.2.3 Quantifying Population Structure

We used a principal component analysis (PCA) to visualize the overall population structure in our samples. The PCA decomposed the genetic variation across all samples and all SNPs into composite axes that explained the most variation in the dataset. We performed PCAs at two levels: one where we used the individual sampling sites as the population units (i.e., each sampling location was considered a discrete population; $n=17$), and another where we pooled sampling sites into three groups, each separated by a large water body (i.e., each group was considered a discrete population; $n=3$; Figure 4.1). We only included one SNP per RAD locus, and only included SNPs present in more than 50% of individuals in the analyses. We used the “sampled” method of imputation for missing data, which randomly samples genotypes based on the frequency of alleles across all samples. For the sampling level where each site was an individual population unit, we ran a second PCA that, in addition to the above filters, also only included SNPs present in at least one individual per sampling location. We visualized and plotted these PCAs in geographic space in R (R Core Team 2021).

To explicitly determine the number of populations best explained by the data and levels of admixture among identified groups, we used the program fastSTRUCTURE (Raj et al. 2014). Genetic admixture occurs when formerly isolated populations experience an introduction of new genetic lineages via immigrants (Rius and Darling 2014, Jaisuk and Wansuk 2018). Because STRUCTURE programs can be sensitive to missing data, we subset our original variant call format to biallelic SNPs present in more than 70% of individuals, and randomly chose one SNP per RAD locus to minimize the effect of linkage disequilibrium (Pritchard et al. 2000; Newman and Austin 2016; Hodel et al. 2017). Linkage disequilibrium is the non-random association of alleles within loci in a single population, and loci are considered to be in linkage disequilibrium when the association among loci is higher or lower than would be expected if they were truly independent of one another (Slatkin 2008). We ran fastSTRUCTURE models testing a range of possible total populations ($K=1-9$). We used a logistic prior instead of the standard prior when running fastSTRUCTURE to better detect fine-scale population patterns. We calculated the number of populations that best fit the data using the ‘chooseK’ function within fastSTRUCTURE.

We next calculated F_{ST} , a metric of population subdivision (Holsinger and Weir 2009, Weir and Goudet 2017). We used the same subset of SNPs as in the fastSTRUCTURE analysis (i.e., we used SNPs present in 70% of individuals). We calculated F_{ST} using the package ‘hierfstat’ in R. F_{ST} ranges from 0 to 1, with lower values indicating more genetic similarity among populations, and higher values indicating more genetic divergence. Values of F_{ST} can be explained by population structure, migration, or other factors that may subdivide a population (e.g., biogeographical events that change landscape or habitat structure). We calculated F_{ST} values for pairwise combinations of populations and conducted these estimates using both

population unit levels: one analysis where each sampling site was identified as individual population units, and another analysis where all sites were grouped into three population units.

2.2.4 Genetic Diversity and Effective Population Size within Sampling Units

We calculated a variety of population genetic statistics to quantify levels of genetic diversity and inbreeding. We used the same subset of SNPs as in the fastSTRUCTURE analysis. We calculated the observed heterozygosity (H_O), within population gene diversity (H_S), and inbreeding coefficient (F_{IS} ; Nei 1987) using the package ‘hierfstat’ (Goudet 2005). Again, all population genetic statistics were estimated for each of the two population unit levels. We removed any sampling locations with only one individual ($n = 4$). We quantified these metrics of genetic diversity for the populations that best explained the data according to fastSTRUCTURE.

We also calculated the effective population size, N_e . Effective population size is the idealized number of individuals that experiences the same amount of genetic drift as the population. It is a measure of genetic diversity, with lower values indicating fewer individuals are contributing to the evolutionary trajectory of the population, and likely lower overall genetic diversity (Waples 2022). We calculated N_e using two methods within NeEstimator: (1) the “heterozygosity excess” method with a cutoff of alleles with more than 2% frequency in the population and used when there is a small sample size per sampling unit; and (2) the “linkage disequilibrium” method, which is the preferable method when there is little overall genetic variation (Waples and Do 2010). The former method was used when sampling units were defined as the individual populations ($n=17$) but the number of tissue samples within those populations were low. The latter method was used when sampling units were defined as all populations filtered into groups separated by a large water body ($n=3$), each with a higher number of tissue samples within the groups.

3. Results

3.1 Sequencing

Our final dataset contained 113 green salamanders from 17 sampling locations. This number is reduced from the number of tissue samples collected because some reads failed to allow the identification of the genetic sequence. The full dataset contained a median of 2,822 SNPs, from a median of 12.3 million raw reads per individual. Because each dataset filters SNPs differently, not all SNPs were used in each analysis to find SNPs shared among different individuals.

3.2 Population Structure

The PCA with SNPs present in more than 50% of individuals used 851 unlinked SNPs. The PCA with SNPs present in more than 50% of individuals and at least one individual per sampling location used 247 unlinked SNPs. Regardless of SNP filtering, no PCA showed strong separation among sampling sites, indicating little population structure (Figure 4.2). The more highly filtered dataset did show some separation (Figure 4.2B), but individuals from the same sampling location were often found across PCA clusters. When population units were evaluated as three populations separated by water bodies, we detected some genetic separation and population structuring between the groups (Figures 4.2C; 4.2D). This pattern is weaker in the more stringently filtered dataset (Figure 4.2D). fastSTRUCTURE analyses used 443 unlinked SNPs and indicated that a single population ($K = 1$) best described the data. All fastSTRUCTURE runs showed little to no admixture among groups, regardless of the number of populations in the model. F_{ST} values ranged between -0.084 and 0.254 (mean = 0.058, SE = 0.008; Table 4.1) when populations were evaluated as individual sampling sites. When F_{ST} values were visualized against geographic distance, there was evidence of isolation by distance,

with some variation notable in the low to intermediate pairwise distances (Figure 4.3; $R^2 = 0.24$, $p < 0.001$). When population units were evaluated as three groups, F_{ST} values ranged between 0.078 and 0.083 (mean=0.080, SE=0.003; Table 4.2).

3.3 Genetic Diversity and Effective Population Size Within Sampling Units

Individual sampling locations show overall low levels of genetic diversity, and correspondingly low effective population sizes. Observed heterozygosity within individual sites ranged from 0.014 to 0.042 (mean=0.030, SE=0.002), F_{IS} values ranged from -0.400 to 0.114 (mean=-0.055, SE=0.036), and the estimated effective populations ranged from 8.6 individuals to 87.8 individuals (Table 4.3). When calculated for sites combined into three groups, each separated by a body of water, observed heterozygosity ranged from 0.025 to 0.033 (mean=0.029, SE=0.002), and F_{IS} was estimated to range between -0.098 to -0.007 (mean=-0.051, SE=0.026; Table 4.4). The results showed no signs of inbreeding depression, and they did not show lower than expected heterozygosity regardless of how we categorized sampling units. Linear regressions between site-specific F_{IS} values and abundance estimates (Chapter 3) showed no evidence that population size influenced inbreeding coefficients (CMR-derived abundance estimates: $R^2=0.004$, $p=0.87$; N-mixture-derived abundance estimates: $R^2=0.007$, $p=0.78$). The estimated effective population sizes, N_e , for Groups 2 and 3 were 180.3 and 316.4 individuals, respectively. The estimated N_e for Group 1 was indistinguishable from the standard error and therefore no value is described.

4. Discussion

Green salamander populations in upstate South Carolina showed low levels of genetic diversity and population structure, and there was no evidence of inbreeding within sampling locations. Population size (Chapter 3) had no relation with the estimated inbreeding coefficients,

which led us to reject our hypothesis that sites with higher abundances would have lower F_{IS} values and, therefore, a larger distinction among individuals. While there was little evidence of strong genetic differentiation among sites, our hypothesis of isolation by distance was supported. PCA plots showed some evidence of genetic divergence when sampling units were split into three groups separated by the Keowee River, and the South Saluda River; however, the F_{ST} values between these three sampling units indicate the genetic differentiation was not very strong. Our results also included negative F_{ST} estimates between some sampling locations, which suggest the populations are expressing more heterozygosity than they would if they were panmictic. However, these negative values are more likely indicative that the individual sites we sampled are not genetically distinct from one another (i.e., our sampling sites are not discrete green salamander populations).

Collectively, our results indicate enough gene flow is occurring among sites to reduce the threat of inbreeding within sites (Hartl and Clark 1997, Lowe and Allendorf 2010, Nielsen and Slatkin 2013). Such findings may be a result of sufficient dispersal to maintain a panmictic population existing across numerous discrete sites of green salamanders in upstate South Carolina (maximum distance between sites=42 km). However, the physiology and behavioral biology of green salamanders lead us to believe large dispersal behaviors is not a viable explanation of genetic homogeneity across this system. Green salamanders (family: *Plethodontidae*) are lungless and fully reliant on cutaneous respiration, and with this restrictive respiration system, the metabolic capacity and oxygen consumption of green salamanders are limited (Full 1986). The continuous movement (e.g., dispersal behaviors) capability of lungless salamanders comprises only 20-40% of what a lunged salamander can sustain (Full et al. 1988). Limitations in movement theoretically affect demographic connectivity patterns across

populations. Green salamanders have been reported to move up to 106 m (Gordon 1961, Smith and Green 2005), which may be enough to connect neighboring populations in adjacent rock outcrops. However, movement among the sites that were the focus of this analysis was only observed once in a three-year period between two rock outcrops separated by 50 m (Chapter 3). We suspect green salamanders may maintain population connectivity via a few dispersers to nearby subpopulations, but we are skeptical that ongoing animal migration among geographically distant sites is occurring frequently enough to produce these genetically homologous population results.

A slow rate of molecular evolution is another potential explanation for the genetic homogeneity observed among the green salamander populations. Slow molecular evolution rates have been observed in other taxa despite geographic barriers across populations (Weisrock et al. 2000, Spinks and Shaffer 2005, Rosenbaum et al. 2007). However, a broader study identifying the divergences of genetic polymorphisms across various species of salamanders would better inform the pace of microevolution by allowing observations of net sequence divergences among clades (e.g., Walker & Avise, 1998). Having only information on one disjunct range of a single species makes this explanation irresolute at best. However, if all green salamander populations within the disjunct Blue Ridge Escarpment (BRE) have a shared historical connection to the larger green salamander species range, a slow rate of molecular evolution coupled with a recent divergence from a larger contiguous population could explain the low levels of genetic differentiation among individual populations. Historic green salamander distribution maps from as far back as 1924 do not indicate any population connectivity across the Appalachian Valley (Figure 4.4), which lies between the BRE and the larger species range along the Appalachian Mountains. It has been speculated that the fragmentation of the BRE populations from the larger

species range may have been the result of the severe decline in the American Chestnut trees in the mid 1900's (Wilson 2003). Some historic green salamander observations were associated with the American Chestnut, a tree that used to dominate the eastern landscape of North America (Braun 1951, Gordon 1952, Wilson 2003). By 1950, a non-native invasive fungus (*Chryphonectria parasitica*) had eradicated almost all American Chestnuts (Ronderos 2000). It is possible that the recent fragmentation event between these two distributions could be responsible for the lack of genetic differentiation found in this study. However, it is worth noting the blight infected chestnuts throughout the Appalachian Mountain range, not just within the Appalachian Valley; therefore, this may not be the sole cause of the disjunction of the BRE but likely contributed to hindering dispersal routes between sites (Wilson 2003).

Whether green salamanders exhibit slow rates of microevolution or have had historically contiguous population structures, our results clearly show that the discrete green salamander locales in South Carolina have low levels of population subdivision through genetic variation. These results allow us to infer that patches of discrete rock outcrops amongst the landscape do not effectively serve as population boundaries, and the structural connectivity between sites should be maintained. However, the mechanism substantial enough to permit the dispersal of individuals between rock outcrops is currently unknown. With green salamanders having been noted as “weakly” arboreal in past literature, perhaps migratory behaviors occur in the less studied tree canopies. A landscape genetic analysis would likely be informative in identifying landscape features that conduct and resist the functional connectivity among green salamander sites that was made evident with these results. We also suggest future studies incorporate the genetic structure of neighboring green salamander populations in North Carolina and Georgia to

identify if this pattern of homogeneity is shared with other green salamander locales within the BRE.

CHAPTER FIVE

ISOLATION BY DISTANCE BEST EXPLAINS SPATIAL GENETIC STRUCTURE IN GREEN SALAMANDERS IN SOUTH CAROLINA

Abstract.—Understanding the effect landscape plays in the genetic structure of populations is an integral component of spatial ecology. Landscape genetic analyses reveal the effects of functional connectivity on evolutionary processes, which can subsequently inform species conservation and landscape management plans. The objective of this study was to evaluate the genetic population structure of green salamanders (*Aneides aeneus*) by comparing an isolation by distance (IBD) model to two isolation by resistance (IBR) models. We used pairwise F_{ST} values across thirteen rock outcrops occupied by green salamanders as the genetic response to evaluate resistance surfaces. We evaluated a resistance surface categorizing water bodies (three features: lakes, rivers, and streams) and another that represented land cover (five features: water, developed space, early successional land, forest, and agricultural land). The IBD model had the most empirical support in explaining the genetic structure of green salamanders across South Carolina. Land cover consistently provided the least resistance against gene flow. With forests being the dominant land cover feature, these results suggest forested land may provide a mechanism for gene flow in a stepping-stone dispersal network to adjacent sites and across the species range in South Carolina.

1. Introduction

The movement of individuals within a landscape matrix influences the genetic and demographic population structure of species within and among sites. These dispersal events may manifest as a few individuals moving among discrete populations for short periods of time, or migrant behavior that includes the long-term settlement in and breeding within the receiving

population (Wright 1943, Lowe and Allendorf 2010). The latter case promotes increased gene flow and can have positive effects on species by increasing or maintaining genetic variation (Wright 1931).

In the absence of significant barriers to movement, genetic differentiation among sites tends to be a function of the geographic distance between populations (Wright 1943). The genetic structure of species with limited movement capabilities or short dispersal behaviors is often described by isolation by distance (IBD). However, IBD has also emerged as the most influential descriptor of genetic structuring for animals with large dispersal capabilities when analyzed across a large scale relative to the extent of the species' range (Khosravi et al. 2018, Bauder et al. 2021*a*).

An alternative hypothesis to IBD is the isolation by resistance (IBR) model, where heterogeneity within a landscape, rather than Euclidean distance, reduces individual movement and subsequently gene flow among populations (McRae 2006). Landscape features that impose resistance costs on gene flow can include natural barriers (i.e., elevational differences, large water bodies, unsuitable natural habitat), or anthropogenic features (i.e., impervious surfaces, open agricultural land, roads, dams, etc.). Isolation by resistance hypotheses can be compared against an isolation by distance model to evaluate whether spatial features better explain the genetic distances among populations. Investigating the comparative relationship between IBR and IBD models for species of conservation concern can therefore identify crucial implications that landscape heterogeneity or spatial distribution can have on species movement, gene flow, and ultimately the population genetic structure. Results of these model comparisons can inform population management plans and long-term landscape development plans. For example, IBD versus IBR models were used to evaluate the genetic structure in white-tailed deer

after the introduction of a fatal disease to identify population management practices and surveillance plans that would help mitigate the spread of the disease (Bauder et al. 2021a). Similar methods were recently used to identify gene flow and animal movement of a keystone squirrel species experiencing habitat loss and fragmentation (Asadi Aghbolaghi et al. 2023).

The green salamander (*Aneides aeneus*) is a fully terrestrial salamander that occurs in vertical rock habitats along the Appalachian Mountains. The species is also known to exhibit arboreal behaviors (Wilson 2003, Waldron and Humphries 2005), though the full extent of this is unknown. While temporal trends in green salamander population abundances are not well documented (Chapter 3), there has been evidence of a population collapse (Snyder 1991, Corser 2001) within the Blue Ridge Escarpment of the species' range (Figure 3.1). Green salamanders are listed as “Near threatened with decreasing populations” by the IUCN Red List (IUCN 2022), and as “Critically imperiled” in South Carolina, within which all populations are a part of the larger BRE population, disjunct from the rest of the species range. Information on green salamander dispersal capabilities indicate the species exhibits limited mobility (generally ≤ 50 m; Gordon 1952, 1961, Williams and Gordon 1961, Waldron and Humphries 2005, John 2017), and population analyses across sites of known green salamander occupancy show poor population structuring with F_{ST} values identifying similar allelic frequencies across sampling sites (i.e., rock outcrops; Table 4.1). Even with evidence of all thirteen green salamander sites showing little to no population structure, a regression between geographic and genetic distances showed evidence of isolation by distance (Figure 4.3). The IBD regression also illustrated genetic variation among sites with near and intermediate pairwise distances, indicating potential for spatial heterogeneity (rather than distance) to explain that genetic differentiation.

The aim of this chapter was to evaluate the impact of landscape heterogeneity on gene flow via IBD versus IBR models across thirteen green salamander locales in upstate South Carolina. We tested the impact of resistance surface models using a landscape genetics framework with pairwise F_{ST} values as the genetic response. Our hypotheses were three-fold. First, we hypothesized large bodies of water would prove more restrictive on gene flow than our land cover. We suspect the lack of genetic differentiation among sites (Table 4.1) may indicate the feature classes within the land cover resistance surface may have been developed too short a time ago to affect gene flow, whereas water features such as lakes rivers and streams may have served as movement barriers long before developed land. Second, we hypothesized that within our resistance surface based on water classifications, the higher-order streams and rivers (4th–6th order) and larger water bodies (i.e., lakes) would act as impervious barriers to movement and restrict gene flow; however, smaller order streams (1st–2nd order) would not. We believe smaller streams would still permit tree canopies to be connected, and that continuous canopy coverage may act as a conductance surface for animal movement and gene flow between rock outcrops. Third, we hypothesized that within our land cover resistance surface, non-forested land would provide a greater risk of restricting gene flow because open (i.e., grassland) and anthropogenic (i.e., agriculture and developed land) landscapes do not provide suitable habitat for green salamanders to inhabit or traverse through.

2. Methods

2.1 Study site and sample collection

We collected tissue samples from green salamanders at 15 sites across Oconee, Pickens, and Greenville counties in South Carolina, USA (Figure 5.1). Sites varied in size from 12–1251 m² (mean=321±78 m²) and were in state parks, protected land owned by the South Carolina

Department of Natural Resources, and private land. Two sites were directly parallel to a major roadway. Two sites were adjacent to powerlines. All sites were within hardwood and pine forests, with Great Laurel (*Rhododendron maximum*) and Mountain Laurel (*Kalmia latifolia*) common in the understory. Geographic distances among sites ranged from 0.05–42.6 km apart, with an average distance of 14.54 km (± 0.77 SE). We identified individual green salamanders using photo-identification to prevent repeated tissue sampling. Tissues were only removed from adult salamanders to avoid samples from mixed life stages affecting genetic parameter estimates (Peterman et al. 2016). We removed 2–5 mm of tissues from the tail tips of individuals. The number of tissue samples collected across sampling locales were not equal. Five sites had two or fewer samples collected, and others ranged from 4–30 samples, with an average of 6.65 (± 1.61 samples per site). Uneven tissue collection was the result of the number of salamanders encountered at each site and the limited success in removing individuals from rock crevices.

2.2 DNA extraction and population genetic analyses

We constructed 3RAD libraries for the genetic sequencing of our samples. We size-selected the library to 400–600 base pairs and sent the pooled library to Azenta Life Sciences (South Plainfield, NJ, USA) for sequencing. We calculated F_{ST} values for all pairwise combinations of site locations as our measure of population subdivision and genetic distance (Holsinger and Weir 2009, Weir and Goudet 2017). Our final data set contained genetic sequences on 113 green salamanders from 17 sampling locations. The full dataset contained a mean of 2,822 SNPs, from a median of 12.3 million raw reads per individual. F_{ST} values ranged between -0.084 and 0.254 (mean=0.058 \pm 0.008; Table 4.1). There was evidence of isolation by distance (IBD) when F_{ST} values were visualized against geographic distance, with some variation notable in the low to intermediate distances (Figure 4.3). These genetic distances were used as the

response variable in our genetic landscape analyses. A comprehensive description of these DNA amplification and genetic analysis methods and results can be found in Chapter 4.

2.3 Resistance models

We created two resistance surfaces in ArcGIS Pro (v. 3.0.1; Figure 5.2). One surface was a composite water map obtained from the National Hydrography Dataset (NHD, USGS 2021). The initial layer was comprised of eight line feature classes and eleven area feature classes. The line and area features were rasterized into a 60x60 m resolution. We then aggregated and reduced the classification scheme down to three classes: large water bodies, small streams, and land (Figure 5.2B). The “large water body” classification combined lakes with streams categorized as third order and higher because we posited third order streams and larger to serve as effective barriers to green salamander movement. The “small streams” class included first and second order streams. We maintained a separate classification for the smaller, lower order streams because we hypothesized green salamander movement would be potentially feasible via overhanging canopy. The second resistance surface was a composite map obtained from the National Land Cover Database (NLCD, Esri 2019). The initial layer grouped land cover into twenty classes. We reclassified the layer into five categories: water, developed space, early successional, forest cover, and agriculture (Figure 5.2C). The “water” classification combined open water, woody wetlands, and emergent herbaceous wetlands. The “developed space” class was the result of merging developed open space, and developed land from low, medium and high intensity. Our “early successional” category conjoined barren land, shrub land, scrub land, grassland, and herbaceous cover. The “agriculture” class incorporated pasture, hay, and cultivated crop land. The NLCD layer was resampled from a 30x30 m resolution to a 60x60 m resolution using the “resample” tool and “majority” resampling technique. Both the water and

land cover resistance surfaces were mapped at a 60x60 m resolution using the WGS 1984 coordinate system and the NAD 1983 StatePlane 3900 projection.

Resistance surfaces were clipped to a 43x11 km area that incorporated a 500 m buffer around the minimum bounding area of our collective site locations. We chose a 500 m buffer because it is five times the furthest distance recorded for a green salamander dispersal event (Gordon 1961, Smith and Green 2005), and past literature has shown landscapes tightly clipped to sample locations produces artificial effects on current flows during the resistance analysis (Koen et al. 2010).

2.4 Resistance surface optimization and evaluation

We optimized our resistance surfaces using the R package ‘ResistanceGA’ (v. 4.1-16 Peterman, 2018). ‘ResistanceGA’ uses a genetic algorithm employed from the ‘GA’ package (Scrucca 2013) to search the input space for the best-fit resistance surface parameterization and the functional form of the relationships between the resistance surface and the landscape covariates. We implemented a monomolecular transformation to the resistance surfaces from which ResistanceGA calculated the cost-distance (i.e., resistance distance) from the transformed surface. The software then fit a linear mixed-effects model using the maximum likelihood population effects (MLPE) parameterization to account for the pairwise nature between the genetic distances and the resistance distances of the sampling points (Bauder et al. 2021b). Resistance distances used within ResistanceGA are estimated using CIRCUITSCAPE (McRae et al. 2014). We used the ‘GA.prep’ function to set the max.cat argument within the function = 500, which establishes a maximum resistance value at 500. Optimization iterations continue until it reaches the maximum number of iterations, or until the program recognizes 25 generations without improvement. We used ‘commuteDistance’ to calculate the landscape distances and

avoid the assumption that individuals select the least cost path during dispersal iterations. We used the “all_comb” function to optimize each resistance surface independently and simultaneously, providing output on the fit of the single surfaces as well as the interaction of the surfaces. ResistanceGA performed three replicate runs to on these optimization methods. Akaike’s Information Criterion adjusted for small sample sizes (AIC_C) was used to evaluate the fit of the resistance surfaces within each replicate run. The models evaluated include (1) the water surface, (2) land cover surface, (3) a simultaneous analysis including both the water and land cover surfaces, (4) distance-only, and (5) intercept only.

3. Results

Results from all three runs of ResistanceGA showed the geographic distance model had the most empirical support relative to the single landscape resistance surfaces (i.e., the water layer and the land cover layer as independent resistance surfaces), the multisurface landscape resistance layer (i.e., the water layer and land cover layer tested simultaneously), and the null surface (Table 5.1). However, among the landscape resistance surfaces, the water model outcompeted the land cover model. Within the water surface, the large water body class produced the highest resistance, followed by small streams and land (Table 5.2).

4. Discussion

The purpose of this study was to evaluate the impact a heterogeneous landscape has on gene flow across green salamander locales in upstate South Carolina. Prior genetic analyses (Chapter 4) established evidence of a single population structure among our thirteen sampling locations, with pairwise F_{ST} values indicating sufficient gene flow was occurring to produce similar allelic frequencies among the sites. However, there was evidence of variation among the genetic distances estimated (Figure 4.3). In this chapter, we analyzed isolation by resistance

models against an isolation by distance model to evaluate if landscape features could explain the variation among the pairwise F_{ST} values. We found no compelling evidence that either water bodies or land cover type provided resistance to green salamander genetic connectivity that was not already explained by geographic distance. These results represent the first landscape genetics study for green salamanders (but see Johnson, 2002 for an analysis on sites ranging 1–3 km apart).

The resistance surfaces optimized and analyzed using ResistanceGA suggested geographic distance was the most important factor for explaining the genetic distances among our green salamander sampling locations. While there was no substantial indication that isolation by resistance explains the genetic distances among our sites, the resistance surface that best explained the data was our water layer. Within that surface, the large water body feature produced the highest resistance against gene flow. Figure 5.2A illustrates these features separating our green salamander sites into three areas, corresponding well with our grouping scheme analyzed in Chapter 4 (Figure 4.1). However, even when sites were aggregated into those three groups and evaluated, F_{ST} values showed little to no genetic differentiation among them (Table 4.1). When compared to other species in genus *Plethodon*, our results are not unique. Isolation by distance have been found to be the primary cause of genetic differentiation among many terrestrial and semiterrestrial plethodontid species (Highton et al. 1990, Highton and Peabody 2000, Mead et al. 2001, Crespi et al. 2003). In fact, prominent geographic structuring describes much of the population genetics among these species and is the often proposed but objectively difficult reason for delimiting different species (Tilley and Mahoney 1996, Kuchta et al. 2016).

Evidence of isolation by distance in a species' genetic structure indicates dispersal distances are limited. Further, geographically close populations are expected to experience more migrant exchange than geographically distant populations; therefore, neighboring populations express higher genetic similarities (Wright 1943, Puebla et al. 2009). Our genetic results and past descriptions of green salamander movement patterns align well with the isolation by distance model. Short-term and within-site studies have found green salamanders to have dispersal distances ranging up to 42 m (Gordon 1952, 1961, Williams and Gordon 1961, Waldron and Humphries 2005, John 2017). The furthest distance recorded for a green salamander was 106 m away from the rock outcrop of origin (Smith and Green 2005), and results from Chapter 3 identified a recaptured individual migrating 50 m to an adjacent occupied rock outcrop. An isolation by distance model describing genetic connectivity perpetuated through limited dispersal distances is congruent with the evidence in past literature of green salamanders consistently moving ≤ 50 m. It is also conceivable that these short-distance dispersal events, in a stepping stone fashion, account for the lack of genetic differentiation across all green salamander locations in this analysis, provided there is a means of population connectivity.

We found no evidence that land cover type is functioning as a resistant surface for gene flow. Forested land is the predominant land cover type represented across our study area, and likely facilitates gene flow. *Aneides* is a genus of salamanders that have arboreal tendencies, and though the extent of the arboreal behaviors of green salamanders is not well known, there are records of individuals being found on trees (Bishop 1928, Gordon 1952, Bruce 1968, Wilson 2003). Generally, green salamanders are considered “weakly” arboreal and predominantly rock-dwelling (Bishop 1928, Snyder 1991), but there is convincing evidence of seasonal occupancy patterns of green salamanders in trees (Waldron and Humphries 2005). Perhaps instances of

migration among sites are permitted through tree canopies serving as corridors among populated rock outcrops. Additionally, a recent study has also found that rock outcrops occupied by green salamanders are less geographically disjunct than previously thought along the linear rocky ridge systems of the Appalachian Mountains in Virginia (Smith et al. 2015). This decreases the distance required to effectively migrate to a neighboring population. Green salamander arboreal behavior coupled with the continuity of suitable rock habitat through the species range suggest a mechanism for gene flow to occur across the short distances green salamanders are capable of dispersing.

Systems adhering to an isolation by distance model while expressing little to no population structure across large landscapes do not solely imply long dispersal behaviors across distant subpopulations. Low genetic differentiation across large areas could result from stepping-stone migration patterns (Gilpin 1980, Gandon and Rousset 1999, Baum et al. 2004). Stepping-stone dispersals have been observed in poor-dispersing habitat specialists including coral reef fish and insects (Baum et al. 2004, Puebla et al. 2009) as well as strong dispersing bird species across inhospitable landscapes (Saura et al. 2014). Networks of step stones across landscape scales larger than organismal dispersal capabilities or across unsuitable habitat are pivotal in conducting and maintaining gene flow throughout population ranges. Small, stepwise green salamander movements over time from one outcrop to an adjacent one could reasonably be the process producing the isolation by distance pattern observed in our results presented here and the lack of genetic differentiation found across sites in South Carolina (Chapter 4).

Given our IBD model had the most empirical support over water and land cover surfaces, we suggest landscape planning corresponding with conservation efforts for green salamanders should maintain connectivity across green salamander habitat to prevent spatial isolation. Future

work should consider analyzing the genetic structure of more sampling locales in the Blue Ridge Escarpment to provide a more refined understanding of the genetic structure of green salamanders in this disjunct population. We also encourage sampling within the more contiguous species range nearest the BRE to determine if there is a similar pattern of low population differentiation, or if there are patterns of ancestry admixture.

CHAPTER SIX

CONCLUSION

This dissertation provided multi-scaled ecological insight into the biology and spatial ecology of a species of conservation concern, the green salamander (*Aneides aeneus*). Results found were often unexpected and changed our perception of green salamander population structures. When I began this work, I assumed outcrops of rock embedded within forested landscapes served as physically discrete patches of homogeneous habitat within a landscape, similar to coral reefs in an open marine habitat, or wetlands within a deciduous forest. I presumed that the discrete perimeters of rock outcrops would serve as natural boundaries for green salamander subpopulations, and this boundary coupled with the limited dispersal capabilities of the small, lungless species would result in limited gene flow and demographic connectivity across salamander populations. However, **results across all questions and spatial scales showed evidence of and emphasized the importance of that connectivity within and across populations.**

In Chapter 2, the smallest spatially scaled project of the cumulative work, results showed that increased crevice density was the strongest predictor that an individual green salamander would be present in a given crevice. A high density of crevices available within a square meter provides a well connected network of potentially suitable microhabitats that would reduce the cost of movement to disperse between. Habitat patches with high structural connectivity are imperative for lungless salamanders, such as green salamanders, that have a limited ability to sustain long continuous movements (Full et al. 1988).

Chapter 3 approached the conservation biology of the green salamander from a larger spatial perspective, focusing on individual subpopulations inhabiting rock outcrops. Green

salamanders have been historically reported as exhibiting primarily rock-dwelling habitation behaviors (Bishop 1928, Snyder 1991). I therefore used the bounds of rock outcrops as discrete delineations between salamander populations, provided the rock outcrops were separated by at least 50 m (an approximated average of longest dispersal distances noted for the species; Gordon 1952, 1961, Williams and Gordon 1961, Smith and Green 2005, Waldron and Humphries 2005, John 2017). The estimated population demographic statistics included abundance, survival probability, and temporary emigration. Green salamander population sizes were shown to increase as the rock outcrop size increased and the number of crevices present increased. These results match the general ecological assumption that habitat size correlates positively with local animal abundances. Interestingly, though, the results also showed lower than expected survival rates, with the monthly estimates ranging from 83% to 100% across rock outcrops. In the context of the robust design analysis employed, survival is defined as retainment of the same individuals across survey periods. The inverse of the survival estimates represents loss rates, which could be the result of death or permanent emigration away from the rock outcrop. I do not believe there was a sufficient biological or ecological reason for green salamanders to experience high monthly death rates throughout the three-year study period; rather, I suspect the loss rates are more likely to be indicative of emigration away from the rock outcrops. **This result was the first occurrence within this dissertation of potential evidence for low fidelity to individual rock outcrops.**

The analyses within Chapters 4 and 5 employed the largest temporal and spatial scale analyses of the dissertation. Within the scope of these chapters, I investigated the genetic (i.e., functional) and landscape (i.e., structural) connectivity across individual rock outcrops in upstate South Carolina. Similar to Chapter 3, my genetic and landscape experimental designs assumed

the 13 individual patches of rock outcrops served as 13 discrete green salamander population units. The genetic analysis revealed no signs of inbreeding (F_{IS} estimates ranged -0.098 to -0.007; mean=-0.051, SE=0.026), and regressions between F_{IS} and population abundances estimated within Chapter 4 showed no evidence that population size influenced inbreeding coefficients ($R^2=0.004$, $p=0.87$). These results indicated that, regardless of rock outcrop size or population abundance, individual salamanders within the same rock outcrop show genetic evidence of a neutral, panmictic population. This was particularly remarkable considering how some populations included in this analysis had low abundance estimates (Figure 3.6). F_{ST} values were also calculated across pairwise combinations of green salamander populations (within rock outcrops) as a means to assess gene flow across the populations. The resulting F_{ST} estimates indicated little evidence of strong genetic differentiation among sites (Table 4.1). Some estimates included negative values, which could suggest the populations are expressing higher heterozygosity levels than if they were panmictic; however, these values are more likely indicative that the individual sites sampled were not genetically distinct from one another. In other words, the rock outcrops sampled do not represent individual green salamander populations. Because of this, I decided to pool individual rock outcrops together to form three green salamander populations instead of 13. In doing this, I also effectively increased the sample size of tissue samples for each of the three populations. F_{ST} results from this pooled dataset still indicated there was sufficient gene flow to maintain similar allelic frequencies across populations. Such findings may be a result of sufficient dispersal to maintain a random mating population across numerous discrete rock outcrops with green salamanders across upstate South Carolina. This supports my findings of low survival (i.e., retention) rates of individual

salamanders within rock outcrops estimated in Chapter 3, and establishes evidence of a **single population structure among the inhabited rock outcrops**.

The genetic results also showed evidence of isolation by distance (IBD) among the sampling sites (Figure 4.3), where genetic similarity decreased as geographic distance between populations increased. I suspect green salamanders may maintain population connectivity via a few dispersers to nearby rock outcrops, but I am skeptical that ongoing animal migrations among geographically distant sites is occurring frequently enough to produce these genetically homologous population results, and evidence of isolation by distance does indicate limited geographic distances are traversed in dispersal behaviors. However, there was variation among the pairwise F_{ST} values between some rock outcrops that were at low or intermediate geographic distances from each other, which indicated potential for spatial heterogeneity (rather than distance) to explain that genetic variation. Therefore, my next chapter aimed to evaluate the impact of landscape heterogeneity on gene flow by comparing isolation by distance models (IBD) with isolation by landscape resistance (IBR) models. Investigating the relationship between IBD and IBR models can identify crucial implications that the landscape or spatial distribution of habitat has on animal dispersal, gene flow, and ultimately the population's genetic structure. I used ResistanceGA to optimize landscape resistance surfaces to best explain the pairwise F_{ST} values that were estimated in Chapter 4. I created IBR models using two resistance surfaces: one containing water features, and the second containing land cover classifications. AICc comparisons of the IBR models against the IBD model showed no compelling evidence that either water bodies or land cover type provided resistance to green salamander gene flow that was not already explained by geographic distance. Forested land was the predominant land cover type represented across the study area, but it demonstrated the lowest resistance estimate

of all land cover types. Perhaps instead, forested land cover facilitates gene flow among discrete rock outcrops.

Aneides is a genus of salamanders that have arboreal tendencies, and while the arboreal behaviors of green salamanders is thought to be subordinate to rock-dwelling habitation behaviors, the extent of our understanding of arboreal tendencies is not well known (Bishop 1928, Bruce 1968, Wilson 2003, Snyder 1991). However, there is convincing evidence of seasonal occupancy patterns of green salamanders in trees (Waldron and Humphries 2005). Additionally, a recent study found rock outcrops occupied by green salamanders are less geographically disjunct than previously assumed in Virginia (Smith et al. 2015). I believe that **the arboreal behavior of green salamanders coupled with the continuity of suitable rock habitat through the species range may suggest a mechanism for gene flow to occur across short distances that the lungless species is capable of dispersing.**

Patchy population systems adhering to an isolation by distance model while expressing little to no genetic differentiation across large landscapes do not imply the populations are dependent on long dispersal behaviors across distant populations. Low genetic differentiation across large areas could result from stepping-stone migration patterns (Gilpin 1980, Gandon and Rousset 1999, Baum et al. 2004). Stepping-stone dispersals have been observed in other poor-dispersing habitat specialists such as insects and coral reef fish (Baum et al. 2004, Puebla et al. 2009). Networks of suitable patches of habitat (i.e., stepping stones) across landscape scales larger than the organism's dispersal capabilities or across unsuitable habitat can be critical components of gene flow throughout patchy population ranges. The cumulative results of this dissertation as a body of work suggest instances of green salamander migrations may be permitted through tree canopies serving as functional corridors for gene flow among populated

rock outcrops. Short, stepwise green salamander movements from one rock outcrop to an adjacent one via movement through tree canopies could reasonably explain my results of low individual survival (i.e., retention) rates (Chapter 3), sufficient gene flow to maintain similar allelic frequencies across “populations” within rock outcrops (Chapter 4), and the lack of resistance forested land cover imposed on gene flow (Chapter 5).

The ecological theater that plays on various levels of time and space can cause different biological patterns to emerge based on the scale of the perspective through which they are viewed (Hutchinson 1965, Wiens 1989). This dissertation evaluated a species of conservation concern across a range of spatial and temporal scales. Throughout each analysis, I took particular care to explicitly design the study to the scale of the question, and at each level, the results consistently highlighted the importance of connectivity within and across patchy populations. Green salamanders are a terrestrial species of salamander thought to be largely restricted to the rock outcrop patch that they are born within. Results from my dissertation suggest otherwise. While green salamanders are lungless and therefore physiologically limited in energy exertion, the connectivity readily available within outcrops through networks of crevices, and between them via forested land cover, the green salamander population in upstate South Carolina is able to maintain gene flow across numerous and distant patches of suitable habitat.

TABLES AND FIGURES

Table 2.1. Predicted (Column 2) and modeled (Column 3) relationships between crevice use and features of the crevice for populations of Green Salamanders (*Aneides aeneus*) across five sites in Greenville, Oconee, and Pickens counties, South Carolina, USA. We expected the features crevice density, nearest crevice, and nearest tree to be the best predictive rock characteristics for salamander presence. Predictions are listed as being either positively (+) or negatively (–) correlated with salamander presence. We had no *a priori* prediction for the effect of crevice length. Columns 3–5 are the results of the Global Logistic Regression Model where site was included as a random effect; crevice width, density, and canopy cover were the three features significantly (*) associated with salamander presence. The abbreviation SE = standard error.

Features	Predicted			
	relationship	Estimate	SE	P-value
Crevice width (cm)	–	-1.75	0.72	0.016 *
Crevice length (cm)	X	-0.27	0.32	0.394
Crevice depth (cm)	–	-0.90	0.56	0.111
Canopy cover (%)	+	1.62	0.67	0.016 *
Crevice density (1/m ²)	+	1.02	0.24	< 0.001 *
Distance to nearest crevice (cm)	–	0.12	0.19	0.520
Distance to nearest tree (m)	–	-0.61	0.53	0.252

Table 2.2. Mean \pm standard deviation of crevice features that were both occupied and unoccupied by Green Salamanders (*Aneides aeneus*) across five sites (rock outcrops) in Greenville, Oconee, and Pickens counties, South Carolina, USA.

Crevice Feature	Occupied	Unoccupied
Crevice width (cm)	1.4 \pm 1.6	3.9 \pm 5.5
Crevice length (cm)	24.0 \pm 21.9	53.2 \pm 63.9
Crevice depth (cm)	3.8 \pm 4.4	11.8 \pm 16.2
Canopy cover (%)	99.0 \pm 4.4	95.5 \pm 9.5
Crevice density (1/m ²)	8.0 \pm 4.9	5.2 \pm 3.2
Distance to nearest crevice (cm)	12.0 \pm 22.1	18.3 \pm 27.9
Distance to nearest tree (m)	3.7 \pm 3.9	3.6 \pm 3.9

Table 2.3. MANOVA (Multivariate Analysis of Variance) results indicating how crevice features differ across the five sites we visited of Green Salamanders (*Aneides aeneus*) in Greenville, Oconee, and Pickens counties, South Carolina, USA. We expected the features crevice density, nearest crevice, and nearest tree to be the best predictive rock characteristics for salamander presence. Canopy cover, crevice density, distance to nearest crevice, and distance to nearest tree differed significantly between sites. The abbreviation df = degrees of freedom.

Features	MANOVA		
	df	F-value	P-value
Crevice width (cm)	5	1.631	0.148
Crevice length (cm)	5	0.382	0.861
Crevice depth (cm)	5	0.555	0.749
Canopy cover (%)	5	3.056	0.010 *
Crevice density (1/m ²)	5	10.376	< 0.001 *
Distance to nearest crevice (cm)	5	2.353	0.042 *
Distance to nearest tree (m)	5	299.920	< 0.001 *

Table 3.1. Descriptions of the capture probability (p), recapture probability (c), and survival (S) parameter covariates incorporated into the robust design framework for our CMR analysis.

	Covariate	Description
Capture Probability, p	~1	Null
	Site	Capture probabilities are site-dependent
	Removal Difficulty	Capture probabilities are best described by one of three a priori categories describing the difficulty of removing a salamander from a crevice: "easy", "medium", and "hard"
	Layout	Capture probabilities specific to binary covariate describing if a site was classified as a single rock or numerous adjacent rocks
	Primary Period	Different capture probability for each primary sampling period
	Secondary Period	Different capture probability for each secondary sampling period
Recapture Probability, c	~1	Null
	= p	Recapture probability is the same as capture probability because there is no logic for trap shyness or happiness
	Site	Recapture probability is site-dependent
Survival, S	~1	Null
	Site	Survival probabilities are different across each site
	Cover	Survival probabilities are influenced by a rock outcrop being either "open" or "covered" by canopy cover
	Layout	Survival between primary periods is a function of the binary covariate describing if a site was classified as a single rock or numerous adjacent rocks

Table 3.2. Descriptions of the detection probability (p), availability probability (Φ), and abundance (λ) parameter models incorporated into the N-mixture models for the unmarked analysis.

	Covariate	Description
<i>Detection Probability,</i> p	~1	Null; constant detection probability across sites and sampling periods
	Temperature	Detection probability varies across secondary visits as a function of temperature
	Humidity	Detection probability varies across secondary visits as a function of humidity
	Temperature + Humidity	Detection probability varies across secondary visits as a function of the additive model of temperature and humidity
	No. of People	Detection probability varies across secondary visits as a function of the number of surveyors present
<i>Availability,</i> Φ	~1	Null; constant availability across sites and primary periods
	Primary Period	Availability probability is constant within but varies across the five primary periods
	Thermal Season	Binary; availability probability is a function of either the "warm" or "cool" season that the primary period is classified as
<i>Abundance,</i> λ	Size	Logical (m ²)
	Elevation	Logical (m)
	Slope	Logical (°)
	Aspect	Logical (radians)
	Total No. Crevices	The total number of crevices at a site
	Layout	Binary; population abundance dependent on whether a site was classified as a "single rock" or "numerous adjacent rocks"
	Elevation + Aspect	Logical
	Elevation + Total No. Crevices	Logical
	Size + Aspect	Logical
	Size + Total No. Crevices	Logical

Table 3.3. AIC_c results for candidate CMR models describing the 214 capture histories of green salamanders (*Aneides aeneus*) across 12 sites by various survival (*S*), capture probability (*p*), and recapture probability (*c*) covariates. ~1 indicates a null model; blank cells indicate the covariate was not incorporated into the model; n_{par} = the number of modeled parameters; *w* = AIC weight.

See Table 2.1 for covariate explanations.

	Movement	<i>p</i>	<i>c</i>	<i>S</i>	n_{par}	AIC_c	ΔAIC_c	<i>w</i>
1	Null	~1		Site	13	1065.57	0.00	2.32E-01
2	Null	Site		Layout	14	1066.78	1.21	1.27E-01
3	Random	Site		Layout	15	1067.41	1.85	9.23E-02
4	Random	~1		Site	14	1067.81	2.24	7.58E-02
5	Null	~1		Layout	3	1067.86	2.29	7.38E-02
6	Null	Site	=p	Layout	15	1067.97	2.40	7.00E-02
7	Null	Site	=p	~1	14	1068.85	3.28	4.51E-02
8	Null	Site		~1	13	1069.02	3.45	4.13E-02
9	Random	Site		~1	14	1069.08	3.51	4.02E-02
10	Random	~1		Layout	4	1069.59	4.02	3.12E-02
11	Random	Site	=p	Layout	16	1069.65	4.08	3.02E-02
12	Null	Site		Site	24	1070.28	4.71	2.20E-02
13	Random	Site	=p	~1	15	1071.05	5.48	1.50E-02
14	Null	Site	=p	Cover	15	1071.07	5.50	1.48E-02
15	Null	Layout	=p	~1	3	1071.14	5.57	1.43E-02
16	Null	Site		Cover	14	1071.26	5.69	1.35E-02
17	Random	Site		Cover	15	1071.33	5.76	1.30E-02
18	Random	Layout	=p	~1	4	1071.85	6.29	1.00E-02
19	Null	Site	Site	~1	25	1071.92	6.36	9.67E-03
20	Random	Site		Site	25	1072.51	6.94	7.22E-03
21	Null	Site	=p	Site	25	1072.60	7.04	6.89E-03
22	Random	Site	=p	Site	26	1073.22	7.65	5.07E-03
23	Random	Site	=p	Cover	16	1073.30	7.73	4.86E-03
24	Random	Site	~1	~1	15	1075.49	9.93	1.62E-03
25	Null	~1		~1	2	1077.14	11.57	7.13E-04
26	Null	~1		Cover	3	1077.86	12.29	4.98E-04
27	Null	Prim. Pd.	=p	~1	3	1078.05	12.48	4.53E-04
28	Random	~1		~1	3	1078.53	12.96	3.56E-04
29	Null	~1	~1	~1	3	1079.01	13.44	2.80E-04

30	Random	~1		Cover	4	1079.35	13.79	2.36E-04
31	Random	Prim. Pd.	=p	~1	4	1079.44	13.88	2.25E-04
32	Markovian	~1		~1	4	1080.30	14.73	1.47E-04
33	Random	~1	~1	~1	4	1080.37	14.80	1.42E-04
34	Null	~Removal Difficulty	=p	~1	4	1081.14	15.57	9.65E-05
35	Markovian	~1	~1	~1	5	1081.92	16.36	6.52E-05
36	Null	Sec. Pd.	=p	~1	9	1082.52	16.96	4.83E-05
37	Random	~Removal Difficulty	=p	~1	5	1082.53	16.96	4.82E-05
38	Random	Sec. Pd.	=p	~1	10	1083.82	18.26	2.52E-05
39	Null	Sec. Pd.	Sec. Pd.	~1	16	1088.67	23.11	2.23E-06
40	Random	Sec. Pd.	Sec. Pd.	~1	17	1090.97	25.40	7.08E-07

Table 3.4. Green salamander (*Aneides aeneus*) survival and capture probability estimates across the surveyed South Carolina populations as described by the top ranked CMR model. Survival (S) was site-specific and capture probability (p) was constant across sites and sampling periods. NA's indicate estimates were removed because the standard errors were larger than the estimates.

Parameter	Covariate	Estimate	Standard Error	Lower CI	Upper CI
Survival, S	Site: 1477	0.948	0.048	0.731	0.992
	Site: HWY	NA	NA	NA	NA
	Site: 1236	0.826	0.073	0.637	0.928
	Site: TR2	0.878	0.052	0.735	0.949
	Site: 1243	0.916	0.054	0.732	0.977
	Site: 3688	0.968	0.029	0.828	0.995
	Site: TR3	1.000	0.000	1.000	1.000
	Site: 1250	0.941	0.025	0.870	0.975
	Site: 1292	NA	NA	NA	NA
	Site: 42105	1.000	0.000	1.000	1.000
	Site: AD1	0.867	0.064	0.686	0.951
	Site: DNR	0.939	0.025	0.868	0.973
Capture Probability, p	Null	0.105	0.013	0.082	0.134

Table 3.5. Green salamander (*Aneides aeneus*) availability probability estimates across the five primary periods. These availability estimates indicate the probability that green salamanders were available for capture within the super-population (i.e., site).

Primary Period	ϕ	SE	lower	upper
1	0.664	0.182	0.285	0.907
2	0.621	0.125	0.366	0.823
3	0.417	0.120	0.214	0.653
4	0.387	0.091	0.230	0.572
5	0.465	0.124	0.246	0.698

Table 3.6. Results of the AIC analysis for candidate N-mixture models describing the unmarked counts of green salamanders (*Aneides aeneus*) across 19 sites by various detection (p), availability (Φ), and abundance (λ) models. n_{pars} = the number of modeled parameters; w = AIC weight. All models are fit to a Poisson distribution. All availability models include the best-fit detection probability covariate (temperature). All abundance models include the top ranked detection covariate and availability covariate (primary period).

	p	Φ	λ	nPars	AIC	Δ AIC	w
1	Temperature	Primary Period	Size + Total No. Crevices	10	998.44	0	8.90E-01
2	Temperature	Primary Period	Size + Aspect	10	1002.57	4.13	1.10E-01
3	Temperature	Primary Period	Size	9	1014.91	16.47	2.40E-04
4	Temperature	Primary Period	Elevation + Total No. Crevices	10	1018	19.56	5.00E-05
5	Temperature	Primary Period	Aspect	9	1027.66	29.21	4.00E-07
6	Temperature	Primary Period	Total No. Crevices	9	1028.62	30.18	2.50E-07
7	Temperature	Primary Period	Elevation + Aspect	10	1035.16	36.71	9.50E-09
8	Temperature	Primary Period	~1	8	1035.26	36.82	9.00E-09
9	Temperature	Primary Period	Layout	9	1037.24	38.8	3.30E-09
10	Temperature	Primary Period	~1	8	1053.16	54.72	1.20E-12
11	Temperature	Primary Period	Slope	9	1054.49	56.05	6.00E-13
12	Temperature	~1	~1	4	1060.15	61.71	3.50E-14
13	Temperature	~1	~1	4	1060.15	61.71	3.50E-14
14	Temperature	Thermal Season	~1	5	1061.48	63.04	1.80E-14
15	Temperature + Humidity	~1	~1	5	1062.13	63.68	1.30E-14
16	Temperature	Primary Period	Elevation	9	1063.67	65.23	6.10E-15
17	No. of People	~1	~1	4	1066.9	68.46	1.20E-15
18	~1	~1	~1	3	1076.99	78.54	7.80E-18
19	Humidity	~1	~1	4	1078.48	80.04	3.70E-18

Table 4.1. Pairwise F_{ST} values for green salamander (*Aneides aeneus*) populations across sampling sites in South Carolina, USA. We have results on thirteen of the seventeen total sites used in this study because four sites were not included in the analysis as they contained only one tissue sample each. Mean $F_{ST}=0.06\pm 0.008$.

	1236	1243	1250	1251	1477	2235	3688	42105	5976	AD1	DNR	HWY
1236												
1243	0.013											
1250	0.109	0.095										
1251	0.091	0.101	-0.038									
1477	0.036	0.099	0.168	0.135								
2235	-0.026	0.019	0.093	0.060	-0.006							
3688	0.016	0.020	0.094	0.095	0.011	0.011						
42105	0.105	0.116	0.254	0.227	0.070	0.086	0.13					
5976	-0.036	-0.049	0.007	-0.023	0.059	-0.003	-0.06	0.049				
AD1	0.020	0.019	0.074	0.053	0.049	0.011	-0.01	0.168	-0.027			
DNR	0.104	0.078	0.004	-0.036	0.156	0.044	0.08	0.205	-0.005	0.063		
HWY	0.096	0.107	0.089	0.091	0.123	0.041	0.08	0.144	0.025	0.081	0.074	
TR3	0.037	0.022	0.015	-0.084	0.073	0.023	0.02	0.211	-0.006	0.030	0.003	0.041

Table 4.2. Pairwise F_{ST} values for populations of green salamanders (*Aneides aeneus*) separated into three groups separated by Lake Jocassee/Eastatoee Creek (between Groups 1 and 2) and the South Saluda River/Table Rock Reservoir (between Groups 2 and 3). Mean $F_{ST}=0.080\pm 0.003$.

	Group 1	Group 2	Group 3
Group 1	-		
Group 2	0.078	-	
Group 3	0.083	0.079	-

Table 4.3. All genetic population statistics estimated for individual green salamander populations in upstate South Carolina, USA. Populations are individual rock outcrops separated by at least 50 m, and n dictates the number of tissue samples removed from the respective site. Sites with only one tissue sample were not included in the population statistic analysis. H_O is a measure of observed heterozygosity, H_S is a measure of expected heterozygosity under Hardy-Weinberg Equilibrium, F_{IS} is the inbreeding coefficient, and N_e represents the estimated effective population size (95% CI). N_e estimates denoted as “NA” indicate the estimate could not be distinguished from the sampling error; it does not indicate an infinitely large population.

Site	n	H_O	H_S	F_{IS}	N_e
1236	12	0.026	0.023	-0.095	14.5 (8.7-46.9)
1243	10	0.026	0.027	0.047	NA
1245	1				
1250	16	0.025	0.023	-0.078	18.7 (12.3-40.7)
1251	5	0.026	0.022	-0.166	10.9 (5.7 - NA)
1292	1				
1477	4	0.036	0.034	-0.035	24.4 (11.5 - NA)
2235	3	0.042	0.044	0.048	NA
3688	7	0.031	0.032	0.047	NA
42105	2	0.041	0.029	-0.400	8.6 (4.3 - NA)
5976	3	0.030	0.031	0.040	NA
AD1	6	0.031	0.029	-0.077	14.4 (8.1 - 82.4)
BB	1				
DNR	24	0.025	0.024	-0.061	NA
HWY	15	0.033	0.030	-0.098	87.8 (17.0 - NA)
TR2	1				
TR3	2	0.014	0.016	0.114	11.5 (3.9 - NA)

Table 4.4. Genetic population statistics estimated for green salamander populations culminated into three groups in upstate South Carolina, USA. Groups are separated by notable water bodies, and n dictates the number of tissue samples removed from the respective site. H_o is a measure of observed heterozygosity H_s is a measure of expected heterozygosity under Hardy-Weinberg Equilibrium, F_{IS} is the inbreeding coefficient, and N_e represents the estimated effective population size (CI). N_e estimates denoted as “NA” indicate the estimate could not be distinguished from the sampling error; it does not indicate an infinitely large population.

	n	H_o	H_s	F_{IS}	N_e
Group 1	15	0.0332	0.0302	-0.0977	NA
Group 2	53	0.0254	0.0243	-0.0475	180.3 (136.9 - 259.9)
Group 3	45	0.0294	0.0292	-0.0066	316.4 (191.4 - 852.9)

Table 5.1. A comparison of the resistance surfaces optimized and evaluated using ResistanceGA (v. 4.1-16) to evaluate isolation by distance versus isolation by resistance models in response to green salamander (*Aneides aeneus*) genetic connectivity. Models include distance-only (Distance), a water resistance layer (Water), a land cover resistance layer (NLCD), an intercept only model (Null), and two resistance layers run simultaneously (nlcd.water). Models were evaluated using Akaike information criterion (AIC_c). K represents the number of parameters, w is the AIC weight, R_m^2 is the marginal r -square, and R_c^2 is the conditional r -square. Results show the distance-only model (IBD).

Surface	Log-likelihood	K	ΔAIC_c	AIC _c	w	R_m^2	R_c^2
Distance	138.4	2	0.00	-271.59	1.00	0.39	0.71
Water	137.89	5	14.39	-257.20	7.49E-04	0.43	0.75
NLCD	141.89	7	24.21	-247.38	5.53E-06	0.53	0.72
Null	115.56	1	42.84	-228.75	4.98E-10	0.00	0.37
nlcd.water	143.17	11	271.26	-0.34	1.25E-59	0.56	0.70

outperformed the other surfaces.

Table 5.2. Resistance values associated with the two resistance models analyzed as single, independent layers within ResistanceGA. Response values for the resistance surface optimization and evaluation were pairwise F_{ST} estimates across green salamander (*Aneides aeneus*) sites across upstate South Carolina. Resistance values were set to a maximum of 500; higher values indicate higher resistance.

Surface	Log-likelihood	K	$\Delta AICc$	AICc	R_m^2	R_c^2	Feature 1	Feature 2	Feature 3	Feature 4	Feature 5
Water	137.89	5	-265.77	-257.20	0.43	0.75	Large Water Bodies	Small Streams	Land		
							500.00	1.34	1.00		
NLCD	141.89	7	-269.78	-247.38	0.53	0.72	Water	Developed space	Early successional	Forest	Agriculture
							1.00	500.00	138.61	1.67	398.45

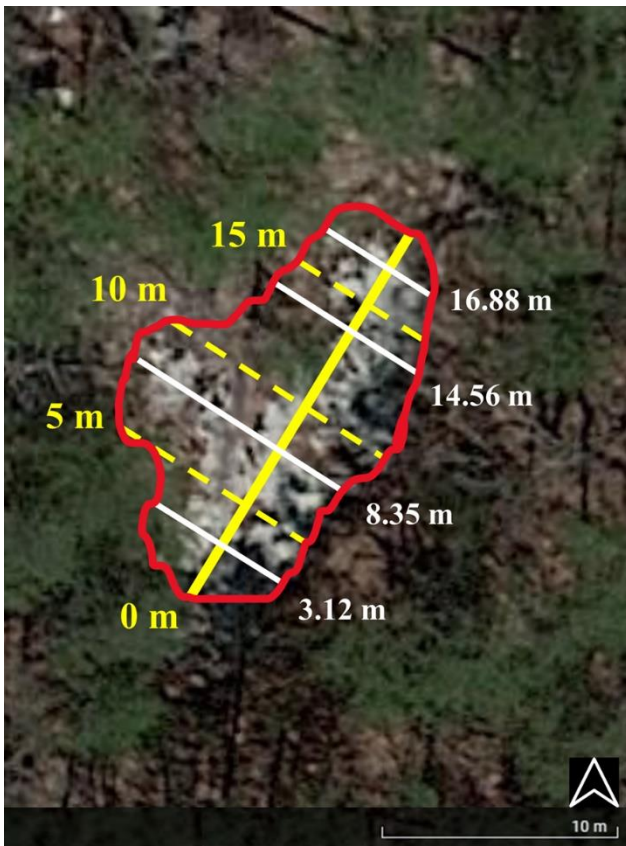


Figure 2.1. Each survey of Green Salamanders (*Aneides aeneus*) of rock outcrops in Greenville, Oconee, and Pickens counties, South Carolina, USA, began by first laying a field tape across the length of the outcrop (solid yellow line). This long axis was divided every 5 m (dashed yellow lines), and a random number generator was used to determine where a perpendicular transect (white lines) was laid within these 5 m segments. Every crevice crossed by these perpendicular transects was surveyed for salamander presence and assessed for crevice depth, width, length, humidity, distance from the nearest tree, distance from the nearest crevice, and crevice density.

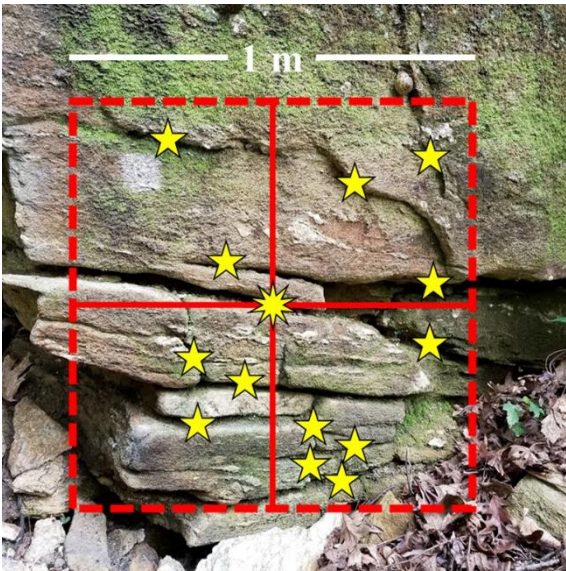


Figure 2.2. Crevice density surrounding the crevice of interest (ten-point center star) of Green Salamanders (*Aneides aeneus*) was calculated by identifying the point within the crevice of interest that is surrounded by the most crevices. A 1-m² area was measured around this point and every crevice that fell within this designated space was counted (shown as individual stars), including the crevice of interest.

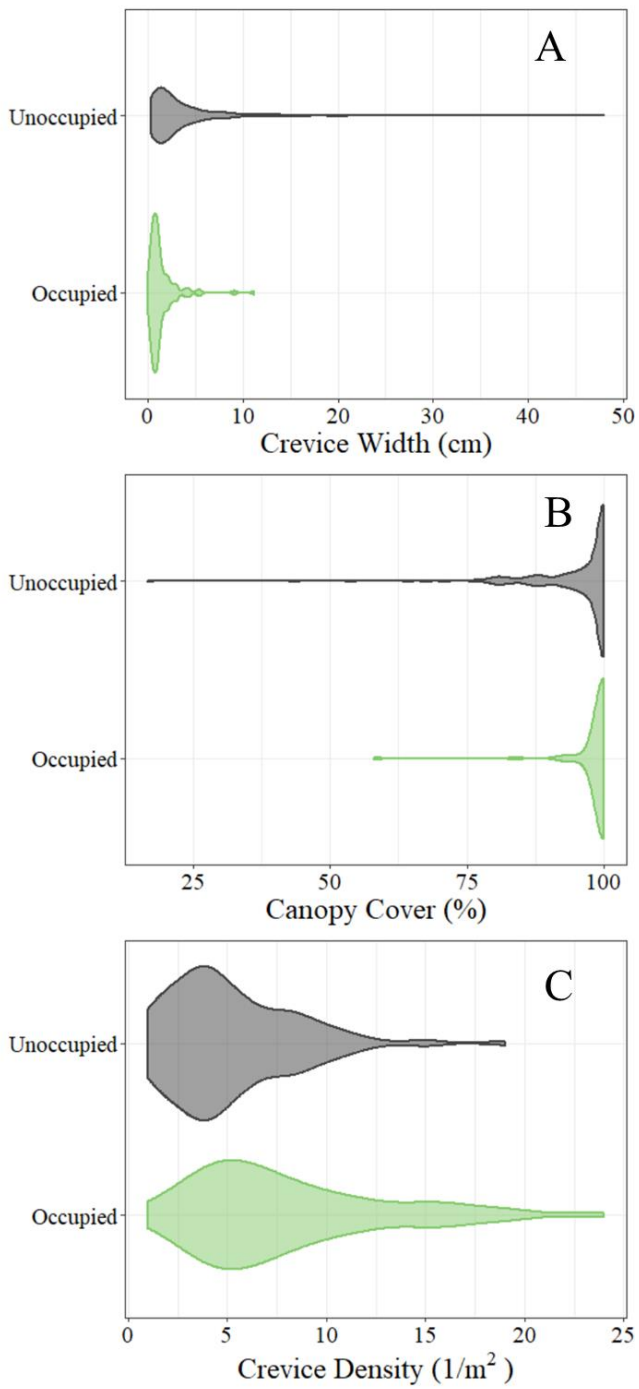


Figure 2.3. Violin plots for the significant ($\alpha=0.05$) site features in crevices unoccupied (grey) and occupied (green) by Green Salamanders (*Aneides aeneus*) in Greenville, Oconee, and Pickens counties, South Carolina, USA. (A) Crevice width; (B) canopy cover; (C) crevice density.

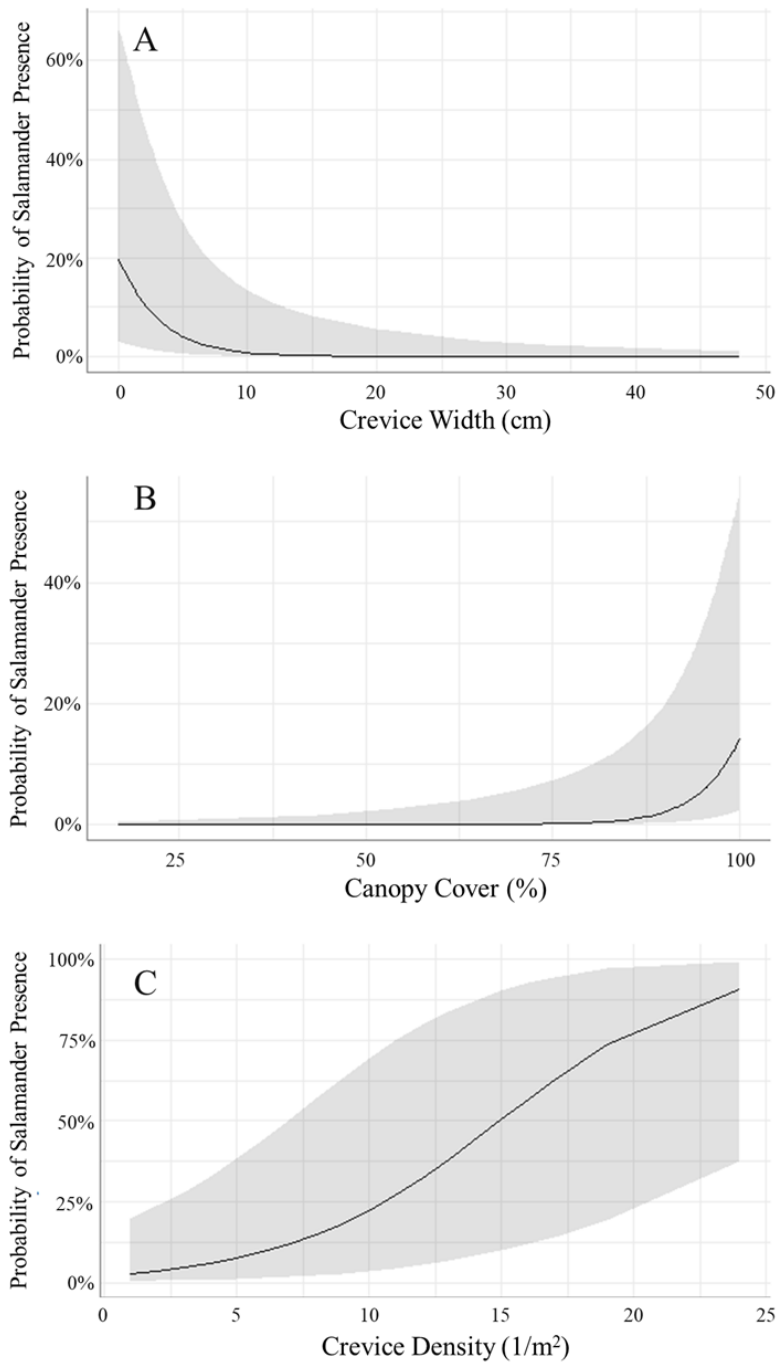


Figure 2.4. Odds ratio curves for probability of presence of Green Salamanders (*Aneides aeneus*) in relationship to (A) crevice width, (B) canopy cover, and (C) crevice density with the respective confidence intervals (gray shading).

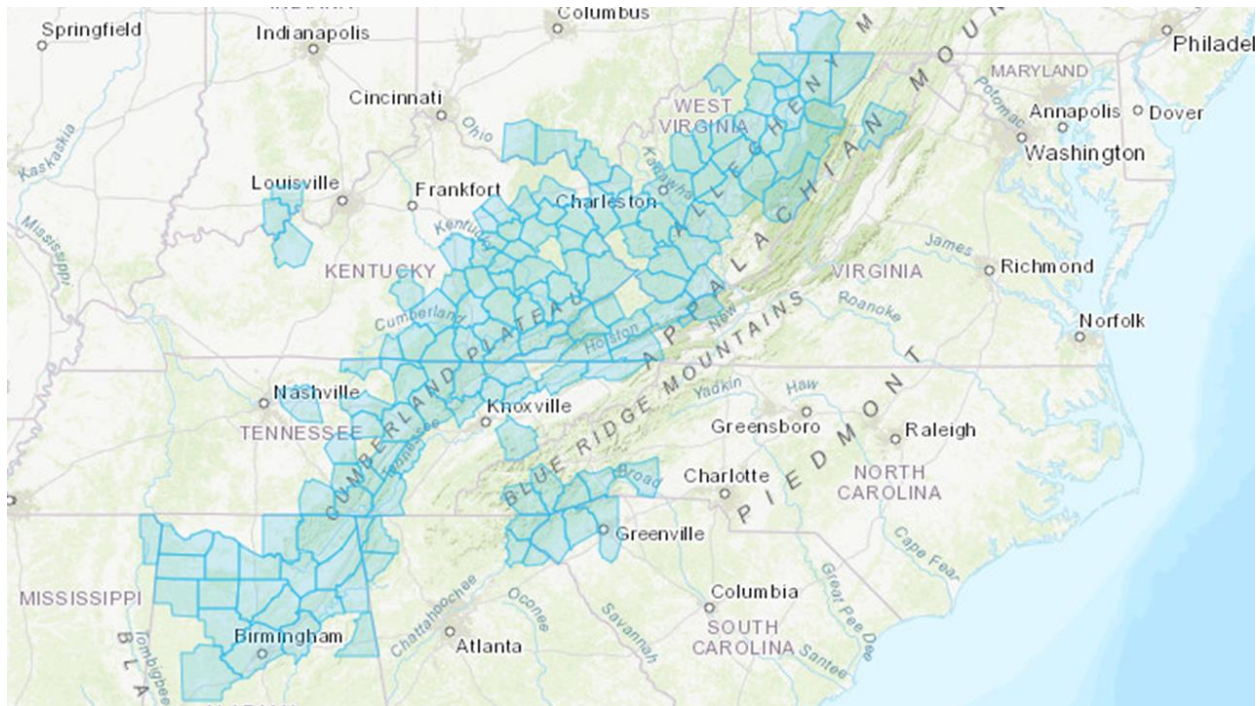


Figure 3.1. County-level distribution of the green salamander (*Aneides aeneus*). The Blue Ridge Escarpment (BRE) populations exist in Georgia, North Carolina, and South Carolina, disjunct from the main Appalachian population. Map downloaded from the Amphibian and Reptile Monitoring Initiative's National Amphibian Atlas website.

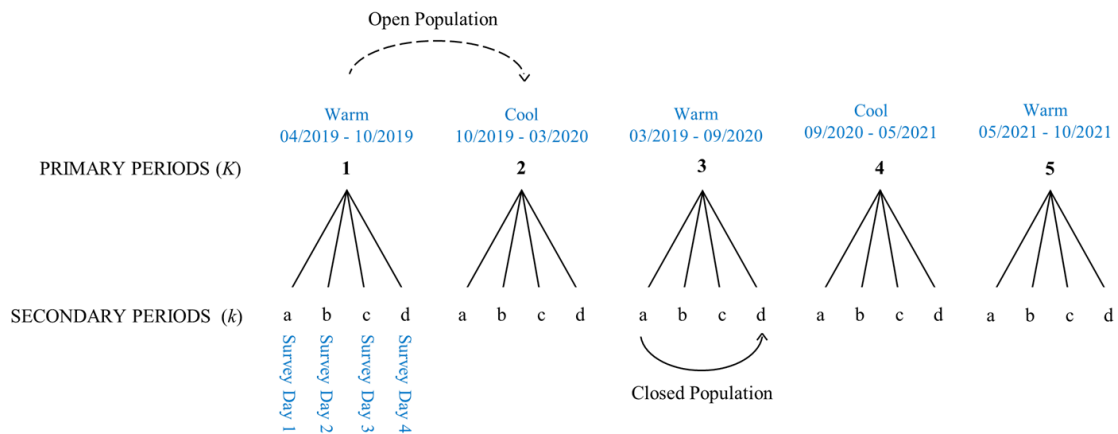


Figure 3.2. The robust design used for the marked population analysis of green salamander (*Aneides aeneus*) populations in the Blue Ridge Escarpment. This design includes primary sampling periods, K , with secondary periods nested within each primary, k . Primary periods were pooled into cool and warm seasons in the year, determined post hoc as sampling days that achieved temperatures higher (warm period) or lower (cool period) than the annual average. Primary periods assume an open population where births, deaths, immigration, and emigration can occur between them. Secondary periods assume a closed population.

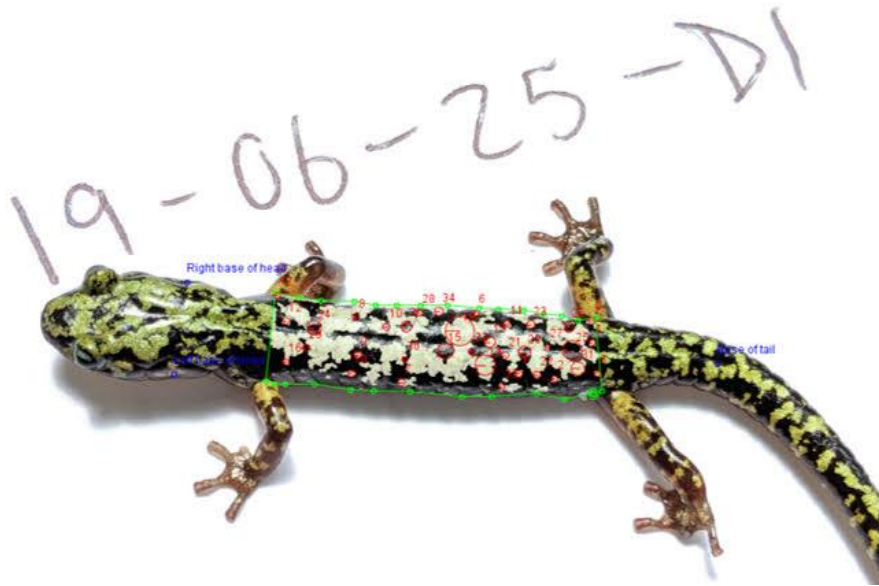


Figure 3.3. Photo-identification process with the Interactive Individual Identification System (I³S) software. Uploaded photographs of individual animals are assessed for reference points (e.g., spots or patterns), and the I³S software compares those reference points to others previously made for individuals already uploaded into the system.

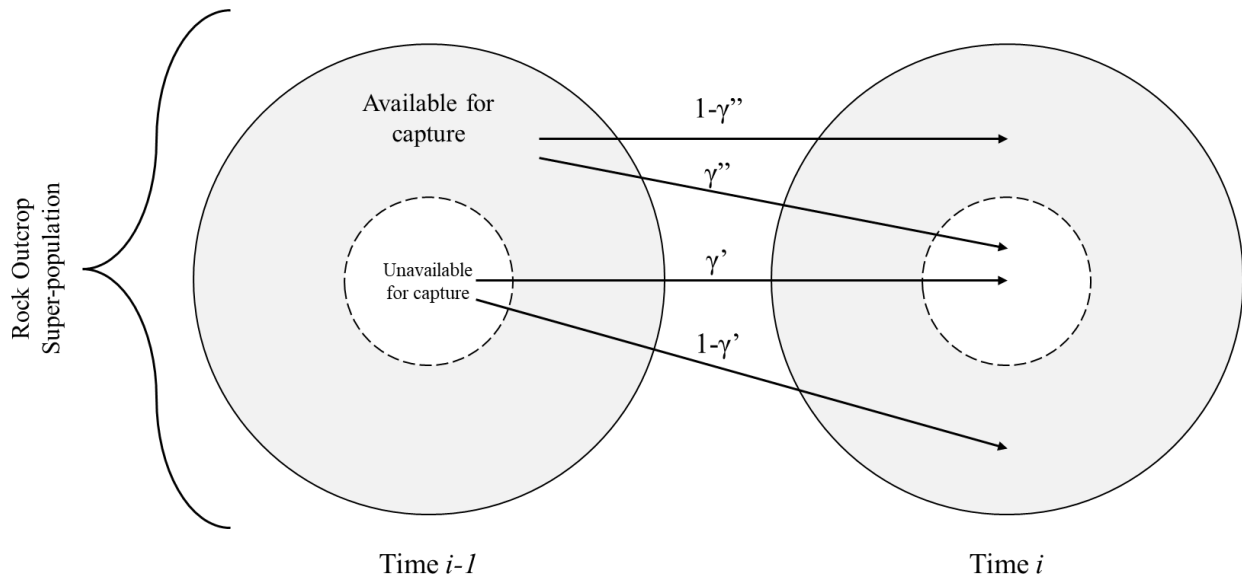


Figure 3.4. An illustration of the relationships between γ' and γ'' at time $i-1$ and i . The super-population is represented by the entire rock outcrop. Crevices on the outer portions of the rock outcrop are easily surveyed, and animals present in these areas are available for capture. Crevices deep within the rock outcrop are unable to be surveyed. Animals present in the inner circle are unable to be encountered by the surveyors, but still members of the super-population. Adapted from Powell and Gale 2015.

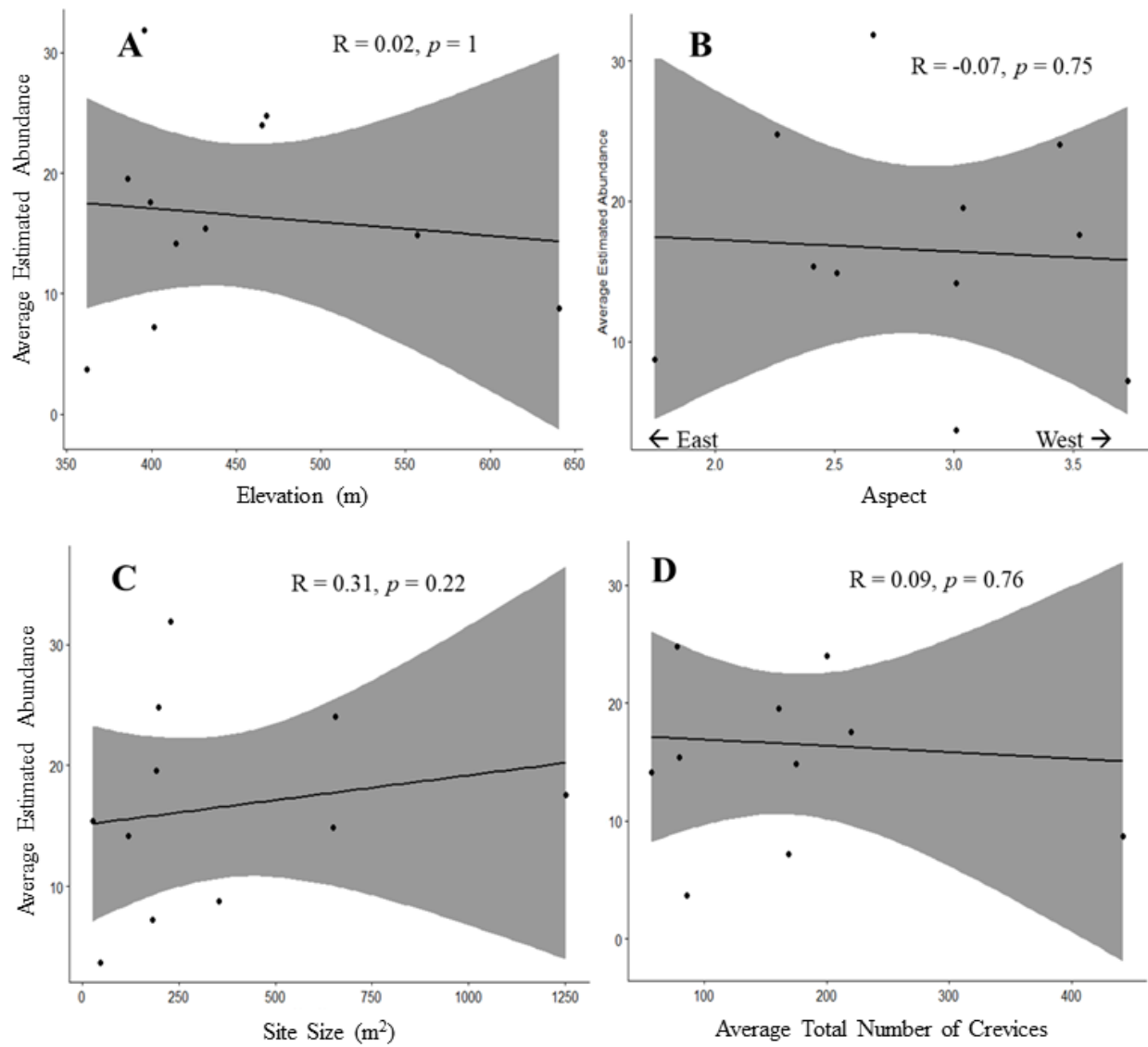


Figure 3.5. Kendall Tau's correlation scatterplots illustrating the relationship between the average abundance as estimated by the CMR analysis and [A] site elevation (m); [B] aspect (degrees); [C] site size (m^2); [D] the average number of crevices totaled across each site.

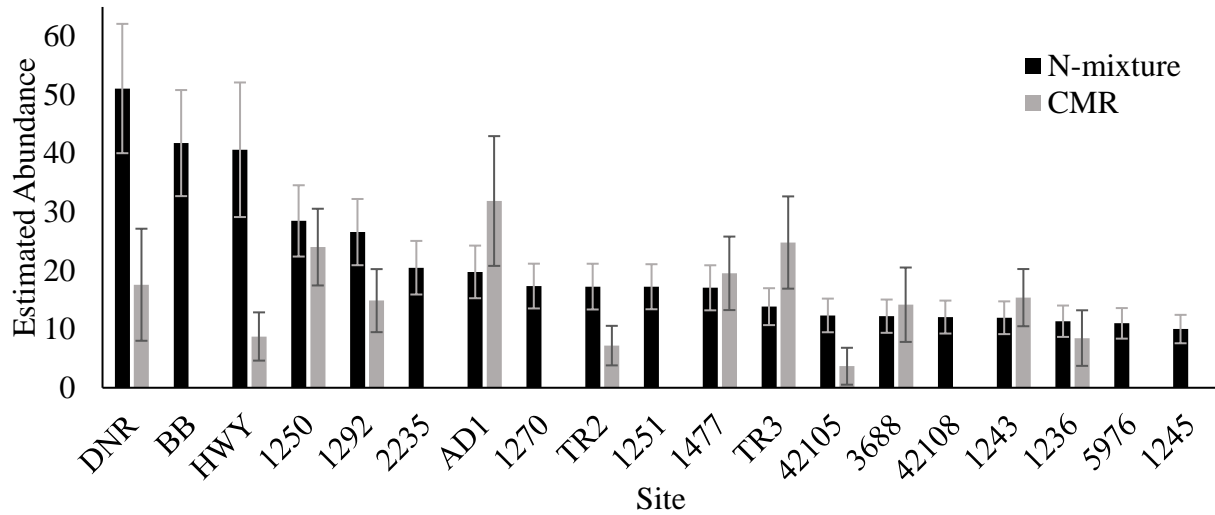


Figure 3.6. Abundance estimates for 19 green salamander (*Aneides aeneus*) populations across upstate South Carolina. Black bars represent site-specific abundances estimated through count data in an N-mixture model framework with count data fit to a Poisson distribution. N-mixture model estimates are informed by $p \sim$ temperature, $\Phi \sim$ primary period, and $\lambda \sim$ site size + total number of crevices. Gray bars represent the site-specific abundances estimated using a CMR approach and averaged across the five primary periods that assumed an open population. Within the CMR model, $\gamma \sim 1$, $p \sim 1$, and $S \sim$ site.

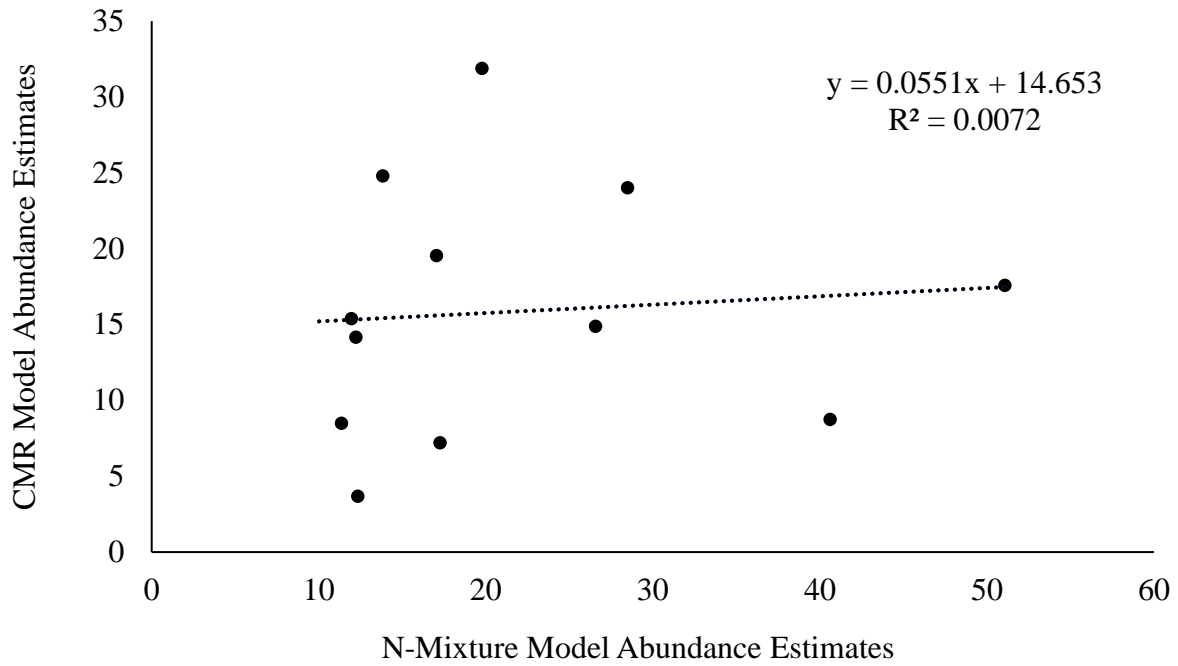


Figure 3.7. Correlative scatterplot illustrating the relationship between our CMR averaged green salamander (*Aneides aeneus*) population abundance estimates and the N-mixture model population abundance estimates. Results indicate a weak relationship ($R^2 = 0.0072$) with no notable association.

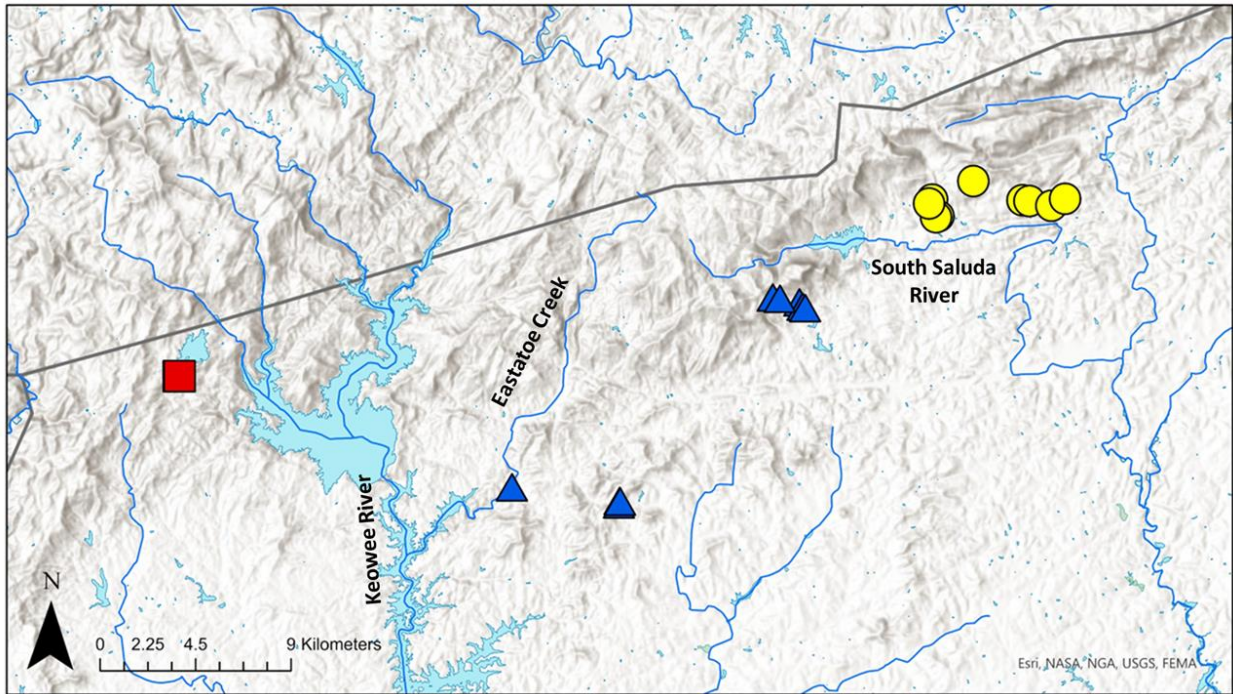


Figure 4.1. Some analyses incorporated population units as numerous sampling locations combined into three groups. This map shows the grouped population units, each separated by a water body that we hypothesized would be large enough to hinder gene flow and create three potential population groupings of green salamanders in upstate South Carolina, USA. Red pin represents Group 1 (n=15 tissue samples); blue pins represent Group 2 (n=53 tissue samples); yellow pins represent Group 3 (n=45 tissue samples).

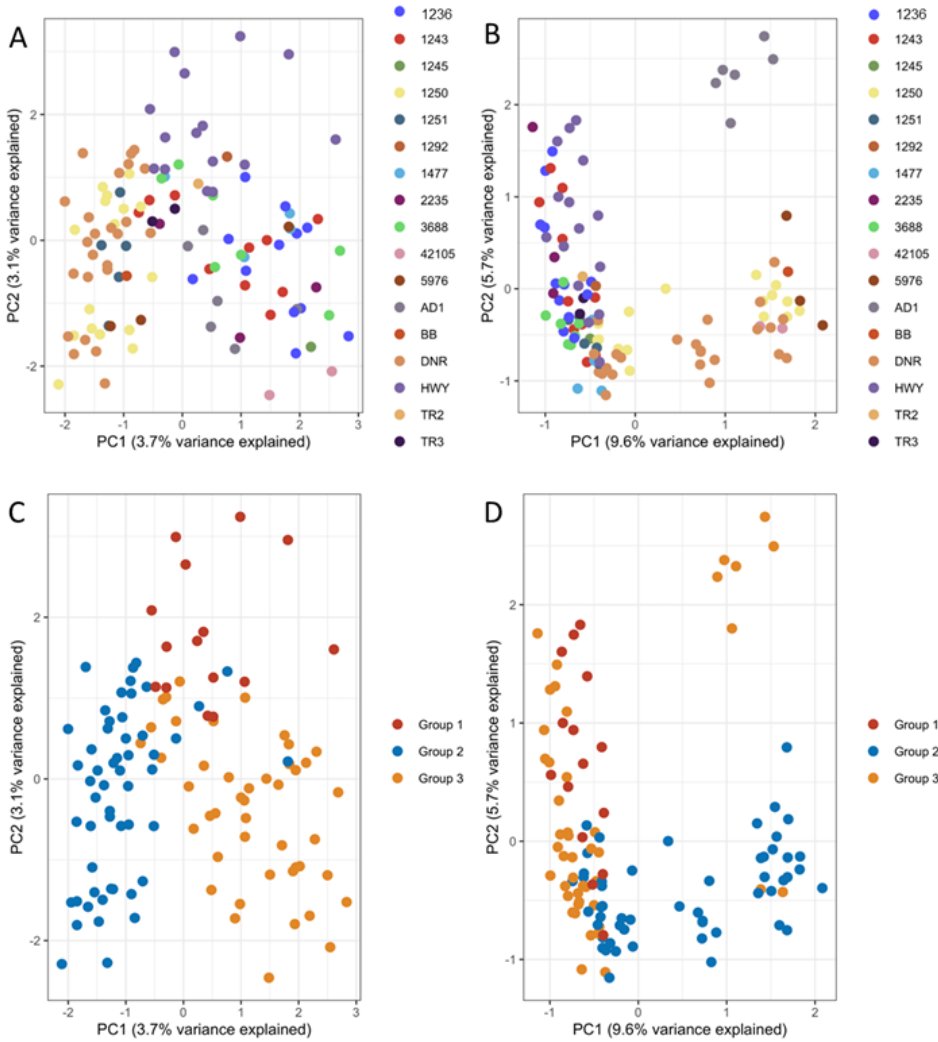


Figure 4.2. Principal component analyses identifying population differentiation among green salamander (*Aneides aeneus*) sites in upstate South Carolina. Each color represents a unique population, and each dot represents an individual green salamander. (A) The analysis conducted with one single nucleotide polymorphism per RAD locus (851 unlinked SNPs). (B) Results of the analysis that included a more stringent filtering scheme that included only SNPs present in more than 50% of individuals, and SNPs present in more than 50% of individuals and SNPs present in at least one individual per sampling location (247 unlinked SNPs). (C) and (D) illustrate the same filtering schemes as (A) and (B), respectively; however, the population units are now separated by geographic grouping rather than individual sites sampled. Neither (A) nor

(B) show strong population separation among sampling sites, but (C) and (D) begin to show more population structure among the three groups

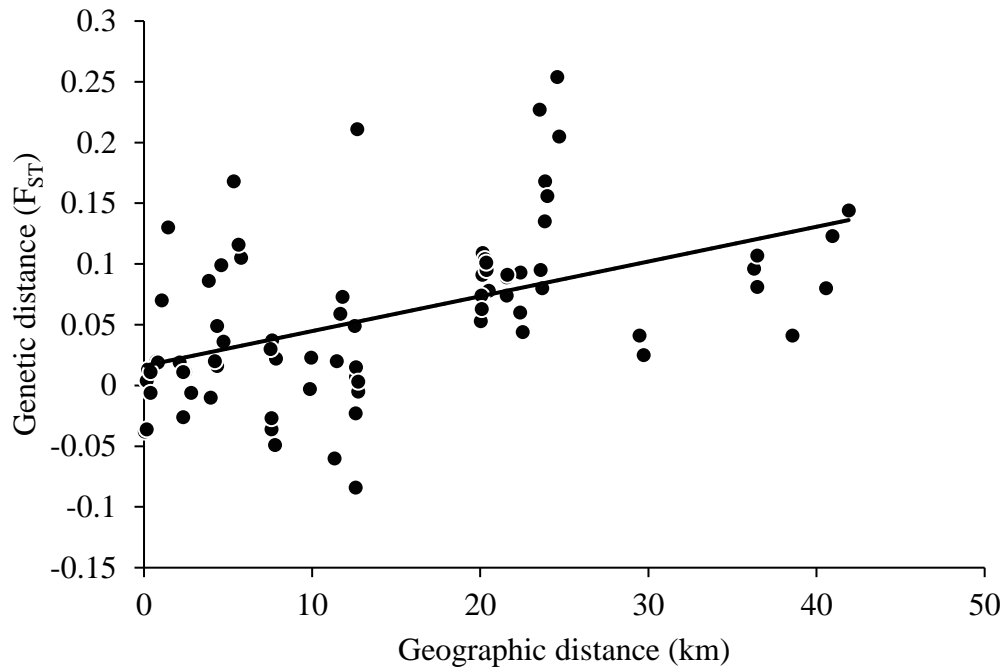


Figure 4.3. Population genetic differentiation showed evidence of isolation by distance ($R^2=0.24$) across pairwise combinations of 17 green salamander (*Aneides aeneus*) populations in upstate South Carolina.

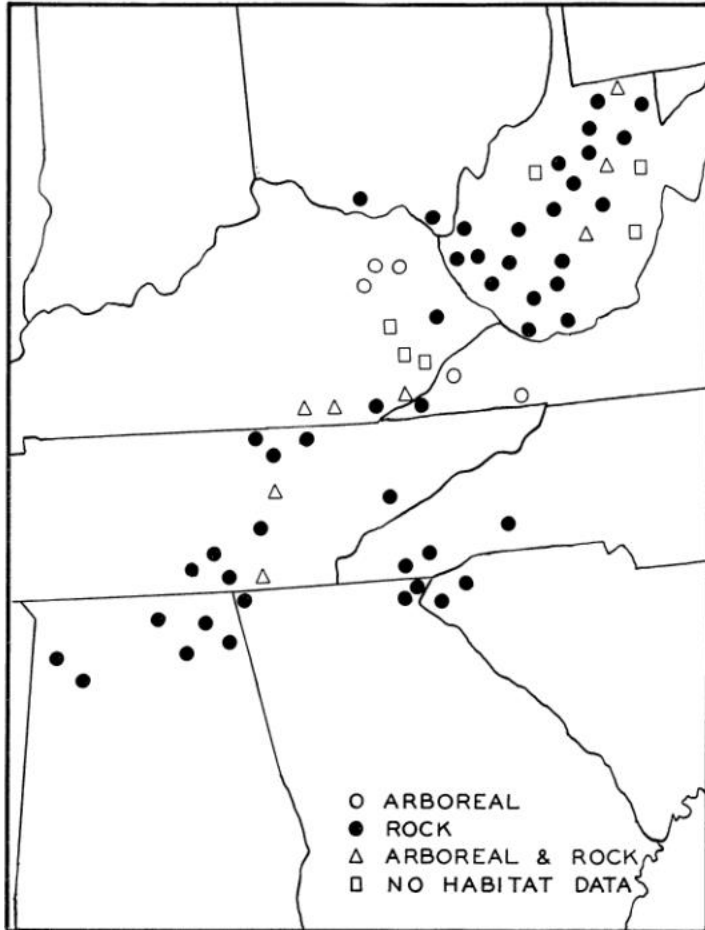


Figure 4.4. Taken from Gordon (1952). A description of population locales and habitat type used by green salamanders (*Aneides aeneus*) along the species range. Population locations were taken from various sources from 1924 to 1950 (see Figure 1 in Gordon 1952). Note no record of green salamander populations within the Appalachian Valley, and apparent disjunct populations within the Blue Ridge Escarpment in North Carolina and South Carolina.

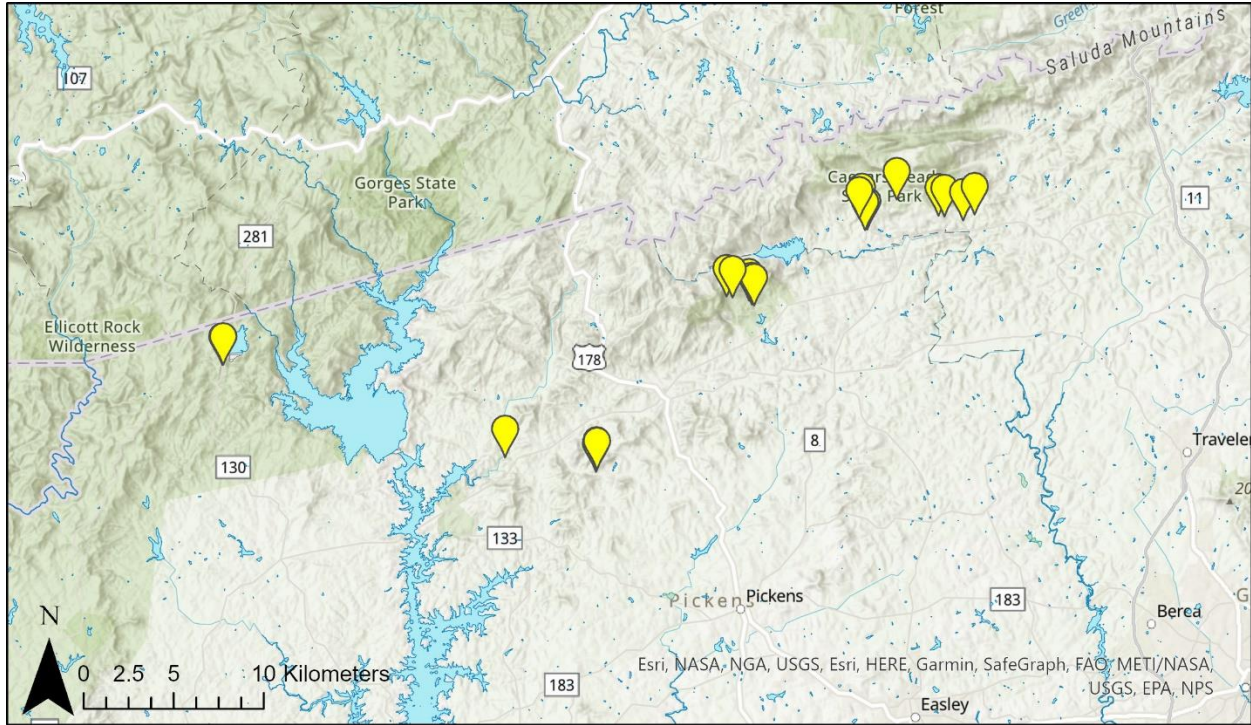


Figure 5.1. Topographic map showing the sampling locations for green salamanders (*Aneides aeneus*) across upstate South Carolina, USA.

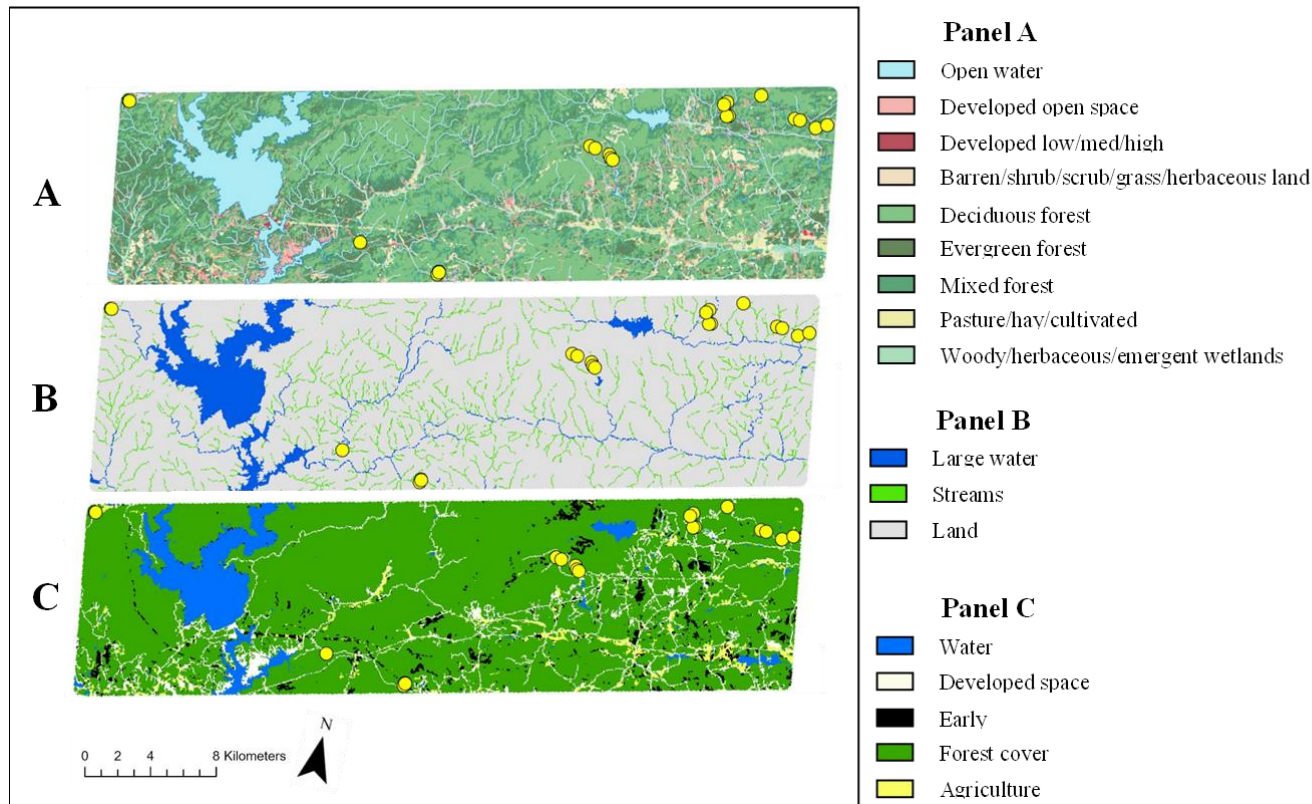


Figure 5.2. Resistance maps made in ArcGIS Pro (v. 3.0.1). Locations of green salamander (*Aneides aeneus*) sampling sites are represented by yellow dots. Panel A shows the original National Land Cover Database (NLCD, Esri 2019) and National Hydrography Dataset (NHD, USGS 2021). Panels B and C represent two resistance surfaces with features aggregated from the original NLCD and NHD layers. Panel B illustrates the water resistance surface with three class features: large water bodies (blue), which combines streams classified as third order and higher as well as lakes; streams (green), which combines first and second order streams; and land

(gray). Panel C illustrates the land cover resistance surface with five class features: water (blue), a combination of open water, woody wetlands, and emergent herbaceous wetlands; developed space (white), which aggregated developed open space, and developed land from low, medium, and high intensities; early successional (black), a category that joined barren land, shrub land, scrub land, grassland, and herbaceous cover; forest cover (green) which combined deciduous, evergreen, and mixed forests; and agriculture (yellow), which incorporated pasture, hay, and cultivated crop land.

APPENDIX

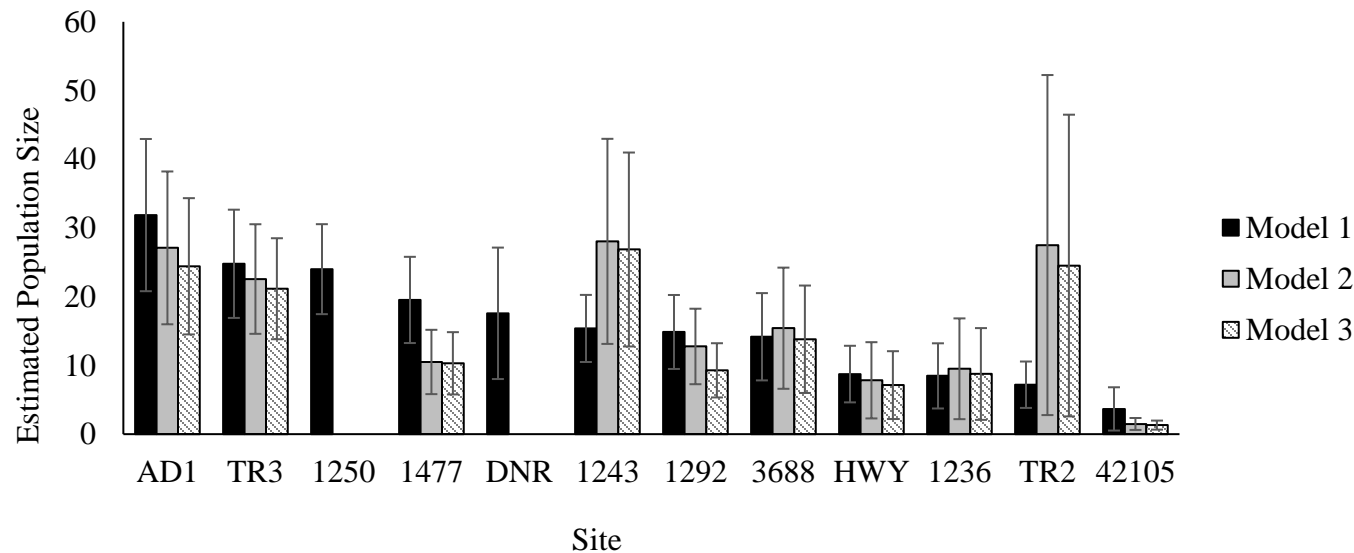
Supplemental 1. Green salamander (*Aneides aeneus*) survival and capture probability estimates across the surveyed South Carolina Populations as described by the second best fit CMR model ($\Delta AIC_C=1.211$, $w=0.127$). Survival (S) was a function of site layout (i.e., the site was comprised of either a single rock, or numerous adjacent rocks). Capture probability (p) was a function of site, and temporary emigration was null. Capture probability estimates from sites 1236 and 1292 were removed because standard error values were larger than the estimates.

Parameter	Covariate	Estimate	SE	Lower CI	Upper CI
Survival, S	Layout: Single Rock	0.876	0.032	0.798	0.926
	Layout: Numerous rocks	0.947	0.016	0.907	0.971
Capture Probability, p	Site: 1477	0.092	0.054	0.028	0.263
	Site: HWY	0.051	0.023	0.021	0.119
	Site: 1236	NA	NA	NA	NA
	Site: TR2	0.127	0.044	0.063	0.240
	Site: 1243	0.137	0.060	0.056	0.299
	Site: 3688	0.096	0.038	0.043	0.199
	Site: TR3	0.331	0.111	0.156	0.569
	Site: 1250	0.126	0.036	0.071	0.214
	Site: 1292	NA	NA	NA	NA
	Site: 42105	0.120	0.078	0.031	0.366
	Site: AD1	0.023	0.017	0.006	0.092
	Site: DNR	0.117	0.028	0.073	0.184

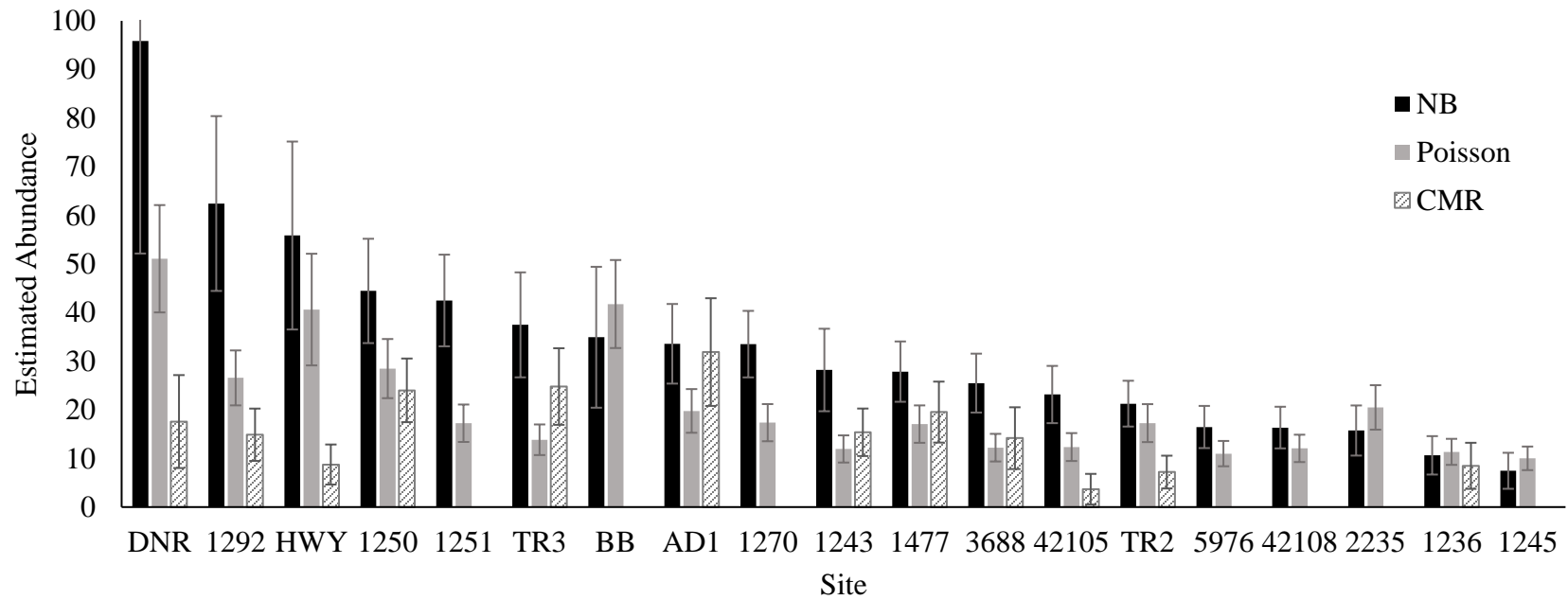
Supplemental 2. Green salamander (*Aneides aeneus*) survival and capture probability estimates across the surveyed South Carolina Populations as described by the third best fit CMR model ($\Delta AIC_C=1.846$, $w=0.092$). Survival (S) was a function of site layout (i.e., the site was comprised of either a single rock, or numerous adjacent rocks). Capture probability (p) was a function of site. Temporary emigration was random. Capture probability estimates from sites 1236 and 1292 were removed because standard error values were larger than the estimates.

Parameter	Covariate	Estimate	SE	Lower CI	Upper CI
Survival, S	Layout: Single Rock	0.898	0.036	0.803	0.950
	Layout: Numerous rocks	0.963	0.020	0.895	0.987
Capture Probability, p	Site: 1477	0.101	0.059	0.031	0.287
	Site: HWY	0.054	0.024	0.023	0.123
	Site: 1236	NA	NA	NA	NA
	Site: TR2	0.132	0.045	0.066	0.248
	Site: 1243	0.140	0.060	0.057	0.303
	Site: 3688	0.108	0.043	0.048	0.226
	Site: TR3	0.404	0.143	0.175	0.684
	Site: 1250	0.141	0.041	0.078	0.242
	Site: 1292	NA	NA	NA	NA
	Site: 42105	0.134	0.088	0.034	0.405
	Site: AD1	0.026	0.019	0.006	0.104
	Site: DNR	0.127	0.030	0.078	0.199
Temporary Emigration, γ	Random	0.295	0.200	0.060	0.734

Supplemental 3. A comparison of green salamander (*Aneides aeneus*) population abundance estimates across the top three CMR models. Black bars represent the site-specific abundances averaged across the five primary sampling periods for the top CMR model. Estimates from the top model were informed by $\gamma \sim 1$, $p \sim 1$, and $S \sim \text{site}$. Gray bars represent the population abundance estimates from the second ranked CMR model ($\Delta\text{AIC}_C=1.211$, $w=0.127$). Estimates from the second model were informed by $\gamma \sim 1$, $p \sim \text{site}$, and $S \sim \text{layout}$. Striped, gray bars illustrate estimated population abundances from the third ranked model ($\Delta\text{AIC}_C=1.846$, $w=0.092$). Within this third model, population abundance estimates were informed by $\gamma \sim \text{random movement}$, $p \sim \text{site}$, and $S \sim \text{layout}$. Abundance estimates were removed from sites 1250 and DNR in the second and third-ranked models because standard error values were larger than the estimated abundances, resulting in biologically unreasonable estimates.



Supplemental 4. A comparison of green salamander (*Aneides aeneus*) population abundance estimates across three analyses. Black bars represent N-mixture model estimates fitting count data to a negative binomial (NB) distribution. Gray bars represent N-mixture model estimates that fit count data to a Poisson distribution. Striped bars represent site-specific abundances estimated using a CMR analysis.



REFERENCES

- Abrahams, M. V., and L. M. Dill. 1989. A determination of the energetic equivalence of the risk of predation. *Ecology* 70:999–1007.
- Asadi Aghbolaghi, M., N. Keyghobadi, Z. Azarakhsh, M. Dadizadeh, S. Asadi Aghbolaghi, and N. Zamani. 2023. An evaluation of isolation by distance and isolation by resistance on genetic structure of the Persian squirrel (*Sciurus anomalus*) in the Zagros forests of Iran. *Ecology and Evolution* 13:e10225.
- Bailey, L. L., T. R. Simons, and K. H. Pollock. 2004. Comparing population size estimators for plethodontid salamanders. *Journal of Herpetology* 38:370–380.
- Barker, R. J., M. R. Schofield, W. A. Link, and J. R. Sauer. 2018. On the reliability of N-mixture models for count data. *Biometrics* 74:369–377.
- Bauder, J. M., C. S. Anderson, H. L. Gibbs, M. J. Tonkovich, and W. D. Walter. 2021*a*. Landscape Features Fail to Explain Spatial Genetic Structure in White-Tailed Deer Across Ohio, USA. *Journal of Wildlife Management* 85:1669–1684.
- Bauder, J. M., W. E. Peterman, S. F. Spear, C. L. Jenkins, A. R. Whiteley, and K. McGarigal. 2021*b*. Multiscale assessment of functional connectivity: Landscape genetics of eastern indigo snakes in an anthropogenically fragmented landscape in central Florida. *Molecular Ecology* 30:3422–3438.
- Baum, K. A., K. J. Haynes, F. P. Dillemath, and J. T. Cronin. 2004. The matrix enhances the effectiveness of corridors and stepping stones. *Ecology* 85:2671–2676.
- Becker, C. G., C. R. Roberto Fonseca, C. F. B. Haddad, R. F. Batista, and P. I. Prado. 2007. Habitat split and the global decline of amphibians. *Science* 318:1775–1778.
- Beebee, T. J. C. 2005. Conservation genetics of amphibians. *Heredity* 95:423–427.

- Benoit-Bird, K. J., B. C. Battaile, S. A. Heppell, B. Hoover, D. Irons, N. Jones, K. J. Kuletz, C. A. Nordstrom, R. Paredes, R. M. Suryan, et al. 2013. Prey patch patterns predict habitat use by top marine predators with diverse foraging strategies. *PLoS ONE* 8:e53348. <https://doi.org/10.1371/journal.pone.0053348>.
- Bishop, S. C. 1928. Notes on some amphibians and reptiles from the southeastern United States with a description of a new salamander from North Carolina. *Journal of the Elisha Mitchell Scientific Society* 43:153–170.
- Blouin-Demers, G., and P. J. Weatherhead. 2001. An experimental test of the link between foraging, habitat selection, and thermoregulation in Black Rat Snakes *Elaphe obsoleta obsoleta*. *Journal of Animal Ecology* 70:1006–1013.
- Bonebrake, T. C., J. Christensen, C. L. Boggs, and P. R. Ehrlich. 2010. Population decline assessment, historical baselines, and conservation. *Conservation Letters*. Volume 3.
- Braun, L. E. 1951. *Deciduous forests of eastern North America*. Second edition. Volume 71. Blakiston, Philadelphia, PA.
- Bruce, R. C. 1968. The role of the Blue Ridge Embayment in the zoogeography of the Green Salamander, *Aneides aeneus*. *Herpetologica* 24:185–194.
- Carey, C., and M. A. Alexander. 2003. Climate change and amphibian declines: Is there a link? *Diversity and Distributions* 9:111–121.
- Carey, C., and C. J. Bryant. 1995. Possible Interrelations among Environmental Toxicants, Amphibian Development, and Decline of Amphibian Populations. *Environ Health Perspect* 103:13–17.
- Chapin, T. G., D. J. Harrison, and D. D. Katnik. 1998. Influence of landscape pattern on habitat use by American Marten in an industrial forest. *Conservation Biology* 12:1327–1337.

- Conde, D. A., Johanna Staerk, F. Colchero, R. Da Silva, Jonas Schöley, H. Maria Baden, L. Jouvett, J. E. Fa, H. Syed, E. Jongejans, S. Meiri, J.-M. Gaillard, S. Chamberlain, J. Wilcken, O. R. Jones, J. P. Dahlgren, U. K. Steiner, L. M. Bland, I. Gomez-Mestre, J.-D. Lebreton, J. González Vargas, N. Flesness, V. Canudas-Romo, R. Salguero-Gómez, O. Byers, T. B. Berg, A. Scheuerlein, S. Devillard, D. S. Schigel, O. A. Ryder, H. P. Possingham, A. Baudisch, J. W. Vaupel, X. Duke, J. W. V Designed, J Staerk, H. S. Performed, J Schöley, J. W. V Contributed, and J. W. Analyzed. 2019. Data gaps and opportunities for comparative and conservation biology. *PNAS* 116:9658–9664.
- Costa, A., A. Romano, and S. Salvidio. 2020. Reliability of multinomial N-mixture models for estimating abundance of small terrestrial vertebrates. *Biodiversity and Conservation* 29:2951–2965.
- Corser, J. D. 2001. Decline of disjunct Green Salamander (*Aneides aeneus*) populations in the southern Appalachians. *Biological Conservation* 97:119–126.
- Courtois, E. A., E. Michel, Q. Martinez, K. Pineau, M. Dewynter, G. F. Ficetola, and A. Fouquet. 2016. Taking the lead on climate change: Modelling and monitoring the fate of an Amazonian frog. *ORYX* 50:450–459.
- Crespi, E. J., L. J. Rissler, and R. A. Browne. 2003. Testing Pleistocene refugia theory: Phylogeographical analysis of *Desmognathus wrighti*, a high-elevation salamander in the southern Appalachians. *Molecular Ecology* 12:969–984.
- Cupp Jr., P. V. 1991. Aspects of the life history and ecology of the Green Salamander, *Aneides aeneus*, in Kentucky. *Journal of the Tennessee Academy of Science* 66:171–174.
- Cushman, S. A. 2006. Effects of habitat loss and fragmentation on amphibians: A review and prospectus. *Biological Conservation* 128:231–240.

- Dail, D., and L. Madsen. 2011. Models for Estimating Abundance from Repeated Counts of an Open Metapopulation. *Biometrics* 67:577–587.
- Dennis, E. B., B. J. T. Morgan, and M. S. Ridout. 2015. Computational aspects of N-mixture models. *Biometrics* 71:237–246.
- Duarte, A., M. J. Adams, and J. T. Peterson. 2018. Fitting N-mixture models to count data with unmodeled heterogeneity: Bias, diagnostics, and alternative approaches. *Ecological Modelling* 374:51–59.
- Dustan, P., O. Doherty, and S. Pardede. 2013. Digital reef rugosity estimates coral reef habitat complexity. *PLoS ONE* 8:e57386. <https://doi.org/10.1371/journal.pone.0057386>.
- Ehrlich, P. R., and R. M. Pringle. 2008. Where does biodiversity go from here? A grim business-as-usual forecast and a hopeful portfolio of partial solutions. *PNAS* 105:11579–11586.
- Falaschi, M., A. Melotto, R. Manenti, and G. F. Ficetola. 2020. Invasive species and amphibian conservation. *Herpetologica* 76:216–227.
- Fasola, E., R. Ribeiro, and I. Lopes. 2015. Microevolution due to pollution in amphibians: A review on the genetic erosion hypothesis. *Environmental Pollution* 204:181–190.
- Ficetola, G. F., B. Barzaghi, A. Melotto, M. Muraro, E. Lunghi, C. Canedoli, E. Lo Parrino, V. Nanni, I. Silva-Rocha, A. Urso, M. A. Carretero, D. Salvi, S. Scali, G. Scari, R. Pennati, F. Andreone, and R. Manenti. 2018. N-mixture models reliably estimate the abundance of small vertebrates. *Scientific Reports* 8:1–8.
- Fiske, I. J., and R. B. Chandler. 2011. unmarked: An R Package for Fitting Hierarchical Models of Wildlife Occurrence and Abundance. *JSS Journal of Statistical Software* 43:1–23.
- Feder, M. E. 1983. Integrating the ecology and physiology of plethodontid salamanders. *Herpetologica* 39:291–310.

- Frankham, R. 2005. Genetics and extinction. *Biological Conservation* 126:131–140.
- Full, R. J. 1986. Locomotion without lungs: energetics and performance of a lungless salamander. *American Journal of Physiology-Regulatory, Integrative and Comparative Physiology* 251:R775–R780.
- Full, R. J., B. D. Anderson, C. M. Finnerty, and M. E. Feder. 1988. Exercising with and without lungs: I. The effects of metabolic cost, maximal oxygen transport and body size on terrestrial locomotion in salamander species. *Journal of Experimental Biology* 138:471–485.
- Fusco, N. A., E. Pehek, and J. Munshi-South. 2020. Urbanization reduces gene flow but not genetic diversity of stream salamander populations in the New York City metropolitan area. *Evolutionary Applications* 14:99–116.
- Gade M. R., and W. E. Peterman. 2019. Multiple environmental gradients influence the distribution and abundance of a key forest-health indicator species in the Southern Appalachian Mountains, USA. *Landscape Ecology* 34:569–582.
- Gallant, A. L., R. W. Klaver, G. S. Casper, and M. J. Lannoo. 2007. Global Rates of Habitat Loss and Implications for Amphibian Conservation. *Copeia* 2007:967–979.
- Gandon, S., and F. Rousset. 1999. Evolution of stepping-stone dispersal rates. *Proceedings of the Royal Society of London. Series B: Biological Sciences* 266:2507–2513.
- Garabedian, J. E., C. E. Moorman, M. N. Peterson, and J. C. Kilgo. 2017. Use of LiDAR to define habitat thresholds for forest bird conservation. *Forest Ecology and Management* 399:14–36.
- Gilpin, M. E. 1980. The Role of Stepping-Stone Islands. *Theoretical Population Biology* 17:247–253.

- Goldberg, C. S., S. Caren, and C. R. Schwalbe. 2004. Habitat use and spatial structure of a Barking Frog (*Eleutherodactylus augusti*) population in southeastern Arizona. *Journal of Herpetology* 38:305–312.
- Gordon, R. E. 1952. A contribution to the ecology and life history of the plethodontid salamander, *Aneides aeneus*. *American Midland Naturalist* 47:666–701.
- Gordon, R. E. 1961. The Movement of Displaced Green Salamanders. *Ecology* 42:200–202.
- Gordon, R. E., and R. L. Smith. 1949. Notes on the life history of the salamander *Aneides aeneus*. *Copeia* 1949:173–175.
- Hafer, M. L.A., and J. R. Sweeney. 1993. Status of the Green Salamander in South Carolina. *Proceedings of the Annual Conference of Southeastern Association of Fish and Wildlife Agencies* 47:414–418.
- Hammerson, G. 2004. *Aneides aeneus*. The IUCN Red List of Threatened Species 2004. International Union for the Conservation of Nature. <http://www.iucnredlist.org>.
- Hartl, D. L., and A. G. Clark. 1997. *Principles of Population Genetics*. Fourth edition. Sinauer Associates, Inc., Sunderland, MA.
- Highton, R., G. C. Maha, and L. R. Maxson. 1990. Biochemical Evolution in the Slimy Salamanders of the *Plethodon glutinosus* Complex in the Eastern United States. *Copeia* 1990:256–258.
- Highton, R., and R. B. Peabody. 2000. Geographic protein variation and speciation in salamanders of the *Plethodon jordani* and *Plethodon glutinosus* complexes in the southern Appalachian Mountains with the description of four new species. Plenum Publishers, New York, New York.

- Holsinger, K. E., and B. S. Weir. 2009. Genetics in geographically structured populations: Defining, estimating and interpreting F_{ST} . *Nature Reviews Genetics* 10:639–650.
- Holt, R. D., J. H. Lawton, K. J. Gaston, and T. M. Blackburn. 1997. On the Relationship between Range Size and Local Abundance: Back to Basics. *Oikos* 78:183–190.
- Hofmann, N., and P. Fischer. 2002. Temperature preferences and critical thermal limits of Burbot: implications for habitat selection and ontogenetic habitat shift. *Transactions of the American Fisheries Society* 131:1164–1172.
- Hoffmann, A. A., C. M. Sgrò, and T. N. Kristensen. 2017. Revisiting Adaptive Potential, Population Size, and Conservation. *Trends in Ecology and Evolution* 32:506–517.
- Holsinger, K. E., and B. S. Weir. 2009. Genetics in geographically structured populations: Defining, estimating and interpreting F_{ST} . *Nature Reviews Genetics* 10:639–650.
- Hopkins, W. A. 2007. Amphibians as Models for Studying Environmental Change. *ILAR journal* 48:270–277.
- Hughes, J. B., G. C. Daily, and P. R. Ehrlich. 1997. Population diversity: Its extent and extinction. *Science* 278:689–692.
- IUCN. 2022. The IUCN Red List of Threatened Species. Version 2022-2.
- Jaisuk, C., and S. Wansuk. 2018. Effects of landscape features on population genetic variation of a tropical stream fish, Stone lapping minnow, *Garra cambodgiensis*, in the upper Nan River drainage basin, northern Thailand. *PeerJ* 6:e4487.
- John, R. R. 2017. Movement, Occupancy, and Detectability of Green Salamanders (*Aneides aeneus*) in Northern Alabama. Master of Science, Auburn University, Auburn, Alabama.

- Johnson, A. 2002. Determining the Genetic Distances between sub-populations of *Aneides aeneus* in the Westvāco Wildlife and Ecological Research Forest. Master of Science, Marshall University, Huntington, WV.
- Johnson, D. H. 1980. The comparison of usage and availability measurements for evaluating resource preference. *Ecology* 61:65–71.
- Jolly, G. M. 1965. Explicit Estimates from Capture-Recapture Data with Both Death and Immigration-Stochastic Model. *Biometrika* 52:225–247.
- Joseph, L. N., C. Elkin, T. G. Martin, and H. P. Possingham. 2009. Modeling abundance using N-mixture models: The importance of considering ecological mechanisms. *Ecological Applications* 19:631–642.
- Jump, A. S., R. Marchant, and J. Peñuelas. 2009. Environmental change and the option value of genetic diversity. *Trends in Plant Science* 14:51–58.
- Kats, L. B., and R. P. Ferrer. 2003. Alien predators and amphibian declines: Review of two decades of science and the transition to conservation. *Diversity and Distributions* 9:99–110.
- Kawamura, K. 2005. Low genetic variation and inbreeding depression in small isolated populations of the Japanese rosy bitterling, *Rhodeus ocellatus kurumeus*. *Zoological Science* 22:517–524.
- Kazitsa, E. G., S. Wei, Y. Pu, X. Wu, L. Song, L. Gao, F. Qiu, Y. Guo, Z. Zhu, and H. Wu. 2018. Population size, genetic diversity and molecular evidence of a recent population bottleneck in *hynobius chinensis*, an endangered salamander species. *Asian Herpetological Research* 9:149–164.

- Keen, W. H. 1984. Influence of moisture on the activity of a plethodontid salamander. *Copeia* 1984:684–688.
- Kendall, W. L., J. D. Nichols, and J. E. Hines. 1997. Estimating temporary emigration using capture-recapture data with Pollock's robust design. *Ecology* 78:563–578.
- Kéry, M. 2018. Identifiability in N-mixture models: a large-scale screening test with bird data. *Ecology* 99:281–288.
- Kéry, M., J. A. Royle, and H. Schmid. 2005. Modeling avian abundance from replicated counts using binomial mixture models. *Ecological Applications* 15:1450–1461.
- Khosravi, R., M. R. Hemami, M. Malekian, T. L. Silva, H. R. Rezaei, and J. C. Brito. 2018. Effect of landscape features on genetic structure of the goitered gazelle (*Gazella subgutturosa*) in Central Iran. *Conservation Genetics* 19:323–336.
- Kilpatrick, A. M., C. J. Briggs, and P. Daszak. 2010. The ecology and impact of chytridiomycosis: an emerging disease of amphibians. *Trends in Ecology and Evolution* 25:109–118.
- Kindlmann, P., and F. Burel. 2008. Connectivity measures: a review. *Landscape Ecology* 23:879–890.
- Koen, E. L., C. J. Garroway, P. J. Wilson, and J. Bowman. 2010. The effect of map boundary on estimates of landscape resistance to animal movement. *PLoS ONE* 5:e11785.
- Krebs, C. J., B. L. Keller, and R. H. Tamarin. 1969. *Microtus Population Biology: Demographic Changes in Fluctuating Populations of M. Ochrogaster and M. Pennsylvanicus in Southern Indiana.* *Ecology* 50:587–607.

- Kuchta, S. R., A. D. Brown, P. E. Converse, and R. Highton. 2016. Multilocus phylogeography and species delimitation in the cumberland plateau salamander, *Plethodon kentucki*: Incongruence among data sets and methods. *PLoS ONE* 11:e0150022.
- Laake, J. 2013. *RMark: An R Interface for Analysis of Capture-Recapture Data with MARK*. Seattle, WA.
- Lewis, J. C., and R. L. Garrison. 1984. Habitat suitability index models: American Black Duck (wintering). FWS/OBS-82/10.68, U.S. Fish and Wildlife Service, Washington DC, USA. 16 p.
- Link, W. A., M. R. Schofield, R. J. Barker, and J. R. Sauer. 2018. On the robustness of N-mixture models. *Ecology* 99:1547–1551.
- Lips, K. R., F. Brem, R. Brenes, J. D. Reeve, R. A. Alford, J. Voyles, C. Carey, L. Livo, A. P. Pessier, J. P. Collins, and D. B. Wake. 2006. Emerging infectious disease and the loss of biodiversity in a Neotropical amphibian community. *PNAS* 103:3165–3170.
- Lowe, W. H., and F. W. Allendorf. 2010. What can genetics tell us about population connectivity? *Molecular Ecology* 19:3038–3051.
- Lunghi, E., R. Manenti, and G. F. Ficetola. 2015. Seasonal variation in microhabitat of salamanders: environmental variation or shift of habitat selection? *PeerJ* 3:e1122 <https://doi.org/10.7717/peerj.1122>.
- Lynch, M., J. Conery, and R. Burger. 1995. Mutation accumulation and the extinction of small populations. *The American Naturalist* 146:489–518.
- McRae, B. H. 2006. Isolation by resistance. *Evolution* 60:1551–1561.
- McRae, B., Viral Shah, Tanmay Mohapatra, VB Shah, and TK Mohapatra. 2014. *CIRCUITSCAPE User Guide*.

- Mead, L. S., S. G. Tilley, and L. A. Katz. 2001. Genetic structure of the blue ridge dusky salamander (*Desmognathus orestes*): Inferences from allozymes, mitochondrial DNA, and behavior. *Evolution* 55:2287–2302.
- Murphy, M. O., K. S. Jones, S. J. Price, and D. W. Weisrock. 2018. A genomic assessment of population structure and gene flow in an aquatic salamander identifies the roles of spatial scale, barriers, and river architecture. *Freshwater Biology* 63:407–419.
- Newman, J. C., K. Barrett, and J. W. Dillman. 2018. Green Salamander estimated abundance and environmental associations in South Carolina. *Journal of Herpetology* 52:437–443.
- Nguyen, T. N., N. Chen, E. J. Cosgrove, R. Bowman, J. W. Fitzpatrick, and A. G. Clark. 2022. Dynamics of reduced genetic diversity in increasingly fragmented populations of Florida scrub jays, *Aphelocoma coerulescens*. *Evolutionary Applications* 15:1018–1027.
- Nichols, J. D., W. L. Kendall, and G. S. Boomer. 2019. Accumulating evidence in ecology: Once is not enough. *Ecology and Evolution* 9:13991–14004.
- Nielsen, R., and M. Slatkin. 2013. *An introduction to population genetics*. Sinauer Associates Inc., Sunderland, MA.
- Nikolakaki, P. 2004. A GIS site-selection processes for habitat creation: estimating connectivity of habitat patches. *Landscape and Urban Planning* 68:77–94.
- Novak, M., and K. Barrett. 2023. Within-site microclimate and connectivity can help predict the presence of discrete patch inhabitants, *Aneides aeneus*. *Herpetological Conservation and Biology* 18:111–117.
- Pan, Y., G. Wei, A. A. Cunningham, S. Li, S. Chen, E. J. Milner-Gulland, and S. T. Turvey. 2016. Using local ecological knowledge to assess the status of the Critically Endangered

- Chinese giant salamander *Andrias davidianus* in Guizhou Province, China. *Oryx* 50:257–264.
- Pauly, D. 1995. Anecdotes and the shifting baseline syndrome of fisheries. *Trends in Ecology & Evolution* 10:430.
- Pearman, P. B., and T. W. J. Garner. 2005. Susceptibility of Italian agile frog populations to an emerging strain of Ranavirus parallels population genetic diversity. *Ecology Letters* 8:401–408.
- Peterman, W. 2018. ResistanceGA: An R package for the optimization of resistance surfaces using genetic algorithms. *Methods in Ecology and Evolution* 9:1638–1647.
- Peterman, W., E. R. Brocato, R. D. Semlitsch, and L. S. Eggert. 2016. Reducing bias in population and landscape genetic inferences: The effects of sampling related individuals and multiple life stages. *PeerJ* 2016:1–19.
- Pflüger, F. J., J. Signer, and N. Balkenhol. 2019. Habitat loss causes non-linear genetic erosion in specialist species. *Global Ecology and Conservation* 17:e00507.
- Pitt, W. C. 1999. Effects of multiple vertebrate predators on grasshopper habitat selection: trade-offs due to predation risk, foraging, and thermoregulation. *Evolutionary Ecology* 13:499–516.
- Pollock, K. H. 1982. A Capture-Recapture Design Robust to Unequal Probability of Capture. *The Journal of Wildlife Management* 46:752–757.
- Powell, L. A., and G. A. Gale. 2015. *Estimation of Parameters for Animal Populations: A primer for the rest of us*. Caught Napping Publications, Lincoln, NE.
- Puebla, O., E. Bermingham, and F. Guichard. 2009. Estimating dispersal from genetic isolation by distance in a coral reef fish (*Hypoplectrus puella*). *Ecology* 90:3087–3098.

- R Core Team. 2021. R: A language and environment for statistical computing. R Foundation for Statistical Computing, Vienna, Austria.
- Reagan, D. P. 1974. Habitat selection in the Three-toed Box Turtle, *Terrapene carolina triunguis*. *Copeia* 1974:512–527.
- Rius, M., and J. A. Darling. 2014. How important is intraspecific genetic admixture to the success of colonising populations? *Trends in Ecology and Evolution* 29:233–242.
- Rosenbaum, P. A., J. M. Robertson, and K. R. Zamudio. 2007. Unexpectedly low genetic divergences among populations of the threatened bog turtle (*Glyptemys muhlenbergii*). *Conservation Genetics* 8:331–342.
- Rossell, C. R., J. Hicks, L.A. Williams, and S. C. Patch. 2009. Attributes of rock crevices selected by Green Salamanders, *Aneides aeneus* on the Blue Ridge Escarpment. *Herpetological Review* 40:151–153.
- Royle, J. A. 2004. N-Mixture Models for Estimating Population Size from Spatially Replicated Counts. *Biometrics* 60:108–115.
- Royle, J. A., and J. D. Nichols. 2003. Estimating abundance from repeated presence-absence data or point counts. *Ecology* 84:777–790.
- Royle, J. A., J. D. Nichols, M. Kéry, and E. Ranta. 2005. Modelling Occurrence and Abundance of Species When Detection Is Imperfect. *Oikos* 110:353–359.
- Sannolo, M., F. Gatti, M. Mangiacotti, S. Scali, and R. Sacchi. 2016. Photo-identification in amphibian studies: A test of I3S Pattern. *Acta Herpetologica* 11:63–68.
- Saura, S., Ö. Bodin, and M. J. Fortin. 2014. Stepping stones are crucial for species' long-distance dispersal and range expansion through habitat networks. *Journal of Applied Ecology* 51:171–182.

- Scrucca, L. 2013. Journal of Statistical Software GA: A Package for Genetic Algorithms in R. *Journal of Statistical Software* 53:1–37.
- Slatkin, M. 2008. Linkage disequilibrium - Understanding the evolutionary past and mapping the medical future. *Nature Reviews Genetics* 9:477–485.
- Smith, M. A., and D. M. Green. 2005. Dispersal and the metapopulation paradigm in amphibian ecology and conservation: Are all amphibian populations metapopulations? *Ecography* 28:110–128.
- Smith, W. H., S. L. Slemp, C. D. Stanley, M. N. Blackburn, and J. Wayland. 2008. Combining Citizen Science with Traditional Biotic Surveys to Enhance Knowledge Regarding the Natural History of Secretive Species: Notes on the Geographic Distribution and Status of the Green Salamander (*Aneides aeneus*) in the Cumberland Mountains of Virginia, USA. *IRCF Reptiles & Amphibians* 22:135–144.
- Smith, W. H., S. L. Slemp, C. D. Stanley, M. N. Blackburn, and J. Wayland. 2015. Combining Citizen Science with Traditional Biotic Surveys to Enhance Knowledge Regarding the Natural History of Secretive Species: Notes on the Geographic Distribution and Status of the Green Salamander (*Aneides aeneus*) in the Cumberland Mountains of Virginia, USA. *Reptiles & Amphibians* 22:135–144.
- Smith, W. H., S. L. Slemp, C. D. Stanley, M. N. Blackburn, and J. Wayland. 2017. Rock crevice morphology and forest contexts drive microhabitat preferences in the Green Salamander (*Aneides aeneus*). *Canadian Journal of Zoology* 95:353–358.
- Snyder, D. 1971. The function of brooding behavior in the plethodontid salamander, *Aneides aeneus*: A field study. Dissertation, University of Notre Dame, Notre Dame.

- Snyder, D. H. 1991. The Green Salamander (*Aneides aeneus*) in Tennessee and Kentucky, with Comments on the Carolinas' Blue Ridge Populations. *Journal of the Tennessee Academy of Science* 66:165–169.
- Soga, M., and K. J. Gaston. 2018. Shifting baseline syndrome: causes, consequences, and implications. *Frontiers in Ecology and the Environment* 16:222–230.
- Spielman, D., B. W. Brook, D. A. Briscoe, and R. Frankham. 2004. Does inbreeding and loss of genetic diversity decrease disease resistance? *Conservation Genetics* 5:439–448.
- Spinks, P. Q., and H. B. Shaffer. 2005. Range-wide molecular analysis of the western pond turtle (*Emys marmorata*): Cryptic variation, isolation by distance, and their conservation implications. *Molecular Ecology* 14:2047–2064.
- Stephens, D. W. 2008. Decision ecology: foraging and the ecology of animal decision making. *Cognitive, Affective, & Behavioral Neuroscience* 8:475–484.
- Stuart, S. N., J. S. Chanson, N. A. Cox, B. E. Young, A. S. L. Rodrigues, D. L. Fischman, and R. W. Waller. 2004. Status and Trends of Amphibian Declines and Extinctions Worldwide. *Science Reports* 99:1783–1786.
- Tilley, S. G., and M. J. Mahoney. 1996. Patterns of Genetic Differentiation in Salamanders of the *Desmognathus ochrophaeus* Complex (Amphibia: Plethodontidae). *Herpetological Monographs* 10:1–42.
- Van Tienhoven, A. M., J. E. Den Hartog, R. A. Reijns, and V. M. Peddemors. 2007. A computer-aided program for pattern-matching of natural marks on the spotted raggedtooth shark *Carcharias taurus*. *Journal of Applied Ecology* 44:273–280.
- Wake, D. B. 1963. Comparative osteology of the salamander genus *Aneides*. *Journal of Morphology* 113:73–118.

- Waldron, J. L., and W. J. Humphries. 2005. Arboreal habitat use by the Green Salamander, *Aneides aeneus*, in South Carolina. *Journal of Herpetology* 39:486–492.
- Walker, D., and J. C. Avise. 1998. Principles of phylogeography as illustrated by freshwater and terrestrial turtles in the southeastern United States. *Annual Review of Ecological Systems* 29:23–58.
- Warkentin, I. G., D. Bickford, N. S. Sodhi, and C. J. A. Bradshaw. 2009. Eating Frogs to Extinction. *Biology* 23:1056–1059.
- Weir, B. S., and J. Goudet. 2017. A unified characterization of population structure and relatedness. *Genetics* 206:2085–2103.
- Weisrock, D., D. W. Weisrock, and F. J. Janzen. 2000. Comparative Molecular Phylogeography of North American Softshell Turtles (*Apalone*): Implications for Regional and Wide-Scale Historical Evolutionary Forces. *Molecular Phylogenetics and Evolution* 14:152–164.
- Williams, K. L., and R. E. Gordon. 1961. Natural dispersal of the salamander *Aneides aeneus*. *Copeia* 1961:353–353.
- Wilson, C. R. 2003. Woody and arboreal habitats of the Green Salamander (*Aneides aeneus*) in the Blue Ridge Mountains. *Contemporary Herpetology* 2003:1–10.
- Wright, S. 1931. Evolution in mendelian populations. *Genetics* 16:97–158.
- Wright, S. 1943. Isolation by distance. *Genetics* 28:114–138.
- Zappalorti, R. T., J. E. Lovich, R. F. Farrell, and M. E. Torocco. 2015. Nest-site characteristics of *Glyptemys muhlenbergii* (Bog Turtle) in New Jersey and Pennsylvania. *Northeastern Naturalist* 22:573–584.

Zarnowitz, J. E., and D. A. Manuwal. 1985. The effects of forest management on cavity-nesting birds in northwestern Washington. *Journal of Wildlife Management* 49:255–263.